Title

Developments in ensemble and finite temperature density functional theory using a model system

Permalink

https://escholarship.org/uc/item/453146cc

Author

Sagredo, Francisca

Publication Date

2020

Peer reviewed|Thesis/dissertation

UNIVERSITY OF CALIFORNIA,
IRVINE

Developments in ensemble and finite temperature density functional theory using a model system

DISSERTATION

submitted in partial satisfaction of the requirements
for the degree of

DOCTOR OF PHILOSOPHY

in Chemistry

by

Francisca Sagredo

Dissertation Committee:
Professor Kieron Burke, Chair
Professor Vladimir Mandelshtam
Professor Craig Martens

2020

DEDICATION

Para la familia Sagredo

TABLE OF CONTENTS

LIST OF FIGURES

List of Tables

ACKNOWLEDGMENTS

First and foremost, I must thank my advisor Professor Kieron Burke, for taking me as a PhD student, and putting up with me for 5 years. While I did not have any previous theory experience, he gave me the opportunity to change my research direction. He provided the space for me to grow as a scientist, and gave me and everyone in the group many valuable opportunities for which I am profoundly thankful. Thank you Kieron for repeatedly answering my questions (even if it was the same question), but most importantly thank you for listening to me and my concerns, even when they were not academic in nature.

I would also like to acknowledge my thesis committee members, Professors Vladimir Mandelshtam and Craig Martens, who also served in my advancement committee. I would like to specially thank Professor Rachel Martin who was the chair of my advancement committee, and who's words of encouragement were always perfectly timed.

I would like to specially acknowledge Dr. Attila Cangi, who recruited me to intern at Sandia National Laboratories during my third year. This internship gave me some much needed time away from my coursework in Irvine. It gave me a peek of what large scale science is like at the national labs. Attila's seemingly endless patience and vast knowledge also gave me the confidence that I could in fact be a competent scientist. Working with Attila, has truly been a pleasure. Being a year round intern at Sandia for the last two years of my degree was unexpected experience for which I am thankful.

Next I must thank all of the friends I made while at Irvine. Our frequent chats and outings made the overall experience much more enjoyable. Special thanks to Kara Thomas, Sabrina Chee, and Sara Taydeon, with whom I worked in the trenches. I would like to acknowledge my childhood friend Sydney Everratt, with whom I shared many fun excursions through out southern CA (and CO), and who most importantly reminded me that life is fun outside of academia (and the sterility of Irvine). I cannot overlook the great discussions and friendships I formed with older theory graduate students. In particular I thank Saswata Roy, Sree Ganesh Balasubramani, and Guo Chen who without hesitation would explain whatever concepts in quantum chemistry I would barge into their office with.

I would like to thank all current and past Burke group members, with whom I shared offices, coffee breaks, and cookies. I must specially thank Dr. Ryan Mccarty who was the best office mate I had, and who's surprisingly relentless optimism made group lunches and meetings more enjoyable. In addition, I must thank Ryan for all of the effort he put into helping pass my advancement exam. I would like to also thank Dr. Dennis Perchak, who's stories always put a smile on my face. His kind words during my exam also gave me some much needed encouragement.

Finally I must thank my family, whom I cherish dearly. My parents are my biggest cheerleaders, and I must thank my father for always pushing me to do my best, and reminding me that that "se hace camino al andar" whenever I was struggling. I would lastly like to thank my sister Maca, who I managed to talk with on almost a daily basis, even though we

were 9 time zones apart. Having the support of family truly is a privilege to which I am eternally grateful.

This dissertation contains verbatim excerpts as they appear in *Journal of Chemical Physics* and *Springer Nature*. Chapter 2 is reproduced from, F. Sagredo and K. Burke, *J. Chem. Phys.* **149**, 134103 (2018), with the permission of AIP Publishing. Chapter 4 is reprinted/adapted by permission from *Springer Nature*, *Frontiers of Quantum Chemisrty* by J. C. Smith, F. Sagredo, and K. Burke (2017). The co-authors listed in these publications directed, supervised, or conducted part of the research which forms the basis for the dissertation.

VITA

Francisca Sagredo

EDUCATION

Doctor of Philosophy in Chemistry	**2020**
University of California, Irvine	*Irvine, CA*
Master of Science in Chemistry	**2018**
University of California, Irvine	*Irvine, CA*
Bachelor of Science in Chemistry	**2015**
Florida International University	*Miami, FL*

RESEARCH EXPERIENCE

Graduate Research Assistant	**2016–2020**
Department of Chemistry, University of California, Irvine	*Irvine, California*
Year-round Intern	**2018–2020**
Center for Computing Research, Sandia National Laboratories	*Albuquerque, New Mexico*
Undergraduate Research Assistant	**2013**
Georgia Institute of Technology	*Atlanta, Georgia*
Undergraduate Research Assistant	**2013-2014**
Florida International University	*Miami, Florida*

TEACHING EXPERIENCE

Teaching Assistant, University of California, Irvine	*Irvine, California*
Density Functional Theory	**2018**
Idiom of Science	**2017**
Math for Chemists	**2016**
Honors General Chemistry	**2015-2016**

REFEREED JOURNAL PUBLICATIONS

Accurate double excitations from ensemble density functional calculations **2018**
F. Sagredo, K. Burke

J. of Chem. Phys., **149**, 134103

Confirmation of the PPLB derivative discontinuity: Exact chemical potential at finite temperatures **2020**
F. Sagredo, K. Burke

Submitted to J. Chem.Theory and Comput.

Construction of exact temperature exchange correlation functional for a model system **2020**
F. Sagredo, K. Burke

in preparation

An exchange correlation functional for bulk, solid, and confinement physics **2020**
F. Sagredo, A. Cangi, A. Mattsson

in preparation

TECHNICAL REPORTS

Semi-local Density Functional Approximations for Bulk Surface and Confinement Physics **2019**
A. Cangi, F. Sagredo, E. Decolvenaere, and A.E. Mattsson

United States: N. p, doi:10.2172/1569522

An Exchange-Correlation Functional for Bulk, Surface, and Confinement Physics **2018**
A. Cangi, F. Sagredo

Center for Computing Research Summer Proceedings 2018, Technical Report SAND2019-5093R

BOOK CHAPTERS

Warming up Density Functional Theory **2017**
J.C. Smith, F. Sagredo, K. Burke

Frontiers of Quantum Chemistry, Springer

The Local Density Approximation **2016**
F. Sagredo, J. P. Perdew

IPAM Book for DFT, submitted

AWARDS

UCI Faculty Mentor Fellowship honorable mention	**2016**
NSF GRFP Honorable mention	**2016**
Chemistry at the Space Time Limit (CaSTL) Diversity Fellowship	**2015**
NSF MDITR Scholarship Recipient	**2013**
Dean's List	**2012-2015**

LEADERSHIP

DECADE Chemistry student representative	**2017-2019**
Mentoring undergraduate students in research	**2019-2020**
Science in Action fellow	**2019**

PROGRAMING LANGUAGES/PACKAGES

Mathematica, Elk, Python

Full CV given upon request

ABSTRACT OF THE DISSERTATION

Developments in ensemble and finite temperature density functional theory using a model system

By

Francisca Sagredo

Doctor of Philosophy in Chemistry

University of California, Irvine, 2020

Professor Kieron Burke, Chair

This dissertation is an accumulation of my contribution to the fundamental understanding of ensemble Density Functional Theory and finite temperature Density Functional Theory, through the use of quantum model systems. Ensemble DFT is a time-independent method to extracting excitation energies, and provides a way to extract multiple excitations. Currently this is not possible with the common approximations used in time-dependent DFT. Chapter 3 of this thesis covers ensemble DFT and verifies an exact exchange approximation that can accurately capture multiple excitations using the Hubbard model. Finite temperature DFT is often incorrectly confused with ensemble DFT, and refers to DFT at non zero temperatures. Its value comes from its applications to warm dense matter simulations. The last three chapters of this dissertation contain several projects in the hopes of improving the understanding of finite temperature DFT. In particular it generalizes the PPLB derivative discontinuity model to finite temperatures, and discusses the construction of an exact finite temperature approximation. These contributions are done with the intention on enhancing warm dense simulations.

Chapter 1

Introduction and outline

Density Functional Theory (DFT) has become the most popular electronic structure method used to date in the fields of chemistry, physics, and material science with at least 30,000 publications cited per year [8]. However most of these papers pertain to ground state, Kohn-Sham (KS) DFT [59, 81], which it is calculated at zero temperature. Naturally this is the case, considering that most calculations look to extract the ground state energies and properties from a given system, which give rise to things like bond lengths and lattice constants.

Over the past decade, substantial progress has been made in the fields of ensemble Density Functional Theory (DFT) and finite temperature DFT, both theories extending past the ground state. Still, a large amount of confusion arises between the two subfields. Mixing of the two theories leads to errors in concepts- and a cause for concern. Both fields arose from different but closely related theories, and hence "live on the same street". However, while being similar in nature, they have different founding papers (therefore live in different houses) and applications. Below, their distinction and relevance is described. Having contributed to both fields, many discussions lead to the same confusions, which lead to the realization that this distinction is not well understood. The use of quantum model systems, in particular, the truncated two site Hubbard model has aided in this clarification. Quantum model systems are a theoretician's tool that provide clear fundamental insight, which is often not possible in more realistic molecular systems. Such insights provide a perfect testing ground needed to make fundamental improvements in the theory. For the work included in this thesis that uses the truncated Hubbard model. The Uniform Electron Gas (UEG) is also discussed briefly in chapter 2. The rest of my graduate work at Sandia National Labs which is not included in this thesis also used quantum model systems, mainly the airy gas, harmonic oscillator gas, and UEG. Below, brief descriptions of ensemble DFT and finite temperature DFT is described, with clear distinctions.

1.0.1 Finite temperature DFT

Finite temperature DFT was originally proposed by Mermin [60], and is a generalization of the Hohnberg-Kohn theorem in ground state DFT to finite temperatures. In this original paper, Mermin specifies the use of the grand canonical ensemble such that the system is attached to a thermal bath, and therefore the particle number fluctuates. In other words, it generalizes the ground state theory, where the chemical potential is normally fixed (and thus the particle is fixed) to include varying particle number. Its applications are relevant to warm dense matter simulations.

Warm dense matter is a high energy density regime, that is not strictly defined. Essentially it is a gray area between condensed matter physics, and plasma physics. Relatively high densities (up to 1000 times denser than condensed matter) and temperatures ($10^4 - 10^7 K$) encapsulate this region. Thus, its understanding and simulation are of the national interest. In particular, warm dense matter is important to understanding planetary cores[101], inertial confinement fusion capsules, and weapons [101, 112, 95, 75, 74, 77, 61, 73, 132, 149, 50]. Using finite temperature DFT in conjunction with MD simulations are vital to understanding warm dense matter, since often experiments are not technologically advanced enough. For instance, an inertial confinement fusion capsule might explode at ignition, before all required measurements are taken, and thus extrapolation of data is required. The inability to experimentally check planetary cores, say Jupiter's core, also shows the necessity of theoretical simulations.

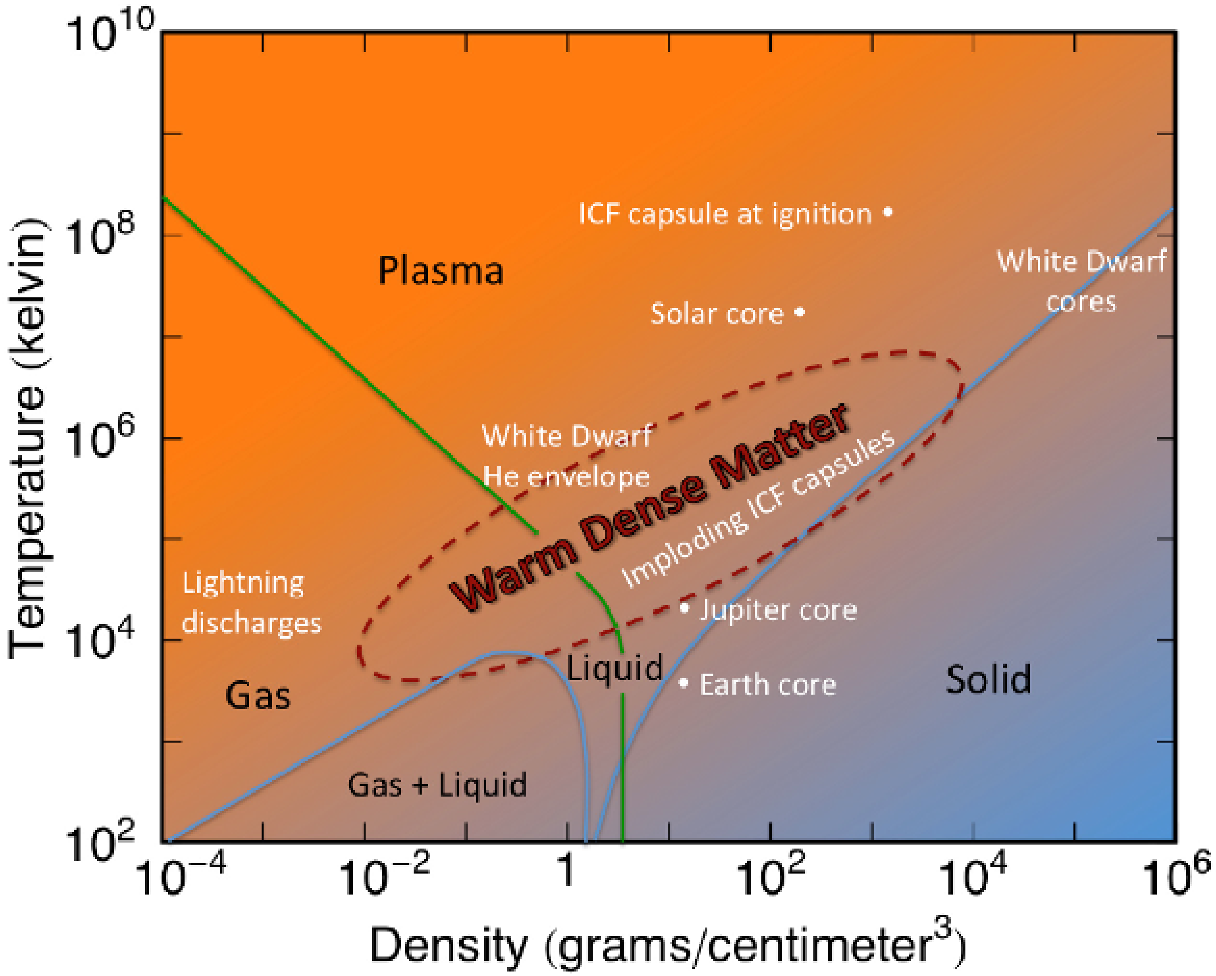

Figure 1.1: Warm dense matter regime. Figure replicated from Ref.[1]

1.0.2 Ensemble DFT

Ensemble DFT came from a generalization of Theophoiou's work on the a variational principle for excited states of wavefunctions. Gross, Olivera, and Kohn (GOK) extended this work to DFT in the 1980s [53]. The purpose of ensemble DFT is to provide a time *independent* alternative to time-dependent DFT. While time-dependent DFT has become the "go to" quantum tool to extract oscillator strengths, and excitation energies, it still has many deficiencies. One of these great pitfalls includes the inability to capture multiple excitations, that is more than one electron in an excited state. Multiple excitations are important in many relevant molecular systems, particularly those of conjugated organic molecules and photochemistry [98, 30, 159, 90, 165]..

Ensemble DFT is often wrongly confused with finite temperature DFT. This is due to many reasons, and partly semantics since finite temperature DFT uses "thermal ensembles". However there is a clear distinction- GOK ensemble DFT occurs *at* zero temperature, and ensembles are of fixed particle number (i.e., canonical ensemble). In addition, the ensemble weights in ensemble DFT are the same in the KS system and the interacting system, and can simply be picked. This is not the case in finite temperature DFT, where the the KS "thermal weights" correspond to the fermi weights, which are naturally temperature dependent and clearly different than those of the interacting system.

1.1 Outline

Chapter 2 covers the first density functional approximation proposed, the Local Density Approximation (LDA). This chapter is part of a book on DFT from a conference hosted by the Institute of Pure and Applied Mathematics (IPAM), at the University of California, Los Angeles. LDA is the most crude functional approximation available, yet its construction still provides some vital insight into the basics of DFT and the construction of functional approximations. LDA is also constructed on the Uniform Electron Gas, a quantum model system.

Chapter 3 includes an ensemble DFT project, which confirmed an exact exchange ensemble DFT approximation using the Hubbard model. This approximation can extract double excitations, which cannot be done using the adiabatic approximation in time dependent DFT by construction.

In chapter 4 finite temperature DFT is more formally introduced in a book chapter that appeared in “Frontiers of Quantum Chemistry”. It provides a review of the field, and current limitations in the fundamental theory.

Chapter 5 is a recent submission and another project within the realm of finite temperature DFT. Here we generalized an approximation from a fundamental theory in DFT that was intended for the zero temperature limit and successfully applied it finite temperature systems. We also show how it is possible to extract free energies that are often required in warm dense matter simulations.

In chapter 6, we conclude with the most recent finite temperature DFT project- the construction of a temperature dependent functional approximation. This project is not yet published, but shows many promising results that are introduced in the chapter.

Chapter 2

The Local Density Approximation

This chapter was written with Professor John P. Perdew. It is from a DFT book written for the "Putting the Theory Back into DFT" conference hosted by the Institute of Pure and Applied Mathematics (IPAM) at the University of California, Los Angeles in 2016. I contributed to writing in this book chapter.

2.1 Abstract

The earliest approximation to the density functional for the exchange-correlation energy is the local density approximation (LDA) of Kohn and Sham 1965. It is also the basis for most of those that followed. LDA was constructed to be exact for any uniform density, but it worked surprisingly well for real solids and to a lesser extent for real atoms and molecules. This was explained by LDA's satisfaction of "hidden universal exact constraints" on the exchange-correlation hole and later on the energy. The local spin density approximation, which adds the spin polarization as an ingredient while preserving the exact constraints, was found to be more accurate than LDA. These facts suggested a strategy to make better

approximations by adding ingredients and satisfying more exact constraints.

2.2 Introduction

The original local density approximation (LDA) was proposed alongside the KS equations in the 1965 paper by Kohn and Sham [81]. It was much better than the simplified Hartree approach. LDA provides the basis for many methods that followed later, such as generalized gradient approximations (GGAs), meta-GGAs, and hybrid functionals, as we will see in later chapters and in the well known Jacob's ladder. Not only do those approximations reduce to LDA for densities that are uniform over space, but they can be constructed non-empirically via a strategy suggested by the effort to understand why LDA worked better than expected: Approximations can be improved by adding more ingredients and satisfying more exact constraints.

2.2.1 Background

As we have seen, in the Kohn-Sham density functional theory (DFT) it is possible to find the exact ground-state energy and electron density of a many electron system by solving the self-consistent one-electron equations [81], if we know the exact exchange and correlation(xc) functionals $E_{\text{XC}}[n]$ or $E_{\text{XC}}[n_\uparrow, n_\downarrow]$. Although in practice we must approximate these functionals, the majority of the 30,000 papers published every year [8] that use DFT also use these approximations. The exact theory tells us that there is an exact density functional to be approximated. It also provides exact constraints and appropriate norms to guide the construction of the functional. Here we define an appropriate norm as a system whose energy can be computed exactly, and for which a given approximate form should be exact or nearly exact. In particular, the uniform electron gas is an appropriate norm for LDA and for other functionals based upon LDA.

As previously noted, the exchange-correlation energy makes up a rather small portion of the total energy of the system, although it provides a vital contribution to the energy differences of interest in both chemistry and physics. For example, if we make the approximation $E_{\mathrm{XC}}[n] = 0$, we are, in a way, doing a Hartree approximation but without the Hartree self-interaction correction. This was the approach that was originally used in solid state physics in the 1950's and 60's. As expected this gives a terrible approximation for lattice constants and bond lengths, about 10-20 percent larger than the exact, and also makes the binding energies of atoms much smaller than they actually are. Here the electrons bind to the atoms due to the external potential, but the atoms themselves bind to other atoms in an unrealistically weak way because of this neglect of $E_{\mathrm{XC}}[n]$. In other words we can see the importance of the approximation used for E_{XC} since it describes the bonding of atoms to one another, and thus the exchange-correlation energy can be considered nature's glue [84].

2.2.2 The Local Density Approximation

It so happens that the LDA is a much more realistic approximation than setting $E_{\mathrm{XC}}[n] = 0$, which will be explained later. The LDA is expressed as:

$$E_{\mathrm{XC}}^{LDA}[n] = \int d^3r n(\mathbf{r}) \epsilon_{\mathrm{XC}}^{unif}(n(\mathbf{r})), \tag{2.1}$$

where $\epsilon_{\mathrm{XC}}^{unif} n(\mathbf{r}) < 0$ is the exchange and correlation energy per particle in an electron gas with uniform density, n. This is a Thomas-Fermi like approximation, which is exact when the electron density is uniform and accurate when the density is slowly varying over space , as seen in (2.2).

$$\frac{|\nabla n|}{n} \ll k_f = (3\pi^2 n)^{1/3}, \frac{|\nabla n|}{n} \ll k_s = \frac{2}{\pi^{1/2}}(3\pi^2 n)^{1/6}. \tag{2.2}$$

Here k_f is the Fermi wave vector, and k_s is the inverse of the Thomas-Fermi screening length. We use atomic units, $\hbar = e^2 = m = 1$.

Kohn and Sham did not expect much out of this approximation for real atoms, molecules, and solids, only that it should be more accurate than using $E_{\text{XC}}[n] = 0$. Surprisingly LDA was found to give huge improvements for lattice constants of solids, phonon frequencies, metal surface energies [86], molecule geometries, etc. [111]. Naturally, the question that arises is: Why is the LDA such a realistic approximation, since virtually nothing has a uniform density? The answer was later found to be [87, 55] that LDA satisfied hidden exact constraints that are true for all systems (that is with any external potential, $v(\mathbf{r})$), not just the uniform gas as it was originally thought. This is further shown in the next section.

2.2.3 Constraints

The exact xc energy is the Coulombic interaction between electrons and the xc holes that surround them. This is expressed as [87, 55]

$$E_{\text{XC}}[n] = \frac{1}{2}\int d^3r \int d^3r' \frac{n(\mathbf{r})n_{\text{XC}}(\mathbf{r},\mathbf{r}')}{|\mathbf{r}'-\mathbf{r}|}. \tag{2.3}$$

We define $n(\mathbf{r})$ as the electron density at $\mathbf{r}$, and likewise $n_{\text{XC}}(\mathbf{r},\mathbf{r}')$ as the density at $\mathbf{r}'$ of the xc hole, the personal space around an electron at $\mathbf{r}$. The exchange-correlation hole density $n_{\text{XC}}(\mathbf{r},\mathbf{r}')$ is actually an average over coupling constant, and not the hole at the physical coupling constant.

Although we cannot evaluate the electron hole density very accurately from the electron density, it is possible to derive some theorems which are simply described below. First the hole density n_{XC} is defined as the sum of the exchange and the correlation part, where $n_{_C}$ is averaged over correlation coupling constant as previously mentioned.

$$n_{\text{XC}}(\mathbf{r},\mathbf{r}') = n_{\text{X}} + n_{_C} \tag{2.4}$$

We note that there are two effects that keep electrons away from one another. The first is the Pauli exclusion principle for fermions, which makes an exchange hole around each electron. The second reason electrons avoid each other is because of the electron-electron Coulomb repulsion which makes a correlation hole.

- The exchange hole density is always negative because, around a given electron, one is missing, and thus if we are to place an electron at point $\mathbf{r}$ it will not be at the point $\mathbf{r}'$.

  $$n_{_X} \leq 0. \tag{2.5}$$

- The integral of the exchange density hole is always -1, again because around a given electron one is missing so

  $$\int d^3r' n_{\text{X}}(\mathbf{r},\mathbf{r}') = -1. \tag{2.6}$$

- The integral of the correlation density hole is always 0, because when electrons are pushed away from a given electron they tend to pile together further away.

$$\int d^3r' n_{_C}(\mathbf{r},\mathbf{r}') = 0. \tag{2.7}$$

Equations 2.5, 2.6, and 2.7 express the hole constraints. Because the LDA $n_{\text{XC}}(\mathbf{r},\mathbf{r}')$ is the same as the $n_{\text{XC}}(\mathbf{r},\mathbf{r}')$ of the uniform electron gas of the same given density at $\mathbf{r}$, LDA satisfies these three constraints. This makes LDA a much more accurate approximation than expected. If $n_{\text{XC}}(\mathbf{r},\mathbf{r}')$ did not satisfy those constraints, then Eq. (3) would be quite uncontrolled for non-uniform densities. It should also be noted that $n_{\text{XC}}(\mathbf{r},\mathbf{r}')$ is in fact not accurate pointwise for LDA, but is more accurate for the system and spherical averages that determine the exchange-correlation energy [55], due to error cancellations that occur reliably because of its satisfaction of the hole constraints. Now to compute LDA we need to know the xc energy $\epsilon_{\text{X}}^{unif}(n)$,

$$\epsilon_{\text{XC}}^{unif}(n) = \epsilon_{\text{X}}^{unif}(n) + \epsilon_{_C}^{unif}(n), \tag{2.8}$$

where the exchange energy part can be determined analytically because the uniform gas has KS orbitals that are plane waves and the energy is simply determined by integrating over plane waves,

$$\epsilon_{\text{X}}^{unif}(n) = -\frac{3}{4\pi}k_f = -\frac{3}{4\pi}(3\pi^2 n)^{1/3}. \tag{2.9}$$

The correlation energy is more difficult to determine since it is based on the physical ground state wave function of the electron gas. The Wigner approximation was the first one used

[?]. Here r_s is a distance- the radius of a sphere that contains one electron on average, which is also known as the Wigner-Seitz radius, and can be defined as $r_s = (3/4\pi n)^{1/3}$. This approximation is qualitatively correct at the high- and low-density limits .

$$\epsilon_C^{unif-Wigner}(n) = \frac{-a}{b + r_s}; n = \frac{3}{4\pi r_s^3}, \tag{2.10}$$

$$r_s \to 0 : \epsilon_C^{unif-Wigner}(n) \to \frac{-a}{b}, \tag{2.11}$$

$$r_s \to \infty : \epsilon_C^{unif-Wigner}(n) \to \frac{-a}{r_s}. \tag{2.12}$$

It should also be noted that $\epsilon_C^{unif}(r_s)$ can be extracted from accurate quantum Monte Carlo calculations [20]. The result has been parametrized to match analytically known high- and low-density limits [56, 168].

Even though the exact exchange energy can be computed from the Kohn-Sham orbitals, it is not a good idea to combine it with a local or semilocal approximation for correlation. In molecules and other multi-center systems, there is a strong error cancellation between local or semilocal approximations for exchange and the corresponding approximations for correlation. That is because the exact exchange-correlation hole is deeper and more localized than the exact exchange hole and correlation hole are separately, and thus more amenable to a local or semilocal approximation.

Note that our arguments for the accuracy of a local or semilocal approximation for the exchange-correlation energy do not justify a local (Thomas-Fermi) or semilocal approximation to the non-interacting kinetic energy, which is always treated exactly in Kohn-Sham theory.

2.2.4 Brief Note on LSDA

It should be noted that in practice the local spin density approximation (LSDA) is used [166]. For a spin-unpolarized density it is the same as LDA. For spin-polarized systems, LSDA is a much better approximation especially for atoms, radical molecules or magnetic solids. In other words, if you add more information to your approximation, you will also get more information out of it.

$$E_{\mathrm{XC}}^{LSDA}[n_\uparrow, n_\downarrow] = \int d^3r n(\mathbf{r}) \epsilon_{\mathrm{XC}}^{unif}(n_\uparrow(\mathbf{r}), n_\downarrow(\mathbf{r})). \tag{2.13}$$

Here the $\epsilon_{\mathrm{XC}}^{unif}(n_\uparrow, n_\downarrow)$ is the exchange-correlation energy per particle of an electron gas with uniform spin densities $n_\uparrow$, $n_\downarrow$. Again, we can also write the LSDA functional in terms of the exchange and correlation hole,

$$E_{\mathrm{XC}}^{LSDA}[n_\uparrow, n_\downarrow] = \frac{1}{2} \int d^3r \int d^3r' \frac{n(\mathbf{r}) n_{\mathrm{XC}}[n_\uparrow, n_\downarrow](\mathbf{r}, \mathbf{r'})}{|\mathbf{r'} - \mathbf{r}|}. \tag{2.14}$$

For the total exchange-correlation energy of an atom or molecule, LSDA underestimates the magnitude by about 10% for small atomic number, and its relative error decreases with increasing atomic number. LSDA overestimates the binding energies between atoms, and underestimates the bond lengths and lattice constants by typically 2%. Thus LSDA is still useful in itself, especially for solids to which its uniform-gas appropriate norm is more relevant. More importantly, LSDA defines a good starting point for later advances in functional approximation.

2.3 Acknowledgments

JPP acknowledges the support of the National Science Foundation under Grant No, DMR-1607868. FS kindly acknowledges support from the US DOE, Award No. DEFG02-08ER46496.

Chapter 3

Accurate double excitations from ensemble density functional calculations

This chapter was replicated from Ref.[137]. It is part of the project on ensemble DFT. It was written in conjunction with my advisor Kieron Burke. I contributed to making figures and writing this paper. Here the truncated Hubbard model is used to check an exact exchange approximation within ensemble DFT, which promises the extraction of double excitations.

3.1 Abstract

The recent use of a new ensemble in density functional theory (DFT) to produced direct corrections to the Kohn-Sham transitions yields the elusive double excitations that are missed by time-dependent DFT with the standard adiabatic approximation. But accuracies are lower than for single excitations, and formal arguments about TDDFT suggest that a correction

kernel is needed. In principle, EDFT with direct corrections at the exchange level must yield accurate doubles in the weakly correlated limit. We illustrate with exact calculations and analytic results on the Hubbard dimer. We also explain the error in formal arguments in TDDFT.

3.2 Introduction

Time-dependent density functional theory (TDDFT) is a popular tool for calculating electronic excitations[135, 16, 100, 161], but with current approximations, has some severe limitations. Within the adiabatic approximation used in almost all practical calculations and all standard codes, double (and multiple) excitations are entirely missed by TDDFT[97]. While in some cases these can be recovered in an ad-hoc fashion using dressed TDDFT [65, 17], which approximates the frequency dependence, there is no general procedure for capturing these relevant excitations.

On the other hand, ensemble DFT (EDFT) is almost as venerable, but is much less used[53, 34, 113]. Unlike TDDFT, which employs linear response around the ground-state to deduce excitation energies, EDFT is based on a variational theorem of ground and excited states (with monotonically decreasing weights), from which individual transition frequencies can be deduced. Using the original ensemble of Gross, Oliveria, and Kohn (GOK) [53], there has been much formal progress over three decades, but accurate approximations have been difficult to develop. An important step forward came with the identification of ghost-interaction errors, and their removal in the work of Papaconstantinou, Gidopoulos, and Gross[106], and in using the symmetry-adapted Hartree-exchange[174, 129], now referred to as the ensemble exact exchange (EEXX)[49]. Furthermore, new work in the generalized adiabatic connection, and the investigation of charge transfer within EDFT [41, 48], as well other recent contributions[107, 108, 155, 2] have all been important to push EDFT forward. But these recent publications rarely focus on double excitations, except in Ref.[173].

In Ref.[173], an alternative ensemble (GOK II) was examined, which has several formal and practical advantages. The GOK ensemble has the same weight for each state, except for its highest multiplet, while the GOK II ensemble also has the same ensemble weight for each state, except for its ground state. Moreover, using the exact-exchange approximation (EEXX) mentioned, and taking the weights of excited states to (almost) zero, Ref.[173] found a simple direct ensemble correction (DEC) to Kohn-Sham transition frequencies, analogous to expressions in TDDFT. Preliminary tests on atoms and a simple model (1D Hooke's atom) showed that, for single excitations, results were comparable to or better than standard TDDFT results. More importantly, double excitations were predicted by the new method, but substantially less accurately than for singles in every case.

While Ref. [173] made progress in understanding EDFT, both in developing the theory and testing it on atoms and a model system, it left an important question unanswered. All test cases had single excitations close to the double excitations, and were chosen to ensure this was the case. This is the condition needed to apply dressed TDDFT, but is not generic. Moreover, in these tests, the accuracy of the double excitations from EDFT was about half of that when compared to single excitations.

It has long been claimed that, by truncating the response equations of linear-response TDDFT with the exchange kernel, the results agree exactly with DFT perturbation theory, both for two electrons[39] and more generally[46]. But for two electrons, the exchange kernel is frequency-independent, and so cannot produce double excitations. The frequency-dependence needed to produce double excitations requires correlation contributions to the kernel in TDDFT[14]. This would imply that double excitations require some correlation contribution to be accurate. But the DEC/EEXX approximation in EDFT is a purely exchange term, so how can it produce these double excitations?

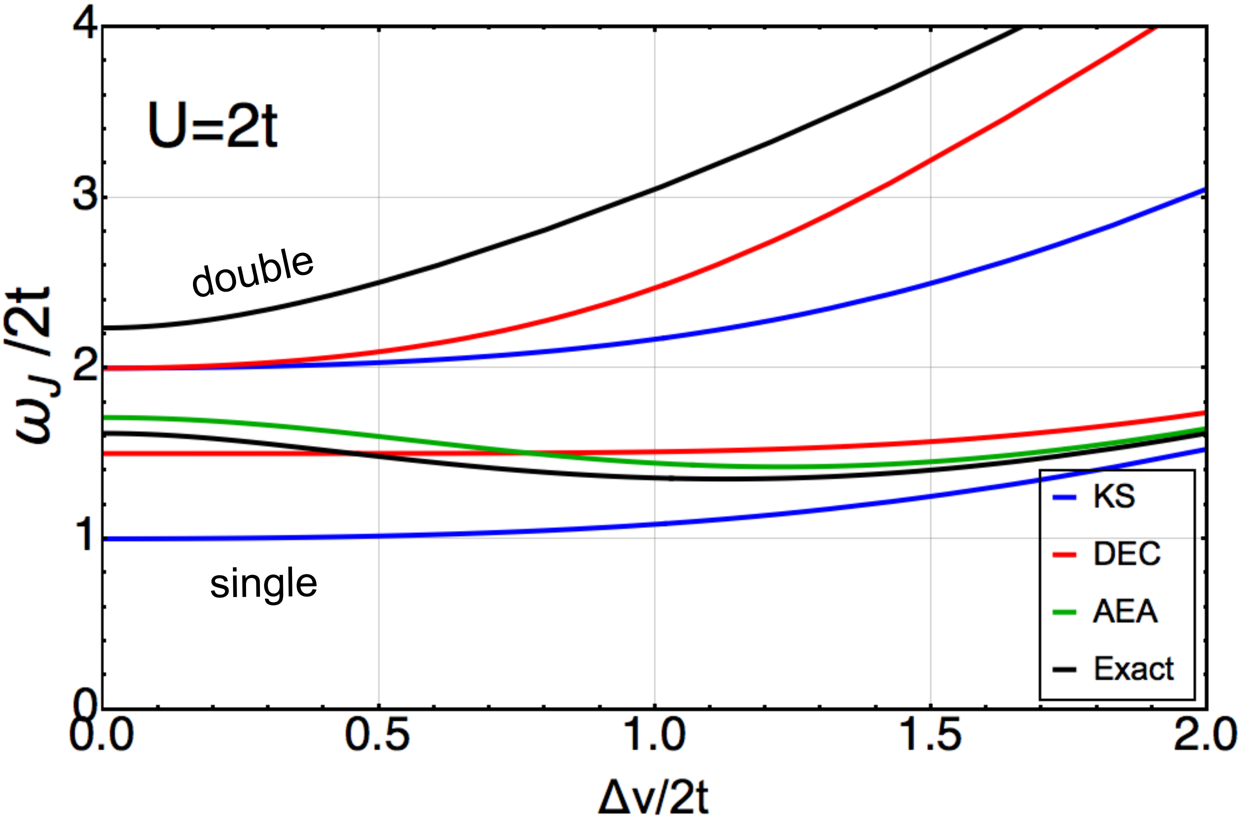

Figure 3.1: Transition frequencies versus onsite potential difference for the weakly correlated Hubbard dimer at with $2t = 1$. The exact many body solution (black) for single (bottom four curves) and double excitation (top three curves) are compared against the Kohn Sham (KS), Adiabatically Exact Approximation (AEA), and Direct Ensemble Correction (DEC).

The present work addresses the question: Does the DEC method of Ref.[173] really produce a useful path toward calculating double excitations, or are their results more-or-less accidental? More precisely, is there any limit in which their method becomes exact for double excitations?

We answer these questions with calculations on a simple model, the asymmetric Hubbard dimer, which provides explicit analytic results, and an in depth analysis of the errors that is not currently possible on larger, more realistic systems. Our principal results are shown in Fig. 3.1, and described in detail within. While DEC in EDFT and adiabatic TDDFT both yield accurate results (but not everywhere) for the first single excitation, only DEC makes a prediction for the double, and is typically accurate for weakly correlated systems. We find a substantial exchange correction to the Kohn-Sham transition of the double-excitation, except in the symmetric case. We also explain the connection with TDDFT, and the relation among various expansions in powers of the coupling constant. Finally, we explain why correlation is needed to find double (and multiple) excitations in TDDFT, but not in EDFT.

3.3 Background

3.3.1 Görling-Levy perturbation theory

Görling-Levy (GL) perturbation theory [47] is the appropriate tool for studying the coupling-constant dependence of individual eigenenergies in DFT for weakly-correlated systems. Expanding the energy of the $J-th$ many-body state in powers of λ, the electron-electron repulsion, while keeping the density fixed (the adiabatic connection[91, 47]), one finds

$$E_J = E_J^{(0)} + \lambda \Delta v_{JJ} + \lambda^2 \left(\sum_{J' \neq J} \frac{|v_{c,J'J}|^2}{E_{J'}^{(0)} - E_J^{(0)}} - v_{c,J,J} \right), \tag{3.1}$$

where $E_J^{(0)}$ is the sum of KS eigenvalues of the occupied orbitals in the $J-th$ many body state, v_{JJ} is the expectation value of the electron-electron repulsion operator minus the Hartree and exchange potentials [175], and $v_{c,J,J}$ is the expectation of the 2nd-order correlation potential. Here we label excitations by the level of the excitation of the adiabatically connected KS determinant relative to the occupation of the KS ground state [14].

3.3.2 Time Dependent DFT

TDDFT yields transition frequencies via linear response. The exact density-density response function is

$$\chi(\mathbf{r}, \mathbf{r}', \omega) = \sum_{J\neq 0} \frac{m_J(\mathbf{r})\, m_J^*(\mathbf{r}')}{\omega - \omega_J + i0_+} + c.c.(\omega \to -\omega), \tag{3.2}$$

where $m_J(\mathbf{r}) = \langle 0|\hat{n}(\mathbf{r})|J\rangle$, $\hat{n}(\mathbf{r})$ is the density operator, and transitions occur at its poles [100]. The KS counterpart is its value when $\lambda \to 0$, keeping the density fixed. Then the wavefunctions become single Slater determinants (typically), and the difference in the inverse of the two response functions is called the Hartree-exchange-correlation kernel[14]. Because the density is a single-particle operator, $m_J^{(0)}(\mathbf{r}) = 0$ unless J is a single-particle excitation, i.e., double excitations do not appear in the KS response. If the kernel is then approximated as frequency-independent (called the adiabatic approximation), it does not affect the pole-structure, so the approximated response has only single excitations. In the specific case of two electrons whose ground-state is a singlet, the exchange kernel is static. Thus, correlation effects (at least second-order in λ) are needed in the TDDFT kernel to extract double excitations. In the approximate kernel of dressed TDDFT, which applies only to doubles that are strongly coupled to singles, the Hamiltonian is evaluated between KS determinants [98, 18], yielding a numerator in the approximate kernel that is second-order in the electron-electron repulsion.

In a generic electronic system, there are many more double excitations than single excitations, and these doubles may or may not be strongly coupled to a particular single excitation. However, in Coulomb systems, there are strong patterns in the positioning of excitations in the spectrum. For example, all double excitations in the He atom are in fact auto-ionizing resonances in the continuum. For small molecules, double excitations that are optically allowed are often close to a single excitation, and for these, the theory of dressed TDDFT yields a practical approach, and hence there are more results for such double excitations using TDDFT in the literature and only those cases were studied in Ref. [173]. The conundrum about this state of affairs is very simple. If double excitations have contributions to first-order in the coupling-constant, then why are correlation contributions needed in the TDDFT kernel in order to find them?

3.3.3 Ensemble DFT

Ensemble DFT is based on a variational principle for ensembles that are a mixture of the lowest M electronic eigenstates, for a chosen set of weights $\mathbf{w} = \{w_J\}_{J=0\ldots M-1}$ that are normalized and monotonically decreasing. Just as in ground-state DFT, one can define $F_{\mathbf{w}}[n]$ which, when added to the external potential and minimized over (ensemble) densities, yields the ensemble energy [53, 34, 113]. The GOK ensemble has weight w for the highest state, and all others chosen equal. One can also define an ensemble KS system of non-interacting electrons by using the same ensemble and the correct minimizing ensemble density. The change in $F_{\mathbf{w}}$ between interacting and non-interacting defines the ensemble Hartree-exchange-correlation energy $E_{_{HXC},\mathbf{w}}[n]$, whose functional derivative yields the corresponding contribution to the KS potential.

One complication of EDFT is that a range of values of w is allowed (as long as normalization is possible), and the total energy of the system E_w is exactly linear with respect to w, so its slope is related to the transition frequencies of the system. For a bi-ensemble of a ground and first excited state, the slope is simply the transition frequency between them. In practice almost all approximations lead to non-linear behavior with w, leading to different predictions depending on the value of w chosen. The (traditional) Hartree energy, being quadratic in the density, has unphysical cross-terms proportional to $w_J w_{J'}$, which are referred to as ghost interaction errors. The careful removal of these errors from Hartree and exchange together yields greatly increased accuracy [106]. Most recently, this ensemble exact exchange (EEXX) [49] has been shown to be the correct (energy-minimizing) choice to first-order in the interaction.

Ref.[173] used an alternative ensemble suggested by GOK (called GOK II), in which each state in the ensemble has weight w, except the ground state. They also considered the limit as $w \to 0$, thereby using only the slope around $w = 0$, yielding a unique answer that is simply a correction to the ground-state KS transitions, i.e., there is no need to do an additional self-consistent cycle for $w \neq 0$. Finally, they also noted that, for the GOK II ensemble, within EEXX, this direct energy correction requires only energy differences between the level of interest and the ground state (and not all intervening states, as is otherwise the case). Plugging in the EEXX into the DEC approximation, and in the absence of degeneracies:

$$\Delta\omega_J^{EEXX} = \lambda(H_J - H_0) \tag{3.3}$$

where H_J is an exchange contribution depending only on the KS orbitals and energies of the J-th state(Eq.(9) of Ref.[173]). They also calculated both single and double excitations for a series of atoms and ions, and for the 1D Hooke's atom. In all cases, the DEC/EEXX yielded single excitations with accuracy comparable to that of TDDFT with standard approximations, while double excitations were also predicted, but with less accuracy. The errors were ascribed to correlation effects missed by DEC/EEXX.

3.3.4 Hubbard dimer

The Hubbard model is a paradigm of strongly correlated physics, and typically consists of an infinite lattice, with hopping and site-interaction terms [64]. The dimer is likely the smallest meaningful model of interacting fermions, with a Hilbert space of just 6 states[15]. It mimics strong correlation effects of bond stretching, but is not a quantitatively accurate model for any first-principle Hamiltonian. In its usual form, it is a simplified version of a minimal-basis model of two electrons on two atoms, with one basis function per atom. The Hamiltonian is

$$\hat{H} = -t \sum_{\sigma} (\hat{c}^{\dagger}_{1\sigma}\hat{c}_{2\sigma} + h.c) + U \sum_{i} \hat{n}_{i,\uparrow}\hat{n}_{i,\downarrow} + \sum_{i} v_i \hat{n}_i. \tag{3.4}$$

Here t is the electron hopping energy, U is the the repulsion between the particles in each site, and the symmetry of the dimer is controlled by the potential difference, $\Delta v = v_2 - v_1$, and the density is characterized by a single number, $\Delta n = n_1 - n_2$. The Hubbard dimer is extremely useful for understanding ground-state DFT [15], especially when correlations are strong, and extensions and variations have been used in many time-dependent problems to understand TDDFT. Its value comes from the ability to solve most problems analytically. Because the double excitation in the dimer is never close to the single excitation, dressed TDDFT cannot be applied [14]. A full discussion of how linear-response TDDFT works for the dimer has just been completed[14]. Recently, the dimer has been used to illustrate EDFT weight-dependence[27], novel approaches to band gaps[144], and approaches to noncollinear magnetism [162].

3.4 Theory

Above, we have given three different formalisms that yield excitation energies with different types of DFT theories. If implemented exactly, they must all yield the same answers. Moreover, the transition frequencies, when expanded in powers of the electron-electron coupling constant, must be the same, term-by-term. However, when approximations are used, such as EEXX in DEC or the adiabatic approximation in TDDFT, there is no such guarantee.

The simplest to compare are the GL perturbative expansion, and the DEC in EDFT. If the EEXX truely yields the exact exchange contribution to any excitation, it must agree with GL to first-order in the coupling constant, for any excitation. In Ref. [173], it was referred to as symmetry-eigenstate Hartree-exchange, as a sensible choice was made for the ensemble eigenstates. It has since been argued[49] that this choice minimizes the ensemble energy, and so should always yield the correct answer (to leading order in the coupling constant).

Below, we confirm that indeed all three approaches agree for the Hubbard dimer, finding the next corrections and explaining the complexities of the kernel in TDDFT that are needed to recover this result.

3.5 Results

Here, we study only singlet states, avoiding the complexities of spin-flipping transitions. There are then only 2 transitions, one to a single and one to a double excitation (the nature of a transition is determined by adiabatically turning off the interaction and labelling it based on its KS determinant). There are two parameters: Δv measures the degree of asymmetry, while U measures the strength of the interaction. When $\Delta v = U = 0$, the dimer is a symmetric, tight-binding problem. When $\Delta v/(2t)$ grows large, the dimer is highly asymmetric, with both particles mostly on one site (in the ground state); when $U/(2t)$ grows large, the dimer has strong correlation effects, just like when a bond is stretched, and many ground-state density functional approximations fail. For $\Delta v = 0$, the expansion about weak correlation diverges at $U = 4t$, while the λ-dependence is found by replacing U by λ for a fixed Δn.

Many of the most important results of this study appear in Fig. 3.1. The solid black lines are the analytic results for the single (lower) and double (higher) excitations [12, 15, 26, 14]. The value $U = 2t$ is chosen to be a significant correlation strength, but still in the weakly-correlated regime. The blue lines are the corresponding KS transitions, with the double at exactly twice the single. These are the exact KS transitions, meaning the transitions between occupied and unoccupied KS orbitals of the exact ground-state KS potential, found from the functional derivative of the exact ground-state XC energy[15].

There are many lessons in this figure. As is typical for weakly correlated systems, the KS transition frequencies are a reasonable zero-order approximation to the exact optical excitations[10]. We define $\Delta\omega_J = \omega_J - J\omega_s$ as the difference between the exact and KS transition frequency. We also note that the accuracy of the KS transitions is not uniform with Δv. At $\Delta v = 0$ (the symmetric case), $\Delta\omega_2 < \Delta\omega_1$. But, as Δv grows, and especially when $\Delta v > U$, the single excitation energy curve approaches its KS alterego, but the double excitation does not. This is because, in the charge transfer regime when $\Delta v > U >> 2t$, both electrons are on the same site for the ground state (e.g. site 1), on opposite sites for the first excitation (and also not interacting), whereas for the double, both electrons are again one site (site 2). The reverse is true for the Mott-Hubbard regime, defined for the region of $U >> \Delta v >> 2t$

Next we consider TDDFT within the adiabatically exact approximation (AEA). The extremely small Hilbert space means the response function is not a matrix but a single function

[14] that vanishes at each excitation:

$$\chi^{-1}(\omega) = \chi_{\rm S}^{-1}(\omega) - f_{HXC}(\omega). \tag{3.5}$$

If f_{HXC} is ignored, transitions occur at $\omega = \omega_s$. If $f_{HXC}(\omega = 0)$ is used (AEA), it shifts the positions of the single excitations, but still misses all higher excitations. This is the best possible performance of the adiabatic approximation, because we used the exact ground state functional to determine $f_{HXC}(\omega = 0)$. This produces the green curve for the single excitation in Fig. 3.1. We see that AEA is extremely accurate and becomes even more so as the asymmetry is increased. Notice that the AEA becomes accurate as correlations weakens, because the coefficient of the numerator of the pole in $f_{\rm XC}(\omega)$ is of the order $O(\lambda^2)$, so its effect on the position of the single excitation vanishes[14] as $\lambda \to 0$. But there is no analogous curve for the double excitation, as there is no way to access the double within linear-response TDDFT without a frequency dependent kernel. (Even higher-order perturbation theory can at most yield doubles that are twice the singles, which would not be accurate [160]).

Next we apply EDFT to the dimer. The results for the ground state and first single excitation are well-known [15, 26], because they can be extracted from a bi-ensemble of the ground and first excited states, where there is no difference between the GOK and GOK II ensembles. But to extract the double excitation we use a three state GOK II ensemble. Applying the DEC/EEXX to the GOK II ensemble, with the exact KS eigenstates of the Hubbard dimer, i.e, Eq. (3.3) we find:

$$\Delta\omega_1^{DEC} = \frac{U}{2}\left(1 - \frac{\Delta n^2}{4}\right), \quad \Delta\omega_2^{DEC} = \frac{U}{2}\Delta n^2. \tag{3.6}$$

These results agree perfectly with Eq.(3.1), applied to the dimer and expressed in terms of the ground-state density [14]. These yield the red lines in Fig.3.1.

To analyze and expand on these results, in Fig. 3.2 we directly plot $\Delta\omega_J$ for each transition.

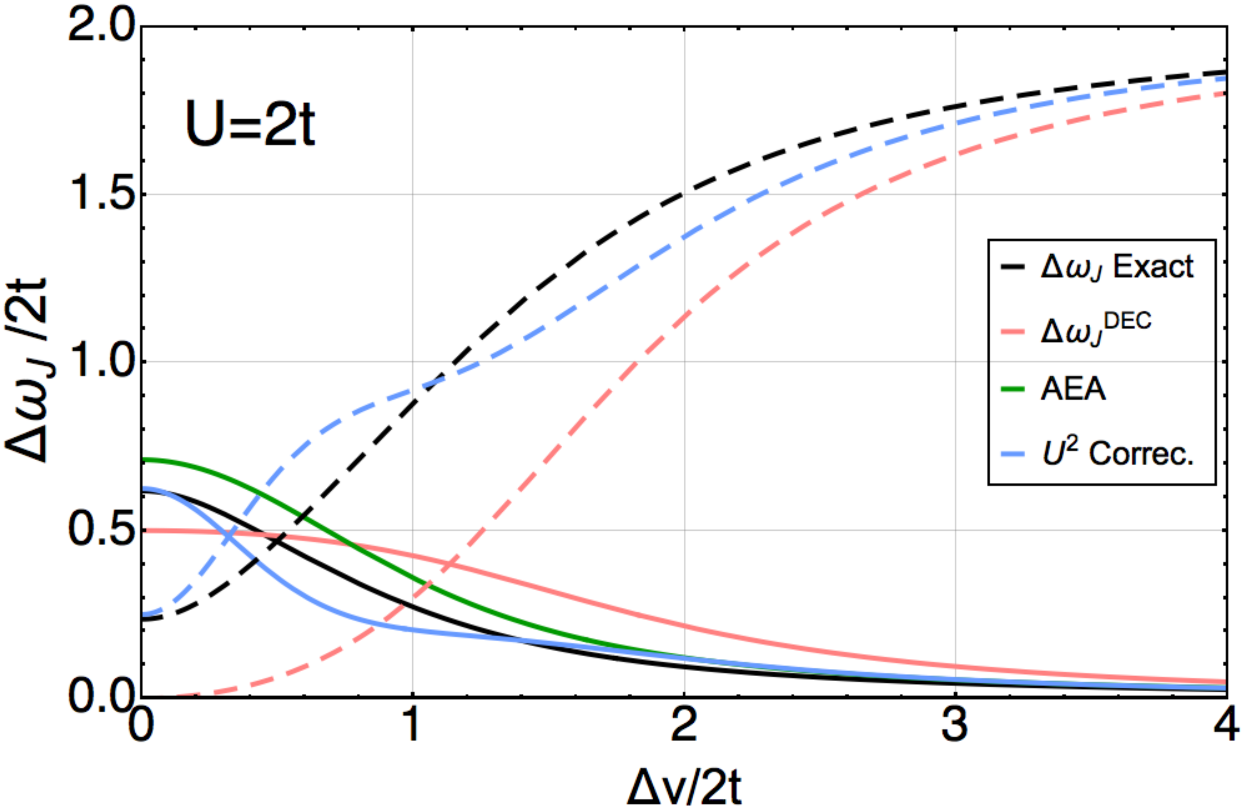

Figure 3.2: Correction to the KS transitions of Fig. 3.1, both exact and various approximations, where solid lines are single excitations, dashed are double. The correction to the single turns off with increasing asymmetry, but not so the double excitation. The DEC/EEXX approximation correctly captures both effects. Also included is the leading correlation contribution (blue), which further improves the results, when the system is weakly correlated. Here the black $\Delta\omega_J$ curves correspond to the exact result (see text for details), the pink $\Delta\omega_J^{DEC}$ curves are for the DEC/EEXX, the green curve is the AEA, and the blue curves are the second order corrections.

This is the true measure of the quality of an approximate treatment of excitations, as the KS transitions are determined entirely by ground-state DFT. We use the single as a test case, as the analytic results are already known. The DEC/EEXX curves are comparable to those of the AEA TDDFT, doing better for $\Delta v < 2t$, but worse as the asymmetry increases, similar to its performance for both atoms and the Hooke's atom [173]. As $\Delta v \to \infty$, $\Delta n \to 2$, turning off the corrections to the single.

Now we focus on the main interest, the double excitation. Here DEC/EEXX yields no correction at $\Delta v = 0$, but everywhere else reduces the error of the KS transition, but with substantially greater error than for the single. This is consistent with the earlier results, but can we discern here if this is accidental or not? To do this, we take advantage of the model's simplicity, and the many results that are already known. One peculiarity is that, performing a many-body expansion for fixed Δv as a function of U, one finds that the double excitation has no first-order correction, i.e., correction to the tight-binding result is of order U^2 [14]. This would appear to make it useless for our purposes. However, ω_s, by virtue of its dependence on the ground-state density, *does* have a first-order correction in λ, which means that $\Delta\omega_2$ is also first-order, and is correctly captured by the DEC/EEXX approximation, as shown. This correction happens to vanish at $\Delta v = 0$. (This means that studying only the symmetric dimer would produce qualitatively incorrect conclusions on this point.)

Because of the simplicity of the model, we can use the results of Ref.[14] to derive the next correction in powers of U (or λ), by converting Δv-dependence to Δn-dependence, yielding

$$\Delta\omega_1^{(2)} = \frac{\sqrt{4-\Delta n^2}(4-13\Delta n^2+3\Delta n^4)U^2}{64(2t)}, \Delta\omega_2^{(2)} = \frac{\sqrt{4-\Delta n^2}(4+11\Delta n^2-3\Delta n^4)U^2}{32(2t)}.$$

Note that these corrections *cannot* be deduced from the DEC/EEXX of Ref. [173], since by definition the DEC/EEXX contains no correlation, and therefore no higher order corrections. These are shown in Fig. 3.2 and (almost) everywhere reduce the error of DEC, as expected in the weakly correlated regime. Moreover, they do produce great improvement in the double at $\Delta v = 0$, and so provide a benchmark for correlation corrections to DEC/EEXX. Finally, we note that these corrections would be extremely difficult to calculate for a system with an ab initio Hamiltonian, as they require knowing the exact ground-state, the exact Kohn-Sham eigenstates, and performing second-order Görling-Levy perturbation theory on those states.

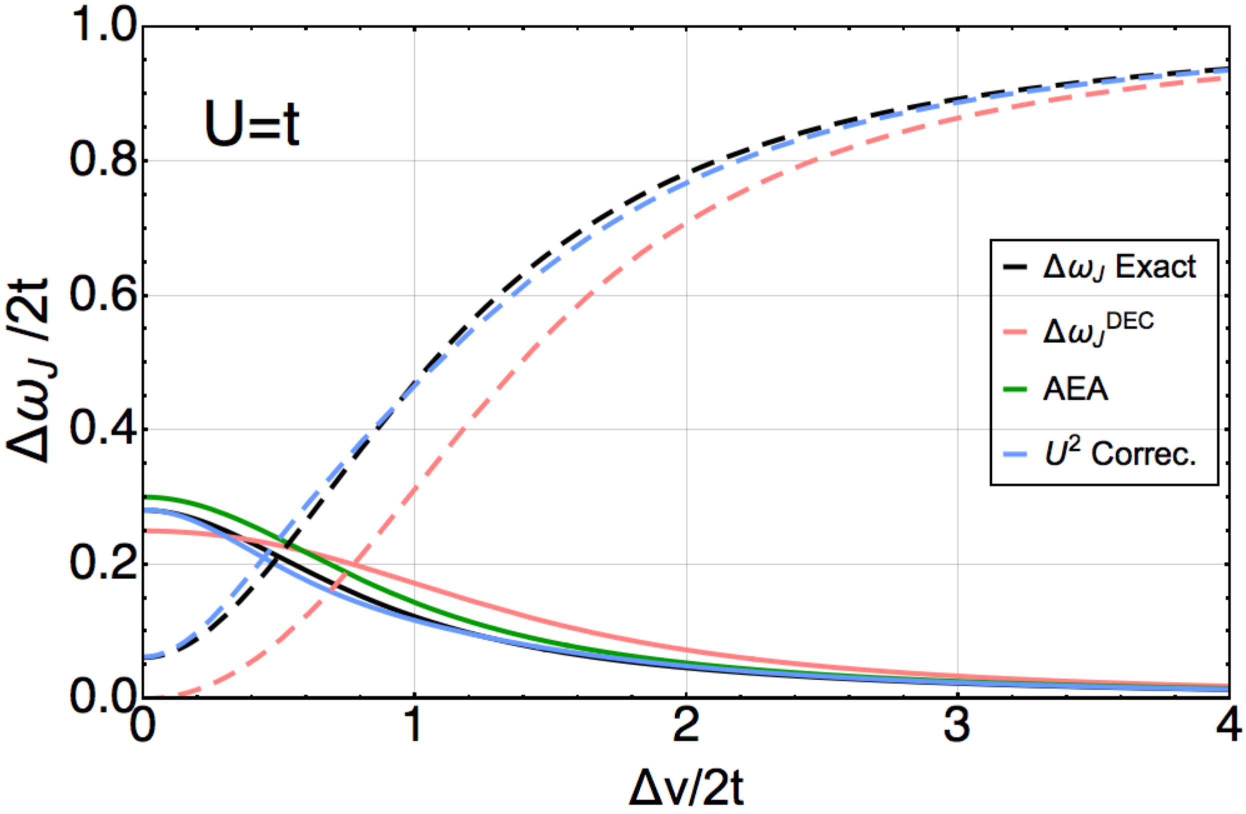

Figure 3.3: Same as Fig. 3.2 but at a weaker correlation of $U = t$, showing that the DEC improves as correlation weakens, and the second order correction agrees even better.

To make sure our understanding is correct, in Fig. 3.3 we show the results when $U = t$, i.e. the same system but with weaker correlation. Now the second-order correction is almost perfect everywhere, showing perturbation theory is converging. Moreover, the absolute errors in DEC have halved, but remain large out to about $\Delta v = 2U$. In our last figure, Fig. 3.4, we show what happens as GL perturbation theory begins to fail. Near $\Delta v = 0$, DEC fails completely, with equal corrections to the first and second excitation, making the gap precisely zero. This is where convergence of perturbation theory breaks down, and the KS transitions

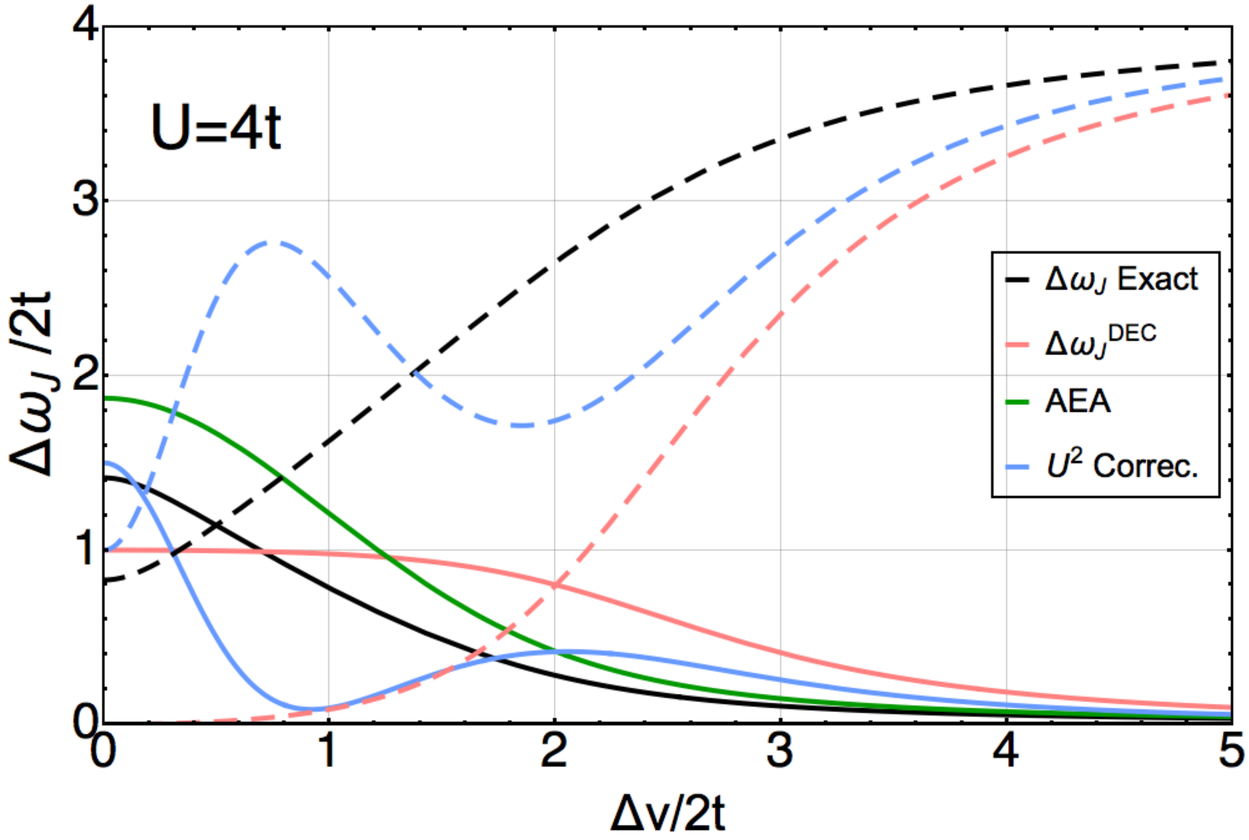

Figure 3.4: Same as Fig. 3.2, but at a stronger correlation of $U = 4t$, showing the failure of DEC when correlation is strong. Here DEC fails for small Δv, but nonetheless agrees for both DEC and its second-order correction for large values of Δv, showing that the system becomes weakly correlated when asymmetry dominates over correlation strength.

are not a good starting point. However, even here, for $\Delta v >> U$, the gap is much larger, and both single and double corrections become accurate. This is consistent with the claims of Ref.[14], that for $\Delta v > U$, a system is always weakly correlated, no matter how large U is, as far as DFT is concerned.

3.6 Discussion

So what can we conclude from this very simple model? The most important thing is that, generically, the DEC/EEXX approximation yields a meaningful and non-zero correction to a double excitation, producing the exact linear term in the GL perturbation for fixed density. In special cases where this term vanishes identically, it is of course useless. In some ways, our case is more typical than either of those studied in Ref.[173], as all cases studied there involved double excitations in regions of the energy spectrum with single excitations nearby (where dressed TDDFT could be applied), but here we have a double excitation without a single nearby (and hence dressed TDDFT would not work).

To understand why TDDFT linear response requires a correlation kernel to capture an exchange contribution, it is crucial to understand that an expansion of the kernel in the coupling-constant is not a meaningful concept. Consider how would TDDFT capture these effects if correlation is included? Ref.[14] gives the answer for this model. There is a pole in the kernel that generates the double excitation. It has the form:

$$f_{_{HXC}}(\omega) \approx \frac{a}{\omega - \omega_p}. \tag{3.7}$$

Now, both the numerator and ω_p have expansions in powers of λ. While ω_p contains all orders, a starts at second-order. It is meaningless to speak of an expansion of the kernel in powers of λ, as this expansion always fails as ω approaches the pole. Both the numerator and the transition frequencies have well-behaved expansions in powers of λ, and can be usefully approximated in a power series when the system is weakly correlated, but the kernel in TDDFT never does. The arguments of Refs. [46] and [39] focus on the denominator alone, neglecting the requirement of having a non-zero numerator to the order given, and so are only correct for single excitations.

Although the Hubbard dimer is not a quantitative model of anything, it roughly approximates a minimal basis model for a diatomic with two valence electrons. In the symmetric case, this would correspond to H_2. As the bond is stretched, $t \to 0$, but U and Δv remain finite, so $U/(2t)$ and $\Delta v/(2t) \to \infty$. For H_2, by symmetry, $\Delta v = 0$, and this may present special difficulties for DEC/EEXX, as the linear contribution might be unusually small. On the other hand, for LiH, it should work well.

Finally, while this model may appear overly simple, its great power lies in the ability to show transparently what is going on. It clearly demonstrates that EDFT *can* accurately capture double excitations, even when using an EEXX approximation, with no correlation. It would be highly non-trivial (and time consuming) to perform all these TDDFT and EDFT calculations on more realistic systems, and impossible to write down and examine the behavior of analytic expressions.

First and foremost, I must thank my advisor Professor Kieron Burke, for taking me as a PhD student, and putting up with me for 5 years. While I did not have any previous theory experience, he gave me the opportunity to change my research direction. He provided the space for me to grow as a scientist, and gave me and everyone in the group many valuable opportunities for which I am profoundly thankful. Thank you Kieron for repeatedly answering my questions (even if it was the same question), but most importantly thank you for listening to me and my concerns, even when they were not academic in nature.

I would also like to acknowledge my thesis committee members, Professors Vladimir Man-

delshtam and Craig Martens, who also served in my advancement committee. I would like to specially thank Professor Rachel Martin who was the chair of my advancement committee, and who's words of encouragement were always perfectly timed.

I would like to specially acknowledge Dr. Attila Cangi, who recruited me to intern at Sandia National Laboratories during my third year. This internship gave me some much needed time away from my coursework in Irvine. It gave me a peek of what large scale science is like at the national labs. Attila's seemingly endless patience and vast knowledge also gave me the confidence that I could in fact be a competent scientist. Working with Attila, has truly been a pleasure. Being a year round intern at Sandia for the last two years of my degree was unexpected experience for which I am thankful.

Next I must thank all of the friends I made while at Irvine. Our frequent chats and outings made the overall experience much more enjoyable. Special thanks to Kara Thomas, Sabrina Chee, and Sara Taydeon, with whom I worked in the trenches. I would like to acknowledge my childhood friend Sydney Everratt, with whom I shared many fun excursions through out southern CA (and CO), and who most importantly reminded me that life is fun outside of academia (and the sterility of Irvine). I cannot overlook the great discussions and friendships I formed with older theory graduate students. In particular I thank Saswata Roy, Sree Ganesh Balasubramani, and Guo Chen who without hesitation would explain whatever concepts in quantum chemistry I would barge into their office with.

I would like to thank all current and past Burke group members, with whom I shared offices, coffee breaks, and cookies. I must specially thank Dr. Ryan Mccarty who was the best office mate I had, and who's surprisingly relentless optimism made group lunches and meetings more enjoyable. In addition, I must thank Ryan for all of the effort he put into helping pass my advancement exam. I would like to also thank Dr. Dennis Perchak, who's stories always put a smile on my face. His kind words during my exam also gave me some much needed encouragement.

Finally I must thank my family, whom I cherish dearly. My parents are my biggest cheerleaders, and I must thank my father for always pushing me to do my best, and reminding me that that “se hace camino al andar” whenever I was struggling. I would lastly like to thank my sister Maca, who I managed to talk with on almost a daily basis, even though we were 9 time zones apart. Having the support of family truly is a privilege to which I am eternally grateful.

This dissertation contains verbatim excerpts as they appear in *Journal of Chemical Physics* and *Springer Nature*. Chapter 2 is reproduced from, F. Sagredo and K. Burke, *J. Chem. Phys.* **149**, 134103 (2018), with the permission of AIP Publishing. Chapter 4 is reprinted/adapted by permission from *Springer Nature*, *Frontiers of Quantum Chemisrty* by J. C. Smith, F. Sagredo, and K. Burke (2017). The co-authors listed in these publications directed, supervised, or conducted part of the research which forms the basis for the dissertation. This work was supported by the Department of Energy under grant number DE-FG02-08ER46496.

Chapter 4

Warming up density functional theory

This chapter was replicated from Ref.[148]. It was written in conjunction with Justin C. Smith and my advisor, Kieron Burke. I contributed to making figures and writing. This book chapter provides a good review and introduction to the field of finite temperature DFT.

4.1 Abstract

Density functional theory (DFT) has become the most popular approach to electronic structure across disciplines, especially in material and chemical sciences. In 2016, at least 30,000 papers used DFT to make useful predictions or give insight into an enormous diversity of scientific problems, ranging from battery development to solar cell efficiency and far beyond. The success of this field has been driven by usefully accurate approximations based on known exact conditions and careful testing and validation. In the last decade, applications of DFT in a new area, warm dense matter, have exploded. DFT is revolutionizing simulations of warm dense matter including applications in controlled fusion, planetary interiors, and other areas of high energy density physics. Over the past decade or so, molecular dynamics cal-

culations driven by modern density functional theory have played a crucial role in bringing chemical realism to these applications, often (but not always) with excellent agreement with experiment. This chapter summarizes recent work from our group on density functional theory at non-zero temperatures, which we call thermal DFT. We explain the relevance of this work in the context of warm dense matter, and the importance of quantum chemistry to this regime. We illustrate many basic concepts on a simple model system, the asymmetric Hubbard dimer.

4.2 Paper

4.3 Introduction

Warm dense matter: The study of warm dense matter (WDM) is a rapidly growing multidisciplinary field that spans many branches of physics, including for example astrophysics, geophysics, and attosecond physics[101, 112, 95, 75, 74, 77, 61, 73, 132, 149, 50]. Classical (or semiclassical) plasma physics is accurate for sufficiently high temperatures and sufficiently diffuse matter[67]. The name WDM implies too cool and too dense for such methods to be accurate, and this regime has often been referred to as the malfunction junction, because of its difficulty[112]. Many excellent schemes have been developed over the decades within plasma physics for dealing with the variety of equilibrium and non-equilibrium phenomena accessed by both people and nature under the relevant conditions[7]. These include DFT at the Thomas-Fermi level (for very high temperatures) and use of the local density approximation (LDA) within Kohn-Sham (KS) DFT at cold to moderate temperatures (at very high temperatures, sums over unoccupied orbitals fail to converge). The LDA can include thermal XC corrections based on those of the uniform gas, for which simple parametrizations have long existed[146, 71].

Electronic structure theory: On the other hand, condensed matter physicists, quantum chemists, and computational materials scientists have an enormously well-developed suite of methods for performing electronic structure calculations at temperatures at which the electrons are essentially in their ground-state (GS), say, 10,000K or less[8]. The starting point of many (but not all) such calculations is the KS method of DFT for treating the electrons[81]. Almost all such calculations are within the Born-Oppenheimer approximation, and ab initio molecular dynamics (AIMD) is a standard technique, in which KS-DFT is used for the electronic structure, while Newton's equations are solved for the ions[13].

DFT in WDM: In the last decade or so, standard methods from the electronic structure of materials have had an enormous impact in warm dense matter, where AIMD is often called QMD, quantum molecular dynamics[50]. Typically a standard code such as VASP is run to perform MD[73]. In WDM, the temperatures are a noticeable fraction of the Fermi energy, and thus the generalization of DFT to thermal systems must be used. Such simulations are computationally demanding but they have the crucial feature of including realistic chemical structure, which is difficult to include with any other method while remaining computationally feasible. Moreover, they are in principle exact[60, 81], if the exact temperature-dependent exchange-correlation free energy could be used because of Mermin's theorem establishing thermal DFT(thDFT). In practice, some standard ground-state approximation is usually used. (There are also quantum Monte Carlo calculations which are typically even more computationally expensive[105, 38, 104, 140, 31, 141, 28]. The beauty of the QMD approach is that it can provide chemically realistic simulations at costs that make useful applications accessible[102].) There have been many successes, such as simulation of Hugoniot curves measured by the Z machine[132] or a new phase diagram for high density water which resulted in improved predictions for the structure of Neptune[101]. Because of these successes, QMD has rapidly become a standard technique in this field.

Missing temperature dependence: However, the reliability and domain of applicability of QMD calculations are even less well understood than in GS simulations. At the equilibrium level of calculation, vital for equations of state under WDM conditions and the calculation of free-energy curves, a standard generalized gradient approximation (GGA) calculation using, e.g., PBE[119], is often (but not always) deemed sufficient, just as it is for many GS materials properties. Such a calculation ignores thermal exchange-correlation (XC) corrections, i.e., the changes in XC as the temperature increases, which are related to entropic effects. We believe we know these well for a uniform gas (although see the recent string of QMC papers[141, 28] and parametrizations[71]), but such corrections will be unbalanced if applied to a GGA such as PBE. So how big a problem is the neglect of such corrections?

(A little) beyond equilibrium: On the other hand, many experimental probes of WDM extract response functions such as electrical or thermal conductivity[101]. These are always calculated from the equilibrium KS orbitals, albeit at finite temperature. Work on molecular electronics shows that such evaluations suffer both from inaccuracies in the positions of KS orbitals due to deficiencies in XC approximations, and also require further XC corrections, even if the *exact* equilibrium XC functional were used[158, 130, 80].

Acronym	Meaning	Acronym	Meaning
GGA	Generalized Gradient Approx.	RPA	Random Phase Approximation
GS	ground-state	TDDFT	Time-dependent DFT
HXC	Hartree XC	thDFT	thermal DFT
KS	Kohn-Sham	unif	uniform gas
LDA	Local Density Approx.	XC	exchange-correlation
PBE	Perdew-Burke-Ernzerhof	ZTA	Zero-Temperature Approx.
QMC	quantum Monte Carlo		

Table 4.1: Acronyms frequently used in this chapter.

4.4 Background

Generalities: Everything described within uses atomic units, is non-relativistic and does not include external magnetic fields. Unless otherwise noted, all results are for the electronic contributions within the Born-Oppenheimer approximation. While all results are stated for density functionals, in practice, they are always generalized to spin-density functionals in the usual way. In Table **??** we provide a summary of frequently used acronyms.

4.4.1 Ground-state DFT

Hohenberg-Kohn functional: Just over 50 years ago, in 1964, Hohenberg and Kohn wrote down the foundations of modern DFT[59]. They start with the many-body Hamiltonian

$$\hat{H} = \hat{T} + \hat{V}_{\text{ee}} + \hat{V}, \tag{4.1}$$

where $\hat{T}$, $\hat{V}_{\text{ee}}$, and $\hat{V}$ are the kinetic, electron-electron, and potential energy operators, respectively. Assuming a non-degenerate ground-state, they proved by *reductio ad absurdum* that the external potential, $v(\mathbf{r})$ is a unique functional of the density $n(\mathbf{r})$, and therefore all observables are also density functionals. More directly Levy defines the functional

$$F[n] = \min_{\Psi \to n} \langle \Psi | \hat{T} + \hat{V}_{\text{ee}} | \Psi \rangle, \tag{4.2}$$

where Ψ is normalized and antisymmetric, and uses it to define the energy functional

$$E_v[n] = F[n] + \int d^3r \, v(\mathbf{r}) n(\mathbf{r}), \tag{4.3}$$

whose minimization over normalized non-negative densities with finite kinetic energy yields the ground-state energy and density[92].

Kohn-Sham scheme: In 1965, Mermin generalized the Hohenberg-Kohn theorems for electrons in the grand canonical potential with fixed non-zero temperature τ and chemical potential μ[60]. Later in 1965, Kohn and Sham created an exact method to construct the universal functional (see Eq. (4.6)). The Kohn-Sham scheme imagines a system of N non-interacting electrons that yield the electronic density of the original interacting N electron system. These fictitious electrons sit in a new external potential called the KS potential. The KS scheme is written as a set of equations that must be solved self-consistently:

$$\left\{-\nabla^2 + v_{\mathrm{S}}(\mathbf{r})\right\} \phi_i(\mathbf{r}) = \epsilon_i \phi_i(\mathbf{r}), \quad n(\mathbf{r}) = \sum_i^N |\phi_i(\mathbf{r})|^2, \tag{4.4}$$

$$v_{\mathrm{S}}(\mathbf{r}) = v(\mathbf{r}) + v_{\mathrm{H}}(\mathbf{r}) + v_{\mathrm{XC}}(\mathbf{r}), \quad v_{\mathrm{XC}}(\mathbf{r}) = \frac{\delta E_{\mathrm{XC}}[n]}{\delta n(\mathbf{r})}, \tag{4.5}$$

where $\phi_i(\mathbf{r})$ and ϵ_i are the KS orbitals and energies, $v_{\mathrm{H}}(\mathbf{r})$ is the classical Hartree potential, and $v_{\mathrm{XC}}(\mathbf{r})$ is the exchange-correlation potential defined by the unknown XC energy, E_{XC}, in Eq. (4.5). These must be solved self-consistently since the Hartree potential and E_{XC} depend explicitly on the density. Lastly, the total energy can be found via

$$F[n] = T_{\mathrm{S}}[n] + U_{\mathrm{H}}[n] + E_{\mathrm{XC}}[n] \tag{4.6}$$

where T_{S} is the kinetic energy of the KS electrons and U_{H} is the Hartree energy.

In practice, an approximation to E_{XC} must be supplied. There exists a wealth of approximations for E_{XC}[99]. The simplest, LDA, uses the XC per electron of the homogeneous electron gas[118]:

$$E_{\mathrm{XC}}[n] = \int d^3r \, e_{\mathrm{XC}}^{\mathrm{unif}}(n(\mathbf{r})) \tag{4.7}$$

where $e_{\mathrm{XC}}^{\mathrm{unif}}$ is the XC energy density of a uniform gas with density $n(\mathbf{r})$. We can imagine going up a ladder by adding in more ingredients (like gradients of the density[119]) and obeying different or additional conditions to make more complicated and more accurate functionals[123]. For the exact E_{XC}, these equations have been proven to converge[167].

4.4.2 Asymmetric Hubbard dimer and its relevance

Throughout this chapter we illustrate results with the simplest interesting model of an interacting system. This model is the asymmetric Hubbard dimer[15]. The Hubbard dimer crosses the divide between the weakly and strongly correlated communities. Previous work has shown that the basic concepts of ground-state KS-DFT apply to this model and here we demonstrate similar applicability to thermal DFT. The Hamiltonian is given by

$$\hat{H} = -t \sum_{\sigma} (\hat{c}_{1\sigma}^{\dagger} \hat{c}_{2\sigma} + H.c.) + \sum_{i=1}^{2} (U \hat{n}_{i\uparrow} \hat{n}_{i\downarrow} + v_i \hat{n}_i) \tag{4.8}$$

where $\hat{c}_{i\sigma}^{\dagger}(\hat{c}_{i\sigma})$ are electron creation (annihilation) operators and $\hat{n}_{i\sigma} = \hat{c}_{i\sigma}^{\dagger} \hat{c}_{i\sigma}$ are number operators. t is the strength of electron hopping between sites, U is the ultra-short range Coulomb repulsion for when both electrons are on the same site, and v_i is the on-site external potential. We choose, without loss of generality, $v_1 + v_2 = 0$ then $\Delta v = v_2 - v_1$ and the occupation difference, the analog of density, is $\Delta n = n_2 - n_1$.

In Fig. 4.1 we plot the density Δn versus asymmetry Δv in the Hubbard dimer. The Hohenberg-Kohn theorem applies to this Hamiltonian, and guarantees $\Delta n(\Delta v)$ is an invertible function for any value of U. The main physics is a competition between asymmetry and interaction strength. The weakly correlated regime is $U < \Delta v$ and the opposite is strong correlation. Increasing Δv pushes the electrons onto a single site, thus Δn approaches 2. Likewise, for small Δv or large U the electrons are apart and Δn tends to 0. This is made

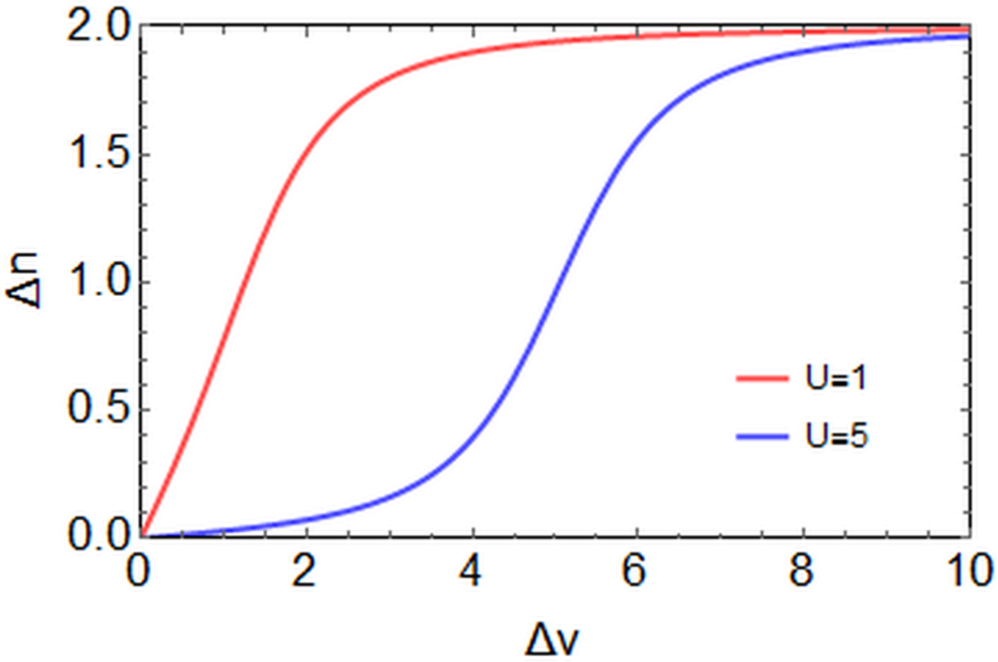

Figure 4.1: Difference in on-site occupations as a function of on-site potential difference for $U = 1$ and 5 in the asymmetric Hubbard dimer. The HK theorem guarantees that each function is invertible. There is a simple analytic result for $U = 0$, and for large U, the relation tends toward a (smoothed) step function, with the step at $\Delta v = U$.

most clear by the extreme cases, i.e.,

$$|\Delta n_{U=0}(\Delta v)| = 2\Delta v/\sqrt{(2\,t)^2 + \Delta v^2}, \qquad |\Delta n_{U\to\infty}(\Delta v)| \to 2\theta(\Delta v - U), \tag{4.9}$$

where $\theta(x)$ is the Heaviside step function. The ability to vary U and move continuously from weak to strong correlation in a model that is analytically solvable makes the Hubbard dimer an excellent illustrator of how KS-DFT works[15].

4.4.3 Ensemble DFT as a route to excitation energies

In this section we take a quick aside to overview ensemble DFT (eDFT), a close cousin of thermal DFT.

Excitations in DFT: Although time-dependent DFT (TDDFT) is the standard method used to determine the excited states of a system [97], there are still many deficiencies, due to crude approximations to the XC functional as well as being unable to approximate multiple excitations, charge transfer excitations, conical intersections, and polarizabilities of long-chain polymers; all things that can be important for photochemistry[98, 30, 159, 90, 165]. Ensemble DFT is a time-independent alternative to the standard TDDFT that can be a useful method for extracting excited states. Naturally, since eDFT and TDDFT are based on two different fundamental theories, it is possible to use eDFT on different systems to those of the traditional method and expect different successes and likewise different failures.

Ensemble variational principle: eDFT is based on a variational principle made up of ensembles of ground and excited states [156]. These ensembles are made of decreasing weights, with the ground state always having the highest weight.

$$E^{\mathbf{w}} \leq \sum_{k=0}^{M-1} w_k \langle \Psi_k | \hat{H} | \Psi_k \rangle, \qquad w_0 \geq w_1 \geq ... \geq w_k \geq 0 \tag{4.10}$$

where all Ψ_k are normalized, antisymmetric, and mutually orthogonal, $\mathbf{w} = (w_0, w_1, ...w_k)$, and the sum of all weights is 1. The ensemble-weighted density is

$$n^{\mathbf{w}}(\mathbf{r}) = \sum_{k=0}^{M-1} w_k n_{\Psi_k}(\mathbf{r}). \tag{4.11}$$

Just as in the ground-state case, a one-to-one correspondence from the weighted density to the potential can be established [53], and applying this to a non-interacting system of the same weighted density can be used to construct a KS eDFT. From this KS system it is in principle possible to extract the exact excited states of the system.

Relation to thermal DFT: The connection to thermal DFT is natural and straightforward. Thermal DFT is a special case of eDFT. In thDFT, one chooses the ensemble to be the grand canonical ensemble with the usual Boltzmann factors for the weights. However, unlike eDFT, the weights themselves depend on the eigenvalues of the Hamiltonian, including the strength of the interaction. Thus the weights in the KS system are different from those of the interacting system. In most applications of eDFT, the weights are chosen to be the same in both the physical and non-interacting systems.

History: Ensemble DFT was originally proposed by Gross-Olivera-Kohn in 1988[53], but, like thermal DFT, there has been slow progress over the last 30 years due to a lack of useful approximations to the XC functional. Many of these difficulties arise from the so-called ghost interaction errors that occur in the Hartree energy[54]. More specifically these ghost-interaction errors appear when only using the ground state definition of the Hartree energy, which causes unphysical contributions and must therefore be accounted for by using a more accurate definition of the Hartree energy for ensembles[129, 174].

Recent progress: More recently, work has been done to extract the weight dependence of the KS eigenvalues, which are required in order to extract accurate transition frequencies[129, 174]. It was also found that a large cancellation of the weight-dependence occurs in the exact ensembles. Further, a new numerical method for inverting ensemble densities was derived for spherically symmetric systems, and this method was also tested for cylindrically symmetric systems. This inversion of densities to extract potentials provides a useful test of eDFT approximations.

Recent work combines linear interpolation with an extrapolation method in eDFT to extract excited states that are independent of ensemble weights[145]. Also, an exact analytical expression for the exchange energy was derived, and a generalized adiabatic connection for ensembles (GACE) was used to connect the ensemble XC functional with the ground state functional[69]. Finally, a ghost interaction correction has been developed for range-separated eDFT[2].

A simple exercise: Here we show an example of the importance of the weight-dependence of functionals in eDFT, in a seemingly simple system. We put only one electron in the Hubbard dimer, so there is no interaction, and its a simple tight-binding Hamiltonian. We will derive the exact kinetic energy functional, which is an example of the non-interacting KS kinetic energy functional. We will also approximate it, as if we were interested in orbital-free eDFT.

There are only two levels, the ground state and a first excited state. Thus we can make only a bi-ensemble. The ensemble-weighted ground-state density is

$$\Delta n^w = (1-w)\Delta n_0 + w\Delta n_1 = (1-2w)\Delta n_0(x), \tag{4.12}$$

where Δn_0, and Δn_1 correspond to the occupational difference of the two sites for the ground and first-excited state, respectively, and $\Delta n_0(x)$ is half of Eq. (4.9) with $U = 0$, since we are looking at a single particle in the dimer. This last result is true only because $\Delta n_1 = -\Delta n_0$ in this simple model. The weight as previously stated is $w \leq 0.5$. Similarly, the kinetic energy for a single particle in the ground-state is known, and $T_{\text{S},1} = -T_{\text{S},0}$, so

$$T_{\text{S}}^w = (1-w)T_{\text{S},0} + wT_{\text{S},1} = (1-2w)T_{\text{S},0} = (1-2w)\frac{-t}{\sqrt{1+x^2}} \tag{4.13}$$

where $x = \Delta v/(2\,t)$. Note that kinetic energy is negative in the Hubbard model. Using $V^w = \Delta v \Delta n^w/2$ and adding it to T_{S}^w yields the ensemble energy, which is exactly linear in w, and passes through E_0 at $w = 0$ and (would pass through) E_1 at $w = 1$.

This simple linearity with w is true by construction of the ensemble, when energies are plotted against w for a fixed potential. But now we show that things get complicated when we consider them as density functionals. Inverting the relation between potentials and densities we find

$$x = \frac{\Delta n^w}{\sqrt{(1-2w)^2 - (\Delta n^w)^2}}, \tag{4.14}$$

and inserting this into the kinetic energy yields

$$T_{\rm s}^{w}[\Delta n^{w}] = -\sqrt{(1-2w)^2 - (\Delta n^{w})^2}/2. \tag{4.15}$$

Even in this trivial case, the the w-dependence of the kinetic energy density functional is non-linear.

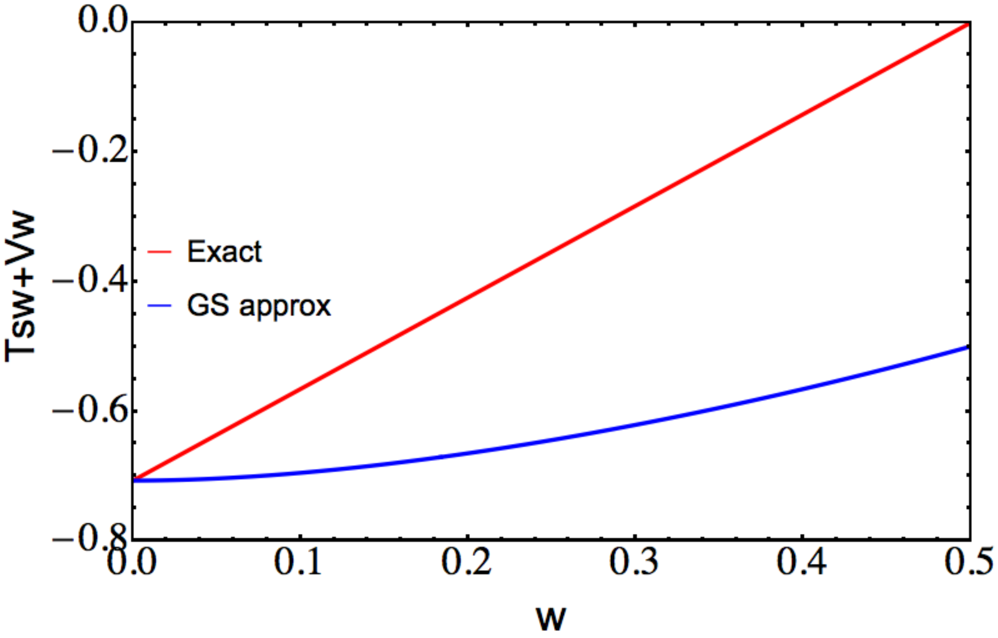

Figure 4.2: The exact energy curve for a single particle in a Hubbard dimer $E_{exact} = T_{\rm s}^{w}[\Delta n^{w}] + V^{w}$ (red), when $x = 1$, in units of $2t$. The blue line is the approximate energy when $T_{\rm s}^{w}$ is replaced by its ground-state analog, $T_{\rm s}^{0}$. Notice that $w = 0$ corresponds to E_0, which is $1/\sqrt{2}$ in these units.

Next, we make the most naive approximation, namely to replace $T_{\rm s}^{w}[\Delta n]$ with its ground-state counterpart. This yields an approximate eDFT theory from which, in principle, we can estimate the energy of the first excited state. To do this, we insert the exact w-dependent density of Eq. (4.12) into the ground-state functional, add the exact V^{w}, and plot the resulting energy. The exact and approximate results are shown in Fig. 4.2. The approximation is very bad, yielding an energy value that is too negative by 0.5, using the value at $w = 1/2$. But it illustrates the difficulties of capturing an accurate w-dependence in an ensemble density functional.

4.4.4 Thermal DFT in a nutshell

Mermin-Kohn-Sham equations: In a thermal system, Eq. (4.4) and (4.5) are generalized such that the density and XC potential become $n^\tau(\mathbf{r})$ and $v^\tau_{\text{XC}}(\mathbf{r})$, i.e. temperature dependent, and $E_{\text{XC}}[n]$ in Eq. (4.5) becomes $A^\tau_{\text{XC}}[n]$, the exchange-correlation *free* energy density functional. The density becomes

$$n^\tau(\mathbf{r}) = \sum_i f_i |\phi^\tau_i(\mathbf{r})|^2 \tag{4.16}$$

where the sum is now over all states and $f_i = (1 + e^{(\epsilon^\tau_i - \mu)/\tau})^{-1}$, the Fermi occupation factors. One of the core difficulties in thermal DFT calculations is this sum, since a huge number of states are required once the temperature is sufficiently high. This leads to large computational demands and convergence issues. We call these the Mermin-Kohn-Sham equations.

To extract the total free energy from the MKS equations, we write

$$A^\tau[n] = A^\tau_{\text{S}}[n] - U_{\text{H}}[n] + A^\tau_{\text{XC}}[n] - \int d^3r\, n(\mathbf{r}) v^\tau_{\text{XC}}[n](\mathbf{r}), \tag{4.17}$$

where the MKS free energy is

$$A^\tau_{\text{S}}[n] = \sum_i \epsilon^\tau_i[n] - \tau S^\tau_{\text{S}}[n], \quad S^\tau_{\text{S}}[n] = -\sum_i \left[f_i \log(f_i) + (1 - f_i) \log(1 - f_i) \right], \tag{4.18}$$

and S_{S} is the MKS entropy.

Exchange-correlation free energy: Compared to ground-state DFT, relatively few approximations have been developed for A^τ_{XC}. In active use are two approximations: thermal LDA (thLDA) and the Zero-Temperature Approximation (ZTA). The former uses the temperature-dependent XC free energy of the uniform gas instead of its ground-state analog in Eq. (4.7). The ZTA means simply using any ground-state XC functional instead of a temperature-dependent one. We denote use of the exact ground-state XC functional as exact ZTA (EZTA).

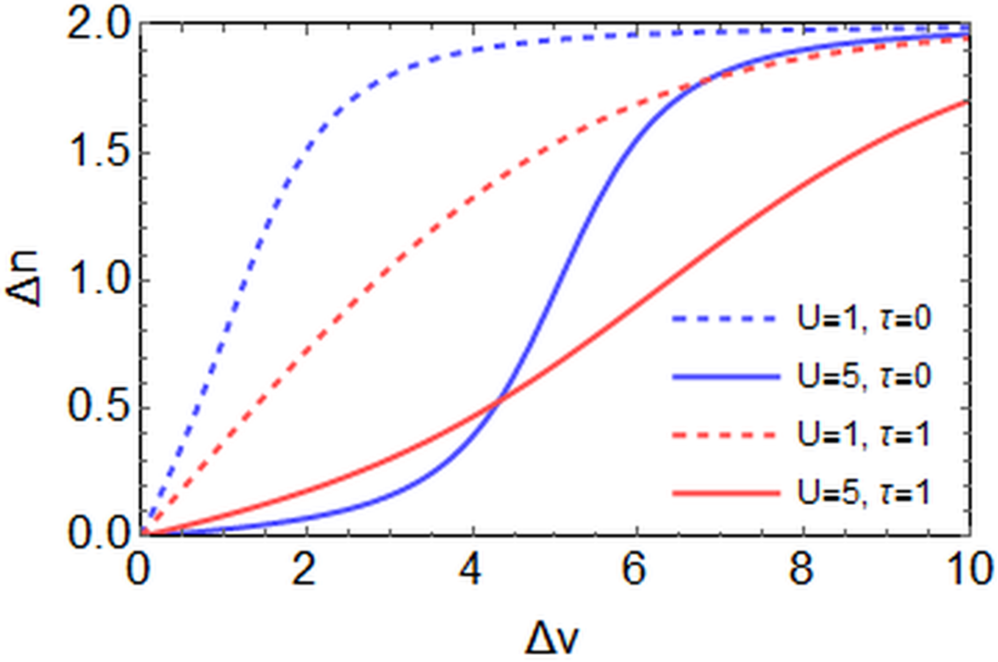

Figure 4.3: Effects of temperature on the difference in on-site occupations as a function of on-site potential difference for $U = 1$ and 5 in the asymmetric Hubbard dimer (see Sec. 4.5.2) with and without temperature. Increasing temperature pushes the electrons towards opposite sites and lowers Δn while increasing Δv pushes electrons to the same site and raises Δn.

In Fig. 4.3 we demonstrate the effects of turning on temperature for the Hubbard dimer (see Sec. 4.5.2 for more information). Even a small increase in temperature can have a big impact on a system regardless of the strength of correlation.

4.5 Some recent developments in thermal DFT

The formalism for thermal DFT was originally developed alongside that of ground-state DFT, but in the intervening decades ground-state DFT (and TDDFT, for that matter) has received significantly more attention and consequently more developments[10, 8]. However, In the past couple decades thermal DFT has seen more use, and with that much more development in the past ten years. In this section we outline some recent developments to thermal DFT from our group.

4.5.1 Exact conditions and their relevance

Zero temperature: One of the most crucial steps in understanding and developing functionals beyond LDA is exact conditions. These conditions take many forms with some common examples being coordinate and interaction scaling conditions[91], and bounds on the XC energy[93]. There are well over a dozen conditions in ground-state DFT (a recent meta-GGA functional even uses seventeen[154]!), but the use of exact conditions is much more nascent in thermal DFT.

Coordinate-temperature scaling and the thermal connection formula

Uniform coordinate scaling: The most straightforward application of exact conditions to thermal DFT is by uniform scaling of the density[91]. The very basic conditions that this procedure generates in ground-state DFT are built in to almost all modern approximations. In a sense, this is simply dimensional analysis, but while keeping the density fixed (which is the tricky bit).

Early work on exact conditions for thermal DFT[125, 128] derived basic conditions such as the signs of correlation quantities, including the separation into kinetic and potential contributions, and the adiabatic connection formula at finite temperature. More conditions come from coordinate scaling of the density, showing that is intimately related to temperature dependence. Examples of a few of these conditions are

$$F_{\rm S}^{\tau'}[n] = \frac{\tau}{\tau'} F_{\rm S}^{\tau}[n_{\sqrt{\tau'/\tau}}], \quad S_{\rm S}^{\tau'}[n] = S_{\rm S}^{\tau}[n_{\sqrt{\tau'/\tau}}], \quad A_{\rm X}^{\tau'}[n] = \sqrt{\frac{\tau}{\tau'}} A_{\rm X}^{\tau}[n_{\sqrt{\tau'/\tau}}], \tag{4.19}$$

where these have been rewritten in terms of temperature scaling instead of coordinate scaling. For any of these functionals, this means that, if you know the functional at *any* one finite temperature, the functional at *all* possible temperatures is available via temperature scaling as long as both temperatures are non-zero.

New formulas: In recent work, many new formulas relating correlation components of the energy to one another were derived[126], such as

$$K_{\scriptscriptstyle C}^{\tau,\lambda}[n] = A_{\scriptscriptstyle C}^{\tau,\lambda}[n] - \lambda \frac{dA_{\scriptscriptstyle C}^{\tau,\lambda}[n]}{d\lambda}, \tag{4.20}$$

where $K_{\scriptscriptstyle C}^{\tau,\lambda}[n] = T_{\scriptscriptstyle C}^{\tau,\lambda}[n] - \tau S_{\scriptscriptstyle C}^{\tau,\lambda}[n]$ is the correlation kentropy. λ is a coupling constant introduced in front of $\hat{V}_{\rm ee}$ where superscript λ indicates quantities defined on $\lambda\hat{V}_{\rm ee}$. There was also a rewriting of the adiabatic connection formula[125, 87], using the relation to scaling mentioned above, yielding the XC free energy at temperature τ:

$$A_{\rm XC}^{\tau}[n] = \frac{\tau}{2} \lim_{\tau''\to\infty} \int_{\tau}^{\tau''} \frac{d\tau'}{\tau'^2}\, U_{\rm XC}^{\tau'}[n_{\sqrt{\tau'/\tau}}], \qquad n_\gamma(\mathbf{r}) = \gamma^3\, n(\gamma\mathbf{r}), \tag{4.21}$$

where $U_{\rm XC}^{\tau}[n]$ is the purely potential contribution to the XC free energy, and the scaling is the usual coordinate scaling of the density introduced by Levy and Perdew[91] for the GS problem. Note that this thermal connection formula uses only information between the desired temperature and higher ones, allowing approximations that begin from the high-temperature end instead of the low-temperature end[126]. A second set of formulas give the many relations among the different correlation energy components (total, potential, and kentropic). These are very important in ground-state DFT[23, 121] for understanding the origins of different physical contributions to the correlation free energy and have guided the construction of many approximations.

Entropy: Lastly for this section, we look at a new set of exact conditions for the electronic entropy as a functional of the density[9]. The most important is that the universal functional can be written solely in terms of a temperature integral over entropy, such as

$$F^\tau[n] = F^0[n] - \int_0^\tau d\tau'\, S^{\tau'}[n], \qquad A^\tau_{\rm XC}[n] = E_{\rm XC}[n] - \int_0^\tau d\tau'\, S^{\tau'}_{\rm XC}[n], \tag{4.22}$$

i.e., the universal contribution to the free energy functional is a simple integral over the electronic entropy, and the second shows that all thermal corrections to the XC free energy are given by an integral over the XC entropy. These formulas have no analog in ground-state DFT. They also lead to fundamental inequalities on the various thermal derivatives of both interacting and KS quantities. Such conditions have long been known for the uniform gas[66], but our results are their generalization to inhomogeneous systems. Analogs are also easily derived from statistical mechanics, but again, the tricky part is to deduce their behavior as functionals of the density rather than the external potential. This is why, for example, all derivatives are total with respect to temperature. The particle number is fixed by the density, so temperature is the sole remaining variable. Our work uses the formalism and methods of ground-state DFT, generalized to finite temperature, but the same results can also be extracted in the language of statistical mechanics[33, 32].

Tiny violations: A minor illustration of the relevance of these conditions is that we found that a recent parameterization of the thermal XC free energy of the uniform gas[71] violates one of our conditions for low densities[9]. This violation is slight, and unlikely to ever influence the results of any thLDA calculation. Nonetheless, it is always better to build parameterizations that satisfy known conditions, so that the corresponding approximate calculations are guaranteed to satisfy such conditions[141, 28].

Zero-temperature approximations: This work also showed that any ZTA calculation automatically satisfies most of our conditions, whereas the inclusion of thermal XC corrections risks violating them for specific systems. For example, all approximations in Fig. 4.5 (discussed below) are guaranteed to satisfy these conditions. But practical calculations including approximate thermal XC corrections should be checked for possible violations of exact conditions in the future.

4.5.2 Exact calculations on a simple model system

Importance for ground-state DFT: A crucial step in all DFT development is the exact solution of simple systems and the test of approximate functionals against exact quantities. There are large databases of molecular properties, based either on highly reliable and accurate experimental measurements, or on far more accurate quantum chemical calculations[139, 176, 136, 157]. But these databases usually contain at most a few numbers per system, such as the atomization energy and bond length(s). A substantially more sophisticated test occurs when a highly accurate calculation is performed such as QMC[19, 164] or DMRG[169], and an inversion of the KS equations[142], so that essentially exact KS potentials, eigenvalues, orbitals, etc, can all be deduced. This is a much more powerful test of a DFT approximation, and usually provides detailed insight into its limitations. The QMC calculations of Umrigar and collaborators[163, 40, 63] and their high impact, testify to this fact.

Difficulty of exact thermal calculations: Although almost all practical calculations of WDM are in a condensed phase (with hot ions), almost all high level inversions yielding exact KS quantities are for atoms or small molecules. But even for such systems, it is difficult to imagine accurate inversions at finite temperature, as only the average particle number is fixed, and all possible particle numbers must be considered.

Exact calculations for Hubbard dimer: Exact calculations are only possible for this model because the Hilbert space is severely truncated which allows us to compute all energies analytically (see Fig. 4.4 for complete diagram of the energy spectrum). However, this means the model is not even a qualitatively realistic representation of very high temperatures (though we choose parameters such that the ceiling of the Hilbert space does not effect results). But we are able to do the inversion exactly, and so extract all the different contributions to X and C as a function of both τ and U. These are the first exact inversions of an interacting system at finite temperature. They show us the structure of the underlying functionals, but cannot tell us which approximations will be accurate. For example, there is no real analog of LDA for this system (although BALDA[94] somewhat plays this role).

Paradox: To see why such simplistic calculations are important, consider Fig. 4.5. The black line shows the exact density difference in the dimer versus temperature for moderate correlation and asymmetry. The blue curve is a Hartree-Fock calculation, while the red curve adds in the high-density limit of GS correlation. Finally, EZTA in green uses the exact GS functional (i.e. the best possible ZTA), which we had already found in Ref. [15], in the MKS equations, which therefore is the best possible calculation that ignores thermal XC contributions. By construction, this becomes exact in the zero-temperature limit. But, to our surprise, we found that the relative error in the free energy and density vanishes in the *high* temperature limit. In fact, as temperature increases, the fractional errors in the energy at first increase, and then start to lessen.

Resolution of paradox: How can this counterintuitive result be right? The answer is very simple. For high temperatures, the XC components of the energy remain finite (and actually shrink, see Fig. 4.6), while the KS contributions grow, at least in this simple case. Thus *any* XC approximation will produce the same effect. This is why all the approximations merge onto the exact line in Fig. 4.5 for sufficiently high temperatures. Of course, there can still be a significant absolute error in the free energy which might have important effects on

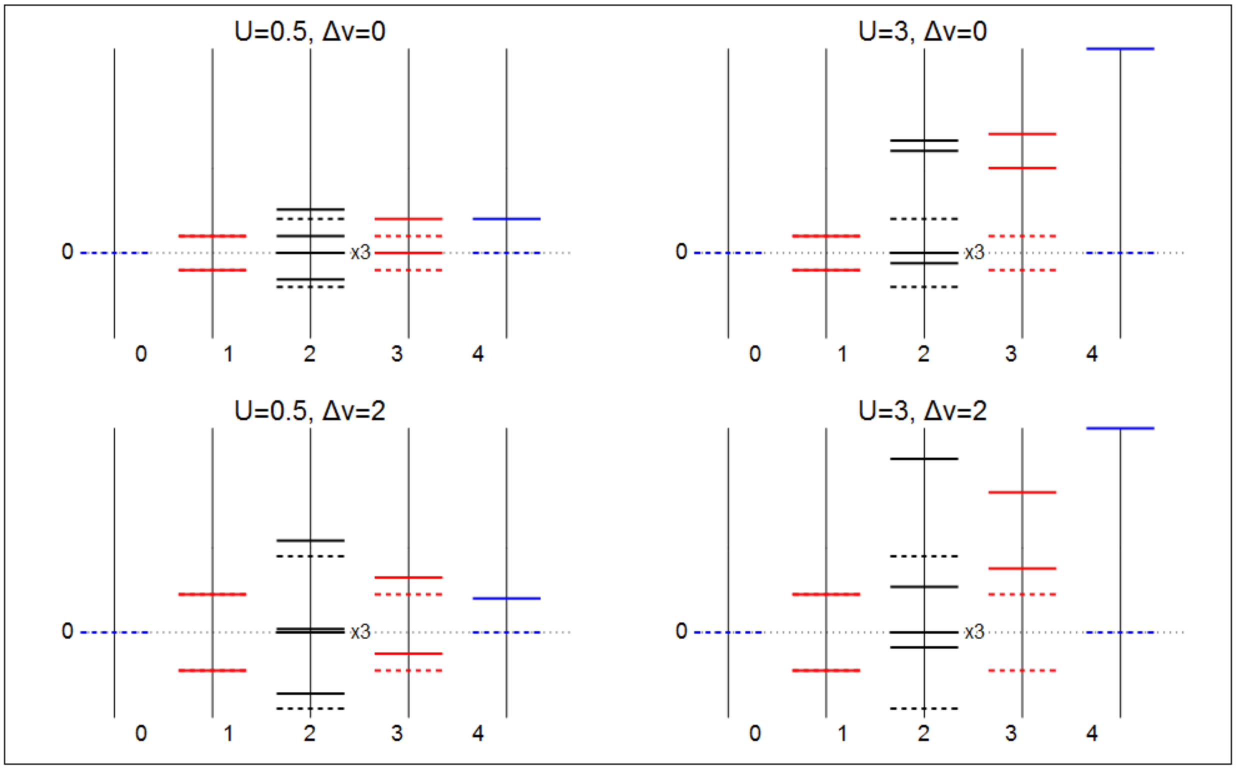

Figure 4.4: Energy spectrum for the Fock space of the asymmetric Hubbard dimer at various parameters ranging from weakly to strongly correlated. The x-axis is labeled by the number of particles. The dashed lines correspond to the non-interacting (tight-binding) case. The labels in the figures denote degeneracy. The triplet for $N = 2$ is always at $E = 0$ due to symmetry. The top left is symmetric and weakly correlated, so the spectral lines are close to the dashed ones. The top right is symmetric but strongly correlated, and the energies for $N = 2$ are substantially raised. We also see pairs of levels pushed together. The Hubbard bands of the infinite chain roughly run between these levels. In the lower panels, we turn on asymmetry, and show the effects on U.

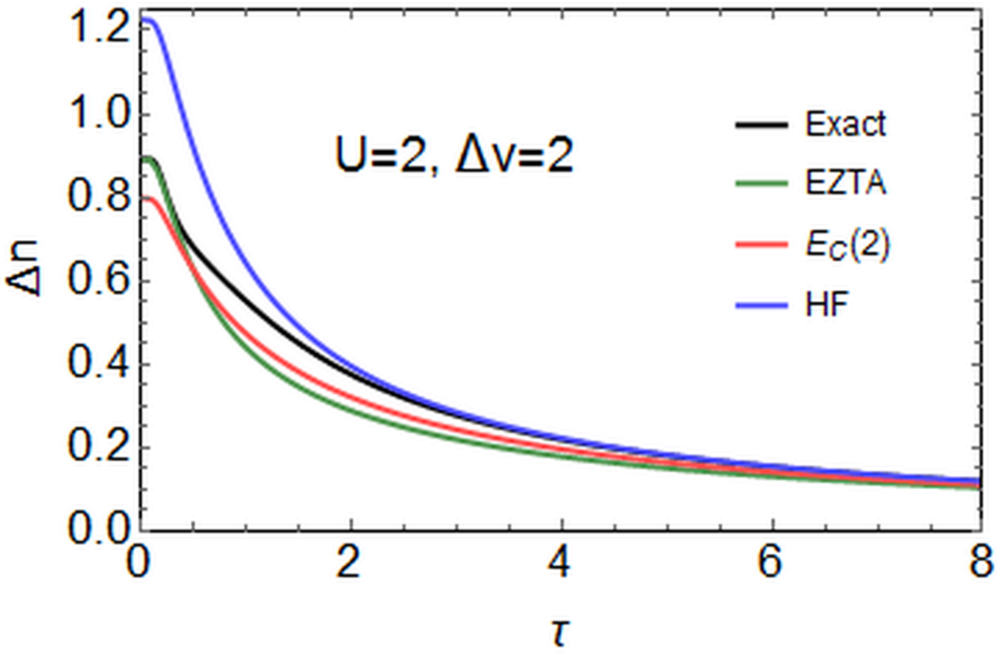

Figure 4.5: Difference in on-site densities as a function of temperature for an asymmetric Hubbard dimer with $U = 2$ and site-potential difference 2 (in units where the hopping parameter $t = 1/2$). The approximate calculations are all MKS-DFT-ZTA equilibrium calculations where HF denotes Hartree-Fock, $E(2̧)$ includes the leading correlation correction to HF in powers of the interaction, while EZTA denotes using the exact ground-state XC functional[15].

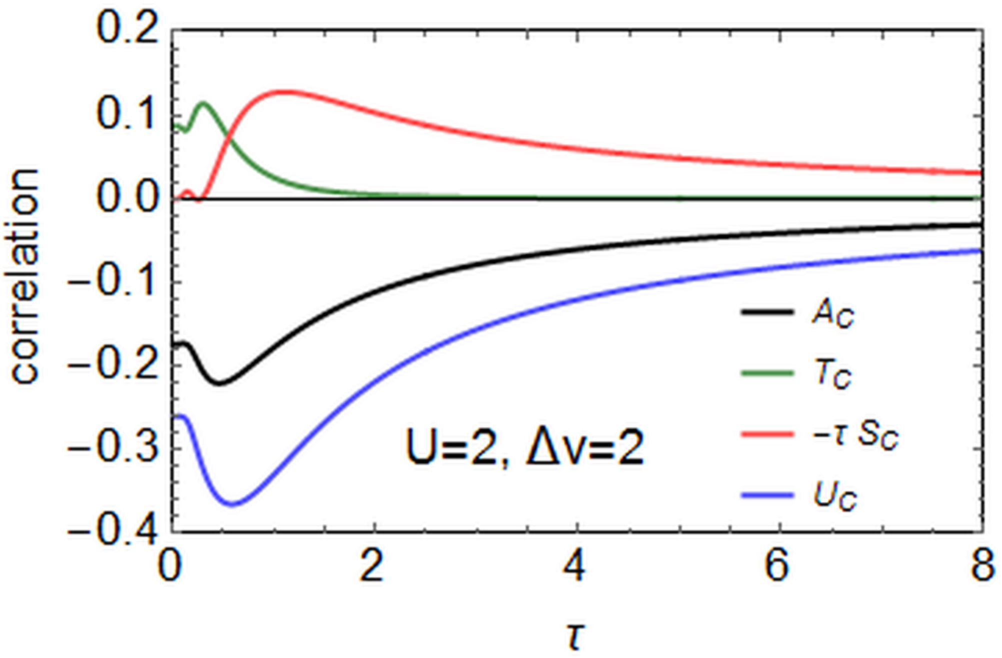

Figure 4.6: Correlation energy components as a function of temperature. All inequalities proven in Ref. [125] are satisfied. This figure shows that the naive assumption that $A_{_C}^{\tau}$ is bounded by $E_{_C} = A_{_C}(\tau = 0)$ is not true. Fig. 1 of Ref. [147] shows that the total free energy increases in magnitude as temperature increases, making the XC contribution relatively less important. Thus ZTA (or any reasonably bounded approximation) will yield relatively exact free energies, densities, and KS orbitals, in the limit of high temperatures. Additionally, Ref. [147] notes that exchange is temperature independent and has no effect on this analysis.

quantities of interest. But the principle is clear: EZTA becomes relatively exact in both the low- and *high*-temperature limits. This is also trivially true for the uniform gas, once the (infinite) Hartree energy is included, and we suspect it to be true for all systems.

Relevance for response functions: The increasing accuracy of the density with temperature has very important implications for calculations of conductivity. This means that the error in the KS orbitals, used in the construction of KS conductivities, starts to decrease beyond some temperature. This is true for *any* GS approximation for XC (within reason). All these conclusions may explain the tremendous success so far gotten by ignoring the thermal XC effects, especially for conductivities.

4.5.3 Beyond equilibrium: Linear response thermal time-dependent DFT

Zero temperature: There are many applications in WDM where the system is perturbed away from equilibrium. At zero temperature, the standard approach to such problems is to apply TDDFT or many-body non-equilibrium Green's function methods[151]. TDDFT in particular[135] can handle both strong perturbations, such as atoms and molecules in intense laser fields, and weak perturbations, where the linear response formulation yields excitation energies and oscillator strengths[11].

General case too difficult: Unfortunately, the situation is very complicated if the perturbation is strong, as then a non-equilibrium treatment is needed. Theories in which the temperature is held fixed do not apply. This is the situation for example in calculations of stopping power[45]. There are many fine attempts to overcome these difficulties under a variety of practically useful conditions[131], but we have not seen a way to construct a general DFT treatment of such problems.

Linear response: For a finite system (which has to be very carefully defined in the thermal case), we proved a limited theorem for the linear density response to a time-dependent external field[127]. This proof allows for (finite numbers of) degeneracies in the excited states, but not in the equilibrium state. Armed with such a theorem, all the usual XC response properties, such as the XC kernel, can be defined at finite temperature. Combined with our thermal connection formula, we have the finite-temperature generalization of the Gross-Kohn response equation[52]:

$$\chi^\tau(12) = \chi^\tau_{\rm s}(12) + \int d3d4\, \chi^\tau_{\rm s}(13) f^\tau(34) \chi^\tau(42), \tag{4.23}$$

where 1 denotes the coordinates $\mathbf{r}, t$, and 2 another pair[70], $\chi^\tau(12)$ is the density-density response function at temperature τ, $\chi_{\rm S}$ its KS counterpart, and $f^\tau(12)$ the thermal Hartree-XC kernel. This becomes the Random Phase Approximation (RPA) when $f_{\rm XC} = 0$. Insertion of this into the thermal connection formula yields an RPA-type equation for the XC free energy[127]:

$$A^\tau_{\rm XC}[n] = \lim_{\tau''\to\infty} \frac{\tau}{2}\int_\tau^{\tau''} \frac{d\tau'}{\tau'^2}\int_0^\infty \frac{d\omega}{2\pi}\coth\left(\frac{\omega}{2\tau}\right)\int d\mathbf{r}\int d\mathbf{r}'\,\frac{\Im\chi^{\tau'}[n_\gamma](\mathbf{r},\mathbf{r}',\omega)}{|\mathbf{r}-\mathbf{r}'|} \tag{4.24}$$

where γ is defined in Eq. (4.21). If XC contributions to the kernel are neglected, this becomes the long-known random-phase approximation to the XC free energy, albeit using the KS orbitals. Since random-phase approximation calculations have become standard within the GS materials world[138], there is little additional computational demand in performing them at moderate finite temperatures. Inclusion of any approximate treatment of the XC kernel yields an entirely novel approach to XC approximations for equilibrium thermal DFT. In particular, one can consider making a uniform approximation in both space and time, and also decide whether or not to include thermal corrections in an approximate kernel. All such treatments can be first tested on a uniform gas, for which the XC free energy is accurately known from QMC calculations[28].

4.6 Recent applications of DFT in WDM

Planetary science: The materials of interest in WDM research span the periodic table. Accurate thermal conductivities for inertial confinement fusion fuel materials such as deuterium and tritium are needed to find the calculated total neutron yield in fusion science (the simulated mixing between the fuel and coating on inertial confinement fusion capsules is very sensitive to thermal conductivities)[62]. Accurate iron thermal conductivities are used to determine whether the conventional model for how the Earth's core developed is valid because heat flux contributes to the Earth's geomagnetic field. Differential heating experiments at ALS, LCLS, Omega, and Titan facilities are all done slightly differently (heating via optical lasers, XFEL, x-rays, or proton heating), to fit hydrodynamics models because of their high accuracy and because other approaches (SESAME, Purgatorio, and Lee-More) all differ[6, 88, 170]. Our work suggesting that ignoring XC thermal corrections nevertheless yields accurate KS eigenstates and eigenvalues[147] helps explain why conductivities can be accurate in these calculations.

Much WDM research is motivated by the desire to understand planetary interiors. The Juno mission is measuring Jupiter's gravitational field extremely accurately, constraining theories of its interior[103], while Kepler has shown that many notions of planetary formation must be rethought with our new data on extra-solar planets[21]. But there is limited understanding of whether initial planetary protocores remain stable during accretion or if they dissolve into outer metallic hydrogen layers. Recent DFT-MD calculations show that MgO is surprisingly soluble in hydrogen under these conditions[171]. Similarly, the moon is thought to have formed in an enormous impact, but such a scenario depends crucially on the equation of state of MgO under extreme conditions. Recent DFT calculations and Z-machine experiments have nailed this EOS more accurately than before, and far better than unreliable extrapolations from more mundane conditions[134].

Alternate methods: Path integral Monte Carlo is an excellent tool for studying WDM, and has been recently extended beyond small atoms to include water and carbon, and has recently been shown to match reasonably well with DFT calculations at lower temperatures[31], validating both. Meanwhile, DFT calculations have predicted new superionic phases of H_2O, under conditions relevant to Uranus and Neptune interiors[172].

DFT failure: A less successful application of DFT in WDM is to the liquid insulator to liquid metal transition in dense D_2, at about 1000K and 300 GPa. DFT calculations with several different functionals yield very different results, none of which are in satisfactory agreement with experiment. The interpretation also depends on the accuracy of the conductivity from the DFT calculations. This system remains a challenge to WDM simulations.

X-ray Thompson scattering: Some of the most exciting recent experiments have been from the LINAC at SLAC, allowing X-ray Thompson scattering (XRTS) measurements of shocked materials. These include the first highly resolved measurements of the plasmon spectrum in an ultrafast heated solid[150]. Ref. [24] gives x-ray scattering results from plasmons in dynamically compressed deuterium, from which one can deduce the ionization state as a function of compression. Ionization begins at about the pressure that DFT-MD calculations show molecular dissociation. In a completely different material, X-ray diffraction showed diamond formation on nanosecond timescales, caused by shock compression to about 200 GPa[82]. This helps explain why the lonsdaleite crystal structure occurs naturally close to meteor impacts.

XRTS has been performed on a variety of materials including Be, Li, C, CH shells, and Al. Most experiments probe the electron dynamic structure factor, which is decomposed via the somewhat ad-hoc Chihara decomposition into bound, loosely bound, and free electrons[5]. But by running TDDFT at finite temperatures, one directly calculates the densities, and can then test the accuracy of Chihara for determining the ionization state. The results of Ref. [127] are already being used to justify thTDDFT calculations such as Ref. [5].

4.7 Relation of thermal DFT to quantum chemistry

At first glance, it would appear that warm dense matter has little or nothing to do with chemistry. In fact, this is not true, it is simply chemistry in an exciting new regime with which we are relatively unfamiliar.

To see this, we first note that the plasma physicists who usually study WDM think in terms of average properties of their systems, such as mean densities and numbers of electrons ionized.

They are familiar with density functional methods, but traditionally only at the level of the LDA. Successes with such an approximation are often attributed to systems being somehow ‘locally uniform’.

But the success of DFT methods in chemistry can be directly correlated with the arrival of the GGA and hybrids of it with Hartree-Fock. These approximations were tested on the G2 data set, and shown to yield much better energetics than LDA, because the G2 data set had already been carefully constructed and benchmarked, using both quantum chemical methods and experimental information[22, 85, 115]. This vote of confidence led to their widespread adoption in many branches of chemistry, and also led to the confidence that GGAs were better than LDA for many materials problems.

It is the same GGAs, used in MD simulations, that have led to the revolution in WDM simulations over the past decade or so[89]. The improved accuracy due to GGAs implies that the details of the electronic structure matter, and that these systems are in no way locally uniform. In fact, in many cases, there are large evanescent regions of the HOMO, just as in gas-phase molecules. The KS system is ideal for computing this, and GGAs and hybrid account for the energetic consequences. So the very success of DFT-MD for WDM implies that the detailed chemistry is vital, even if it is happening within simulations of extended systems under high temperature and pressure.

The recent work in our group is almost entirely focused on bringing GGA-level XC technology to the WDM field. Being able to distinguish among different components of the correlation energy, and switch from one to another, is a crucial part of the exact conditions that were used to construct GGAs[126]. The adiabatic connection formula is often invoked in modern DFT research to understand both exact DFT and approximations, and its recasting as a temperature integral should prove useful in the search for accurate thermal XC approximations.

On the other hand, ground-state DFT has benefited enormously from testing on benchmark data[139, 35]. But for thermal effects, even a simple H atom is difficult, as one must include sums over all possible particle numbers in the partition function. The asymmetric Hubbard dimer is the simplest imaginable exactly-solvable model, and can be considered a model for H_2 in a minimal basis when we take the symmetric limit. While the truncated Hilbert space makes it unrealistic at higher temperatures, it also makes it practical to solve exactly. Thus our calculations on this model demonstrate the behavior of correlation at finite temperatures in one simple case. Unfortunately, due to the lack of a continuum, this cannot be used to check the performance of LDA or GGA.

Thermodynamics tells us simple relations between entropy and free energy and other quantities. But it requires very careful reasoning to deduce the corresponding relations among density functionals, as the density must be held fixed, not the external potential. Our relations between entropy and the universal part of the Mermin functional show this, and subtraction of the corresponding KS contributions yields crucial relations among correlation contributions. They also yield simple inequalities that are not automatically satisfied once thermal XC contributions are approximated.

Lastly, the recent proof of TDDFT for finite temperatures within linear response justifies the extraction of conductivities within the Kubo response formalism from KS orbitals and energies. It also shows that the random-phase approximation, which is now routinely calculated for inhomogeneous systems in many codes in both quantum chemistry and materials science[83, 42, 43, 37, 36, 44], might be an excellent starting point for more accurate approximations to the XC thermal corrections, using approximations to the temperature-dependent XC kernel.

Finally, our recent work explains how ignoring thermal XC effects, which is usually done in practical DFT WDM calculations, might not be as poor an approximation as it first appears. Calculations on the Hubbard dimer show that XC effects become relatively less important as the temperature increases. Thus the errors in the self-consistent density and orbitals caused by any approximation to the XC lessen with increasing temperature, so that calculations of the KS conductance should be more accurate as temperature increases (somewhat counterintuitively).

To summarize, the success of modern density functional approximations in WDM simulations strongly implies the importance of chemical phenomena in such simulations, and the need to accurately approximate the energetics.

4.8 Conclusion

Thermal density functional theory is an increasingly utilized tool for calculations of hot systems such as warm dense matter. These WDM systems include inertial confinement fusion, planetary interiors, and shock experiments. There have been many recent developments ranging from exact conditions, improved understanding, and extensions beyond equilibrium with more foreseeable, and exciting, improvements on the horizon. These steps forward set up the foundation for further future success of thermal DFT in the years to come.

First and foremost, I must thank my advisor Professor Kieron Burke, for taking me as a PhD student, and putting up with me for 5 years. While I did not have any previous theory experience, he gave me the opportunity to change my research direction. He provided the space for me to grow as a scientist, and gave me and everyone in the group many valuable opportunities for which I am profoundly thankful. Thank you Kieron for repeatedly answering my questions (even if it was the same question), but most importantly thank you for listening to me and my concerns, even when they were not academic in nature.

I would also like to acknowledge my thesis committee members, Professors Vladimir Mandelshtam and Craig Martens, who also served in my advancement committee. I would like to specially thank Professor Rachel Martin who was the chair of my advancement committee, and who's words of encouragement were always perfectly timed.

I would like to specially acknowledge Dr. Attila Cangi, who recruited me to intern at Sandia National Laboratories during my third year. This internship gave me some much needed time away from my coursework in Irvine. It gave me a peek of what large scale science is like at the national labs. Attila's seemingly endless patience and vast knowledge also gave me the confidence that I could in fact be a competent scientist. Working with Attila, has truly been a pleasure. Being a year round intern at Sandia for the last two years of my degree was unexpected experience for which I am thankful.

Next I must thank all of the friends I made while at Irvine. Our frequent chats and outings made the overall experience much more enjoyable. Special thanks to Kara Thomas, Sabrina Chee, and Sara Taydeon, with whom I worked in the trenches. I would like to acknowledge my childhood friend Sydney Everratt, with whom I shared many fun excursions through out southern CA (and CO), and who most importantly reminded me that life is fun outside of academia (and the sterility of Irvine). I cannot overlook the great discussions and friendships I formed with older theory graduate students. In particular I thank Saswata Roy, Sree Ganesh Balasubramani, and Guo Chen who without hesitation would explain whatever concepts in quantum chemistry I would barge into their office with.

I would like to thank all current and past Burke group members, with whom I shared offices, coffee breaks, and cookies. I must specially thank Dr. Ryan Mccarty who was the best office mate I had, and who's surprisingly relentless optimism made group lunches and meetings more enjoyable. In addition, I must thank Ryan for all of the effort he put into helping pass my advancement exam. I would like to also thank Dr. Dennis Perchak, who's stories always put a smile on my face. His kind words during my exam also gave me some much needed encouragement.

Finally I must thank my family, whom I cherish dearly. My parents are my biggest cheerleaders, and I must thank my father for always pushing me to do my best, and reminding me that that "se hace camino al andar" whenever I was struggling. I would lastly like to thank my sister Maca, who I managed to talk with on almost a daily basis, even though we were 9 time zones apart. Having the support of family truly is a privilege to which I am eternally grateful.

This dissertation contains verbatim excerpts as they appear in *Journal of Chemical Physics* and *Springer Nature*. Chapter 2 is reproduced from, F. Sagredo and K. Burke, *J. Chem. Phys.* **149**, 134103 (2018), with the permission of AIP Publishing. Chapter 4 is reprinted/adapted by permission from *Springer Nature*, *Frontiers of Quantum Chemisrty* by J. C. Smith, F. Sagredo, and K. Burke (2017). The co-authors listed in these publications directed, supervised, or conducted part of the research which forms the basis for the dissertation. The authors acknowledge support from the US Department of Energy (DOE), Office of Science, Basic Energy Sciences under Award No. DE-FG02-08ER46496. J.C.S. acknowledges support through the NSF Graduate Research fellowship program under Award No. DGE-1321846.

Chapter 5

Confirmation of the PPLB derivative discontinuity: Exact chemical potential at finite temperatures of a model system

This chapter was replicated verbatim from a recent submission (Arxiv:2007.03840), and is a project which generalizes a model of the derivative discontinuity at zero temperature from the 1980's to the realm of finite temperature DFT. This paper was written with my advisor Kieron Burke, and I contributed to making figures and writing.

5.1 Abstract

The landmark 1982 paper of Perdew, Parr, Levy, and Balduz (often called PPLB) laid the foundation for our modern understanding of the role of the derivative discontinuity

in density functional theory, which drives much development to account for its effects. A simple model for the chemical potential at vanishing temperature played a crucial role in their argument. We investigate the validity of this model in the simplest non-trivial system to which it can be applied and which can be easily solved exactly, the Hubbard dimer. We find exact agreement in the crucial zero-temperature limit, and show the model remains accurate for a significant range of temperatures. We identify how this range depends on the strength of correlations. We extend the model to approximate free energies accounting for the derivative discontinuity, a feature missing in standard semilocal approximations. We provide a correction to this approximation to yield even more accurate free energies. We discuss the relevance of these results for warm dense matter.

5.2 Paper

A crucial concern for density functional theory (DFT) calculations of semiconductor solids in the 1980's was whether the systematic underestimate of the band gap represented a limitation of approximations, or a fundamental deficiency of Kohn-Sham (KS) DFT [81]. The paper of Perdew, Parr, Levy, and Balduz (PPLB) [122] argued clearly that the band gap of a pure KS DFT calculation does not in general match the fundamental gap, even if the exact functional is used [167]. In the decades since, this understanding has become a cornerstone of modern DFT. Its generalization to include spin-degrees of freedom [4, 117] has led to approximate functionals that explicitly account for delocalization errors [153, 96, 120, 116, 57]. A deep but more accessible background article was written by Perdew only a few years later [114].

A vital step in the logic of this work is the introduction of the grand canonical (gc) ensemble to couple the electronic system of interest to a thermodynamic bath. At any finite temperature [60], even the exact functional is a smooth continuous function of the average particle number $\mathcal{N}$, but develops steps at integers that sharpen as the temperature is lowered. As the temperature tends to zero, the gc ensemble reduces to a linear ensemble between the integers, which in turn leads to the modern theory of ground-state DFT for non-integer particle numbers [29]. As bonds are stretched, or electrons added and removed from solids, the energetic consequences can be directly related to the discontinuities in the slope of the energy as a function of $\mathcal{N}$. Many of these effects, like charge transfer in molecular systems are missed by semi-local approximations which, by construction, have no discontinuities [124, 159, 96, 158, 79, 72, 58, 110]. Hence the ongoing desire to create approximations that can quantitatively account for such effects [153].

In the last two decades, DFT calculations at finite temperature have helped revolutionize the field of warm dense matter, by producing chemically specific quantitative predictions for present-day shock experiments [148]. Their legitimacy stems from Mermin's theorem [60], which generalizes the Hohenberg-Kohn theorem [59] to non-zero temperature, and therefore non-integer average particle numbers. Modern warm dense calculations run standard solid-state codes to solve the KS equations, with finite temperature Fermi occupations. These are used to model shock experiments, [133], understand planetary cores [25, 109], and even model inertial confinement fusion [76, 78]. Thus there is rapidly growing interest in the theory of equilibrium electronic structure beyond the ground-state.

In the current work, we calculate the chemical potential of a simple model system exactly, as a function of average particle number and temperature. We confirm the ansatz behind the PPLB work: their approximation to the chemical potential becomes relatively exact for all particle numbers as the temperature $\tau \to 0$. For our simple system, we also explore up to what temperatures the PPLB formula works. We also generalize the PPLB model to extract the free energy, and explore its accuracy. We explore how the strength of correlations affect the accuracy of the PPLB approximation. Finally, we give a generalization that corrects an obvious limitation of the PPLB model.

Fig. 5.1 illustrates our key results nicely. The chemical potential is very smooth at higher

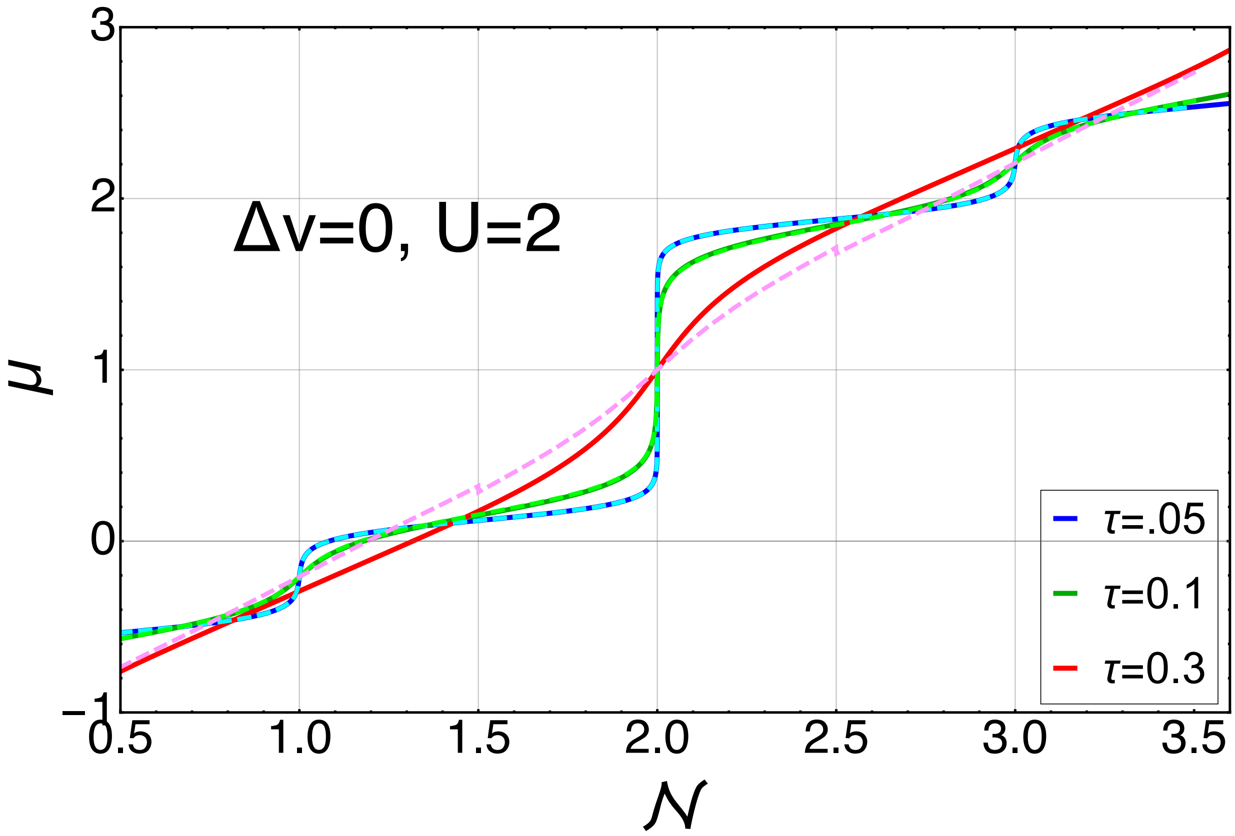

Figure 5.1: Exact (solid) and PPLB (dashed) chemical potentials in the symmetric ($\Delta v = 0$) Hubbard dimer at $U = 2$ with various temperatures τ, with $2t = 1$.

temperatures, but steps develop around integer particle numbers as the temperature is lowered. The PPLB approximation becomes exact in the limit of zero temperature, matching the exact derivative discontinuities, but in this system, the PPLB model continues to work well even at significant warm temperatures, as shown for $\tau = 0.3$. Ironically, unlike local and semi local DFT approximations at zero temperature, the PPLB model's largest error is at half-integers, where it incorrectly jumps discontinuously. The error at these half integer particle numbers is due to its dependence on the nearest integer to $\mathcal{N}$.

We begin with a brief recap of the PPLB argument. For a finite system in contact with a bath at temperature τ, with which it can exchange both electrons and energy, its equilibrium properties are given by the gc ensemble. The gc partition function sums over all particle numbers, N, and eigenvalues [143]. For sufficiently low temperatures, the ground-state energy will dominate over all others for each value of N, so all excited state contributions can be ignored. Moreover, the convexity of $\mu N - E$ ensures that, for $\mathcal{N} = M + \nu$, where $|\nu| \leq$, the partition function will be dominated by only three contributions, from $M-1$, M, and $M+1$. Including just these three terms, one can solve explicitly for the chemical potential, μ, to find the PPLB approximation

$$\mu^{PPLB} = -\tau \log\left(\frac{-\nu + \sqrt{\nu^2 + 4h^- h^+ (1-\nu^2)}}{2h^-(1+\nu)}\right), \tag{5.1}$$

where

$$h^{\pm} = \frac{g_{M\pm1} \exp\left(-(E_M - E_{M\pm1})/\tau\right)}{g_M}, \tag{5.2}$$

and g_M and E_M are the degeneracy and ground state energy for M particles. As stated in Ref.[114], this form was derived only for the limit as $\tau \to 0$. However we will see that it can in fact be used for finite temperatures.

The inclusion of degeneracies first appears in Ref. [114]. In the zero-temperature limit, we make note of a few things. First, that $-\mu$ is simply the Mulliken electronegativity, χ, and second, the iconic results of $\mu = -I$ below an integer and $-A$ above, where I and A are the ionization potential and electron affinity, respectively. Moreover, $\mu = -(I+A)/2$ at the integers. This determines the plateaus in Fig. 5.1 since, at zero temperature, $\mu = \partial E/\partial \mathcal{N}$, so the size of the steps in μ are the derivative discontinuities in $E(\mathcal{N})$. In KS DFT, only part of these steps is in the KS kinetic energy, leaving crucial contributions in the ubiquitous exchange-correlation (XC) energy. As XC potentials are functional derivatives of XC energies, they have spontaneous steps as the particle number moves across an integer [57], and sharp features in the middle of strongly stretched bonds [57].

It is difficult to imagine calculating the analog of Fig. 5.1 sufficiently accurately from any first-principles Hamiltonian, as it requires sums over all states and all particle numbers, including those in the continuum. But the two-site Hubbard model has a tiny Fock space, with only 16 states total. Its Hamiltonian is

$$\hat{H} = -t \sum_{\sigma} (\hat{c}^{\dagger}_{1\sigma}\hat{c}_{2\sigma} + h.c) + U \sum_{i} \hat{n}_{i,\uparrow}\hat{n}_{i,\downarrow} + \sum_{i} v_i \hat{n}_i, \tag{5.3}$$

where $\hat{c}^{\dagger}_{1\sigma}$ and $\hat{c}_{2\sigma}$ are the creation and annihilation operators for each site, t is an electron hopping energy, U is the repulsion between the particles in each site, and $\Delta v = v_2 - v_1$ is the difference in external potential on the left and right sites [15]. We always choose $2t = 1$ to set the energy scale. In chemistry, the symmetric case ($\Delta v = 0$) is the Hamiltonian for H_2 in a minimal basis. For any Δv, $U = 0$ is the tight binding limit. Over the decades, the dimer has been used as a model for testing many concepts in KS DFT [3]. The density is characterized by a single number, $\Delta n = n_1 - n_2$. The analyticity of this model system makes it perfect for testing fundamental aspects in DFT. Recently, it formed the basis of reviews of both ground-state DFT [15] and linear response TDDFT [14]. The dimer was used to check approximations in ensemble DFT [137], to illustrate several theorems in finite temperature DFT [147], and even to study magnetism [162]. Here, we use it simply as the simplest non-trivial model of interacting electrons to which we can apply quantum statistical mechanics, and thus test the PPLB model. Previous work in finite temperature DFT used this model at finite temperature, but always restricted to $\mathcal{N} = 2$ [147]. Here we look at all $\mathcal{N}$, in order to accurately test PPLB.

Our first (and most important) result is already shown in Fig 1. For this simple model, the ansatz behind PPLB is correct, and the PPLB yields the exact zero-temperature limit of the chemical potential. From this fact (for any electronic system), all the subsequent deductions of PPLB follow. It is comforting to know this is true in the one case where μ can be found exactly.

But our next step is to explore PPLB for finite temperatures, and quantify how high in

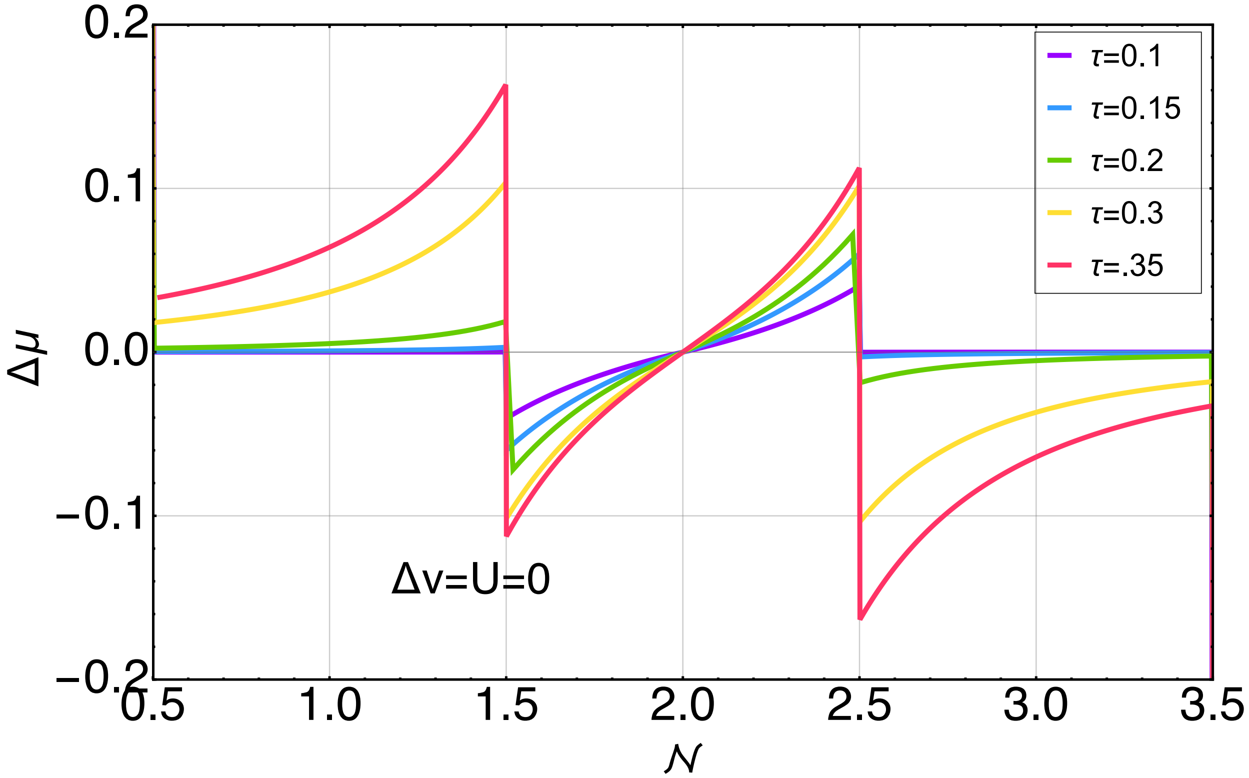

Figure 5.2: The absolute error in the approximate PPLB μ for the symmetric, tight binging case ($U = \Delta v = 0$), plotted with respect to the average particle number $\mathcal{N}$. Here $\Delta\mu = \mu - \mu^{PPLB}$.

temperature it can be considered to be working. This is beyond the original intent of the model, which was designed only to recover the zero-temperature limit. If we accept errors in μ up to some threshold, say 0.1 $a.u.$, then the PPLB chemical potential works for $\Delta v = U = 0$ until almost $\tau = 0.3$, or about 100,000K for $2t = 1$. This result is seen in Fig. 2.

Next, in order to make this more relevant, we use the PPLB model to construct a PPLB approximation to the Helmholtz free energy, A. The exact gc partition function is

$$Z(\tau, \mu) = \sum_{N,i} g_{N}^{(i)} \exp\left((\mu N - E_{N}^{(i)})/\tau \right), \tag{5.4}$$

where $g_{N}^{(i)}$ and $E_{N}^{(i)}$ are the the degeneracy and energy of the i-th state for N particles. The exact average particle number is then found via

$$\mathcal{N}(\tau,\mu) = -\tau \frac{d\log Z(\tau,\mu)}{d\mu}, \tag{5.5}$$

so that the free energy can then be written as

$$A(\tau,\mathcal{N}) = \mu(\tau,\mathcal{N})\mathcal{N} - \tau \log Z(\tau,\mu(\tau,\mathcal{N})), \tag{5.6}$$

where $\mu(\tau,\mathcal{N})$ is the inverse of eq. 5.5. As a step toward deriving eq. 5.1, we break down the derivation into two steps. First we introduce a simple (but different) continuous ground-state approximation, which includes only the ground states in the approximate partition function. Such a partition function, denoted as Z_{0}, is

$$Z_{0}(\tau,\mu) = \sum_{N} g_{N} \exp\Big((\mu N - E_{N})/\tau\Big). \tag{5.7}$$

For the Hubbard dimer at finite temperatures, this is a simple continuous function of μ with only five terms. Then,

$$A_{0}(\tau,\mathcal{N}) = \mu_0(\tau,\mathcal{N})\mathcal{N} - \tau \log Z_{0}(\tau,\mu_0(\tau,\mathcal{N})), \tag{5.8}$$

where $\mathcal{N}_0(\tau,\mu)$ is found from plugging Z_0 into eq. 5.5, and $\mu_0(\tau,\mathcal{N})$ is its inverse. This ground state approximation is plotted in Fig. 5.3 as the dotted lines, and is a smooth well behaved function. $Z_{_0}$ is a better approximation than the PPLB, *but* requires the ground state energies for all N_0 because $\mu^{^{PPLB}}$ is a piecewise function of $\mathcal{N}$, it is not found from a valid (or traditional) partition function. Instead, we define $A^{^{PPLB}}$ with eq. 5.9, inserting eq. 5.1 for μ_0, and truncate Z_0 to the three nearest integers.

$$A^{^{PPLB}} = \mu^{^{PPLB}}\mathcal{N} - \tau \log \widetilde{Z}^{^{PPLB}}(\tau,\mathcal{N},\mu^{^{PPLB}}), \tag{5.9}$$

where

$$\widetilde{Z}^{^{PPLB}}(\tau,\mathcal{N},\mu) = \sum_{J=M-1}^{M+1} g_{_J} \exp\left((\mu J - E_J)/\tau\right), \tag{5.10}$$

and M is the integer closest to $\mathcal{N}$. For the Hubbard dimer, this means that $\widetilde{Z}^{^{PPLB}}$ is a discontinuous, piecewise function. While eq. 5.10 is not a traditional partition function, as it is a function of $\mathcal{N}$, it still does rather well in approximating the free energy of the system. Notice that the difference between $A^{^{PPLB}}$ and $A_{_0}$ becomes negligible as $\tau \to 0$.

A feature that makes the Hubbard dimer extremely useful in DFT studies is that one can make correlation arbitrarily strong. For the symmetric case (that is at $\Delta v = 0$), $U = 2$ is the point at which it switches from weakly to strongly correlated [14, 137]. For strong asymmetry (when $\Delta v >> 1$), this happens near $U = \Delta v$ (see Fig 7 of Ref.[14]). In Fig 5.3, we show the performance of our PPLB free energy model when U is small. In sharp contrast to semi-local approximations, it perfectly captures discontinuities at integer values, but artificially introduces steps at *half*-integers, which are noticeable when the value of τ is

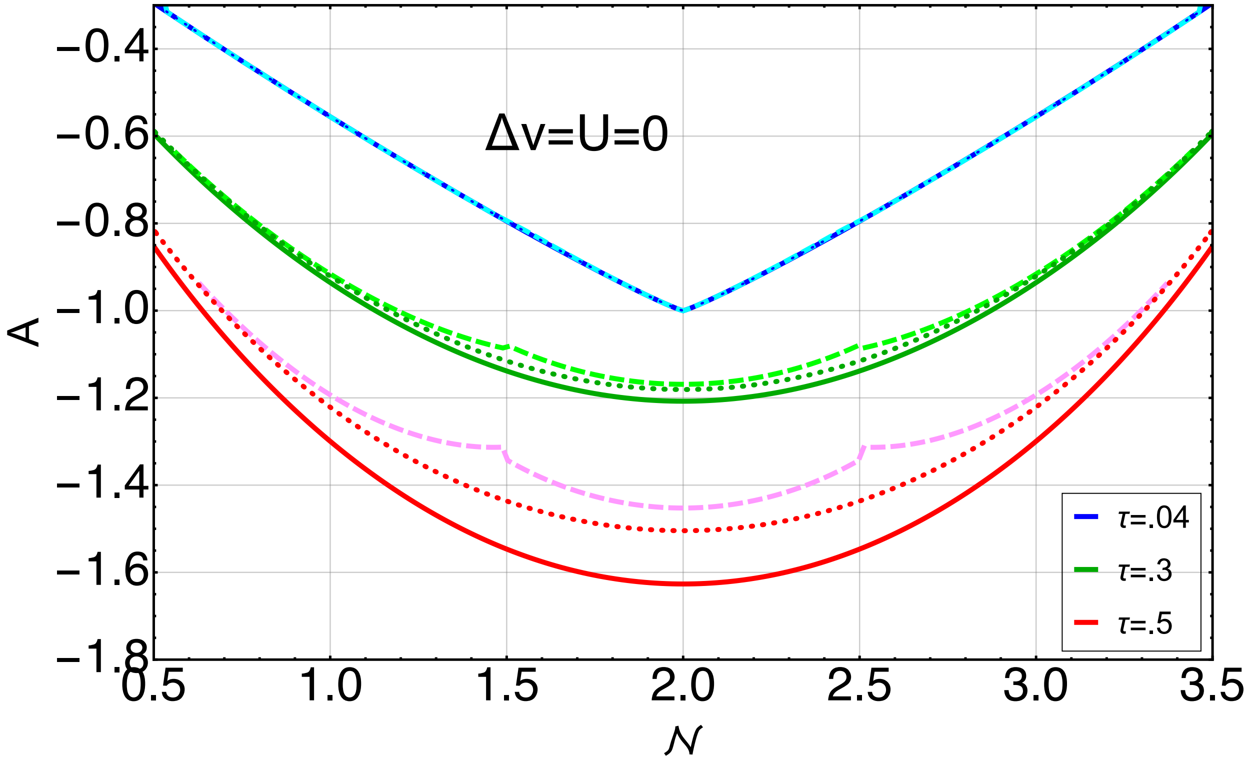

Figure 5.3: Free energy A, plotted for various temperatures, for $U = \Delta v = 0$. Brighter dashed lined correspond to A^{PPLB}, dotted lines are the ground state approximation to the free energy, A_0, and solid lines are the exact values.

large enough.

While the symmetric case for 2 sites (and the homogeneous case for many sites) is the most frequently studied in many-body condensed matter physics, one must consider inhomogeneity to understand the density functional aspects of the problem [14]. We next turn on significant asymmetry ($\Delta v = 5$), and in Fig 4, we plot PPLB for $U = 2$ and $U = 10$. Here a few things are noted. First, that using this A^{PPLB} gives a surprisingly accurate approximation to the free energy, even at finite temperatures. Second, that the largest magnitude of the absolute error *always* appears at either $\mathcal{N} = 2$ or $\mathcal{N} =$ half-integer, with the errors vanishing at the endpoints or when $\mathcal{N} = .5, 3.5$, in this model system. This is in contrast to what was seen in Fig. 5.1, where the errors in μ^{PPLB} *always* vanish at $\mathcal{N} = 2$. Finally, the PPLB free energy works best for weak correlation ($\Delta v >> U$) and fails quantitatively for strong correlation ($\Delta v << U$), just as semilocal functionals do [14, 137]. Most importantly, as stated in the original PPLB paper, the approximation becomes exact at the zero temperature limit, capturing the derivative discontinuities.

We can summarize the efficacy of the PPLB absolute error in the free energy, ΔA, with a contour plot in the $(U - \Delta v)$ plane. We make a crude contour plot of the temperatures at which the absolute error in the free energy using this PPLB approximation is no greater that 0.1 *a.u.* for any value of $\mathcal{N}$, and the colors of the contour correspond to the temperature at which $\Delta A = 0.1$ *a.u* occurs. Fig. 5.5 shows these results. This calculation uses a coarse grid due to computational cost, caused by the discontinuous changes in the PPLB errors, but the structure is clear. There is an obvious divide seen between the strongly and weakly correlated regimes [14, 137]. Clearly, the PPLB approximation works better for the weakly correlated regime where steps are small, and τ reaches high temperatures before the error reaches 0.1 *a.u.* Likewise, as the value of U increases to a point $\Delta v << U$, then the maximum temperature for our benchmark error decreases substantially.

Lastly, we consider how one might extend the temperature range of the accuracy of the PPLB free energy. We simply include the most relevant terms beyond those included in μ^{PPLB}. Since the PPLB partition function includes only the ground-state contribution for each N, the addition to include the first excited state energy to all N seems to be the most obvious. This correction can be included in eq. 5.1, by simply replacing each g_M with $\widetilde{g}_M$, where

$$\widetilde{g}_M = g_M + g_M^{(1)} \exp\left(-(E_M^{(1)} - E_M)/\tau\right), \tag{5.11}$$

$g_M^{(1)}$ and $E_M^{(1)}$ correspond to the degeneracy and first excited state for M particles.

In Fig. 5.6 we compare the exact free energy, the PPLB approximation, the ground state approximation, and our correction to the PPLB free energy. Clearly, there is an improvement when compared to the PPLB formalism at the largest quantitative errors. When the half-integers are the points of largest quantitative errors, that is when $\Delta v >> U$ (and thus weakly correlated), this would cause havoc for any derivatives of the energy in a real system, such as those used to find densities. These steps are places where one value of a parameter is suddenly swapped with another and when the nearest integer changes. So these parameters include the fundamental gap, the ionization energy, and the degeneracies of the energy levels. Any simple smoothing function, or correction to the PPLB could eliminate these. In Fig. 5.7, we compare the results for ΔA with the PPLB approximation, and our correction for various τ. In these figures, it is clearly seen that our correction provides a substantial improvement to A^{PPLB}, even at higher values of τ.

To put this work in context, our Hubbard dimer looks nothing like the systems used in KS DFT warm dense matter simulations [76, 78, 25, 109]. However, such calculations often have features driven by the underlying molecular structure, for which energetic consequences of the derivative discontinuity are known to be quantitatively relevant. Our study here has focussed on the full chemical potential and free energy of the system, not the exchange-correlation contributions that are so important in density functional theory. Our general results apply to finite temperature simulations of localized electrons in any formalism, and so can be used to gain insight into WDM simulations of any kind. The relevance of the PPLB reasoning, and its extension to free energies at finite temperatures given here, is likely unknown in the general WDM community. For example, ionization lowering [68, 152] can now be related to the behavior of both the chemical potential and the free energy. Our work is in the spirit of simple conditions at zero-temperature [147]. We have found that (1) the PPLB was correct as derived for the limit $\tau \to 0$. We have shown what an exact treatment should do, and how well the PPLB model captures this, and (2) how one can understand up to what temperatures it will be accurate. We have (3) used the PPLB formalism to accurately simulate the free energy at finite temperatures, even though this approximation to the chemical potential was originally intended for the zero temperature limit. Last, we have (4) provided a correction to this PPLB model to make it even more useful.

In terms of real-world applications, for any finite temperature KS DFT calculation of a molecular system [51], one could easily construct the PPLB free energy, using only total energy differences as inputs. These could come from either a highly accurate quantum chemical calculation, or even a DFT calculation. The error estimates requiring excitation energies could be extracted from TDDFT [14, 97] or an ensemble DFT calculation [173, 137]. Then an accurate picture of the free energy can be calculated up to reasonable temperatures using PPLB.

5.3 Acknowledgments

F.S and K.B acknowledge support from the Department of Energy, Award No. DE-FG02-08ER46496.

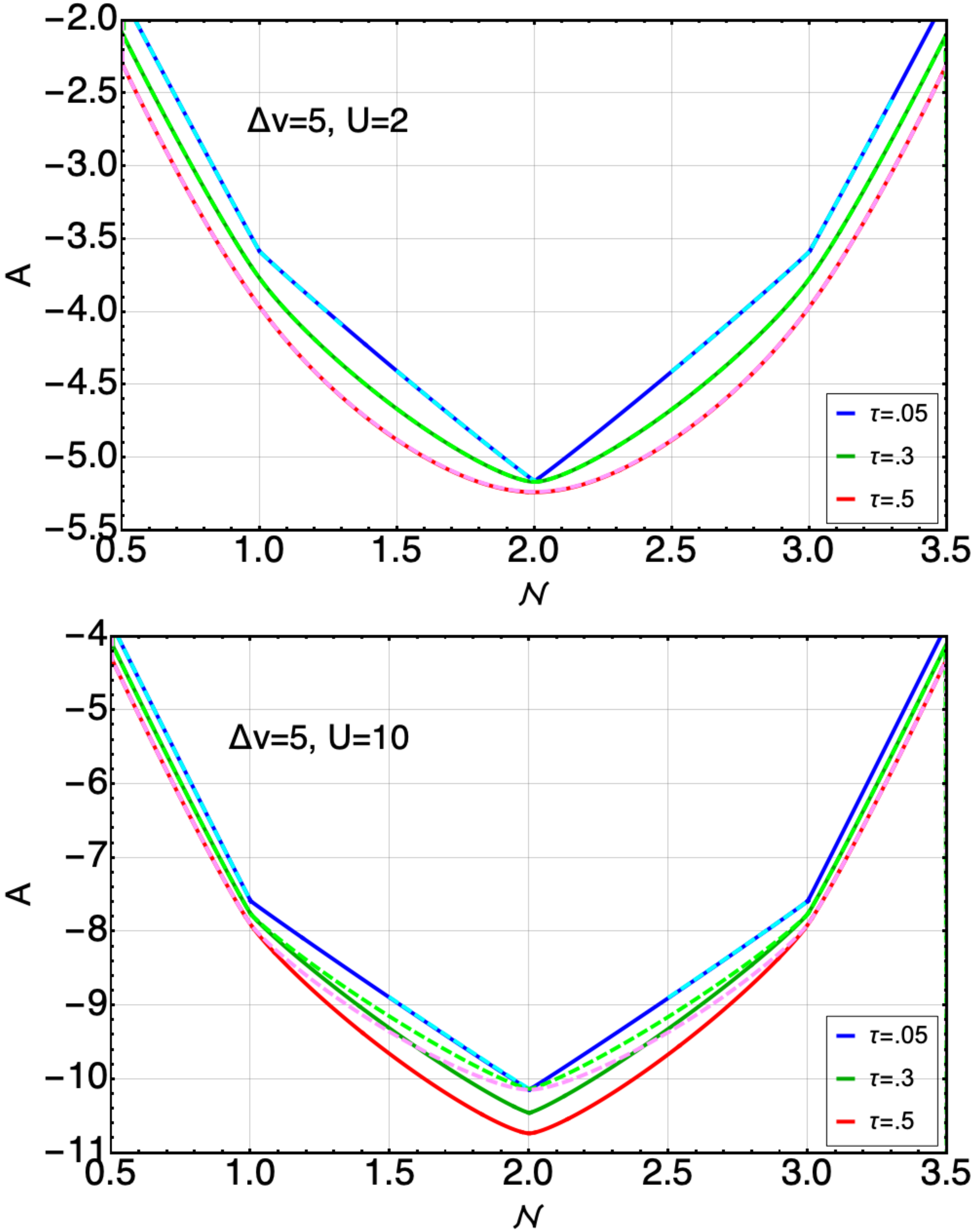

Figure 5.4: Free energy, for weakly correlated, (top panel), and strongly correlated regimes (bottom panel), plotted with respect to the average particle number $\mathcal{N}$.

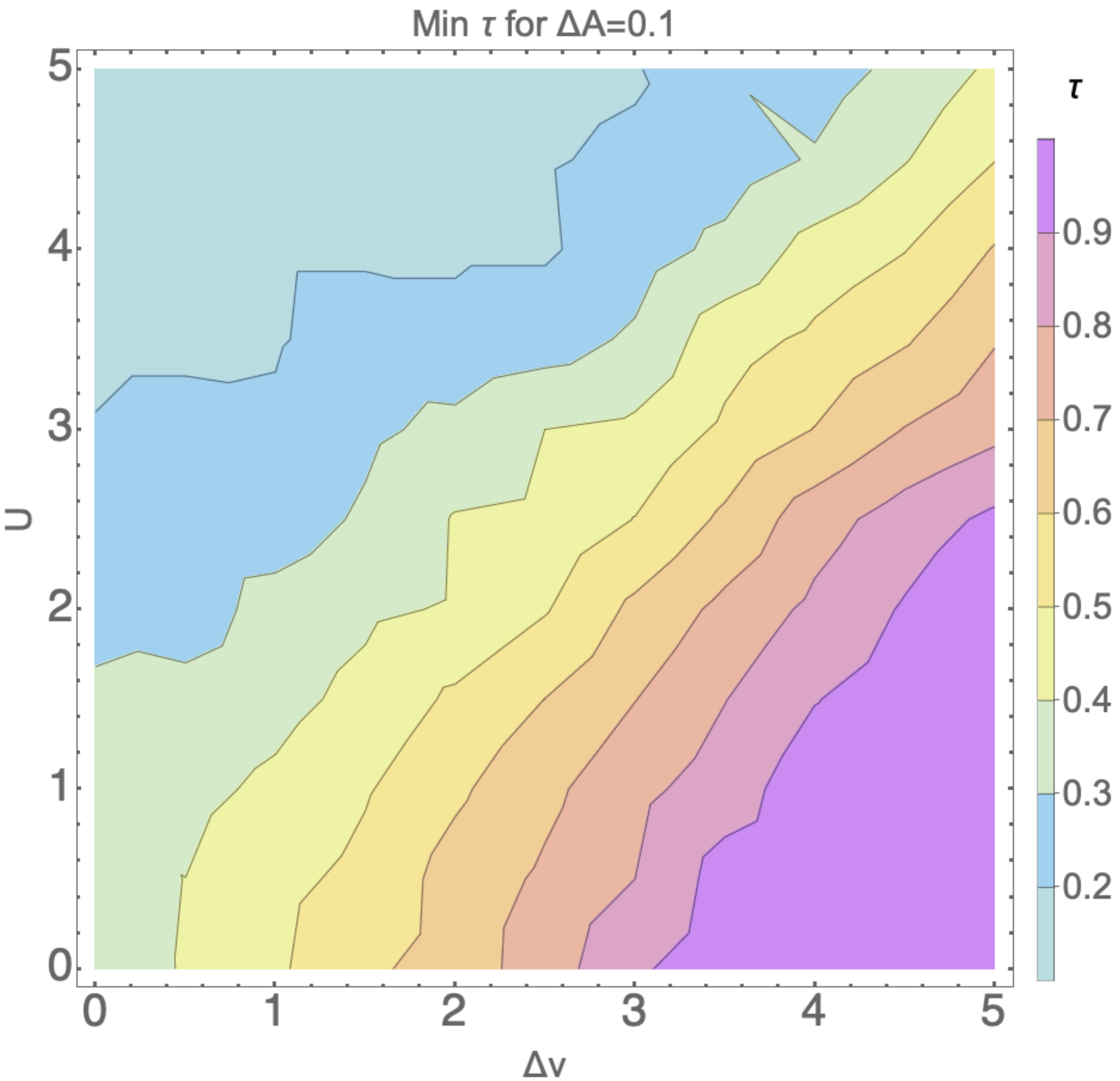

Figure 5.5: Contour plot of the minimum value of the temperature τ which gives absolute errors to the free energy $\Delta A = A - A^{PPLB}$ of 0.1, plotted for various Δv and U.

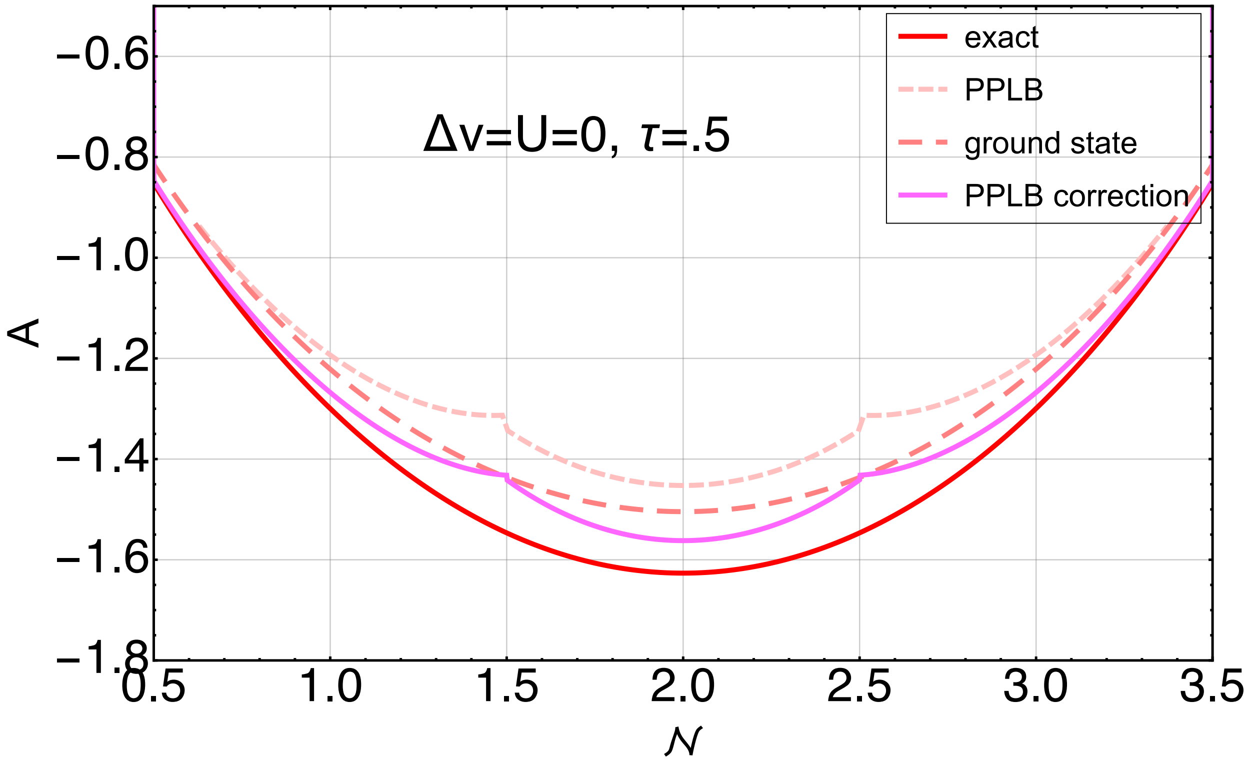

Figure 5.6: Comparing A (eq. 5.6), A^{PPLB} (eq. 5.9), A_0(eq. 5.8), and A^*(eq. 5.11), for $\tau = .5$.

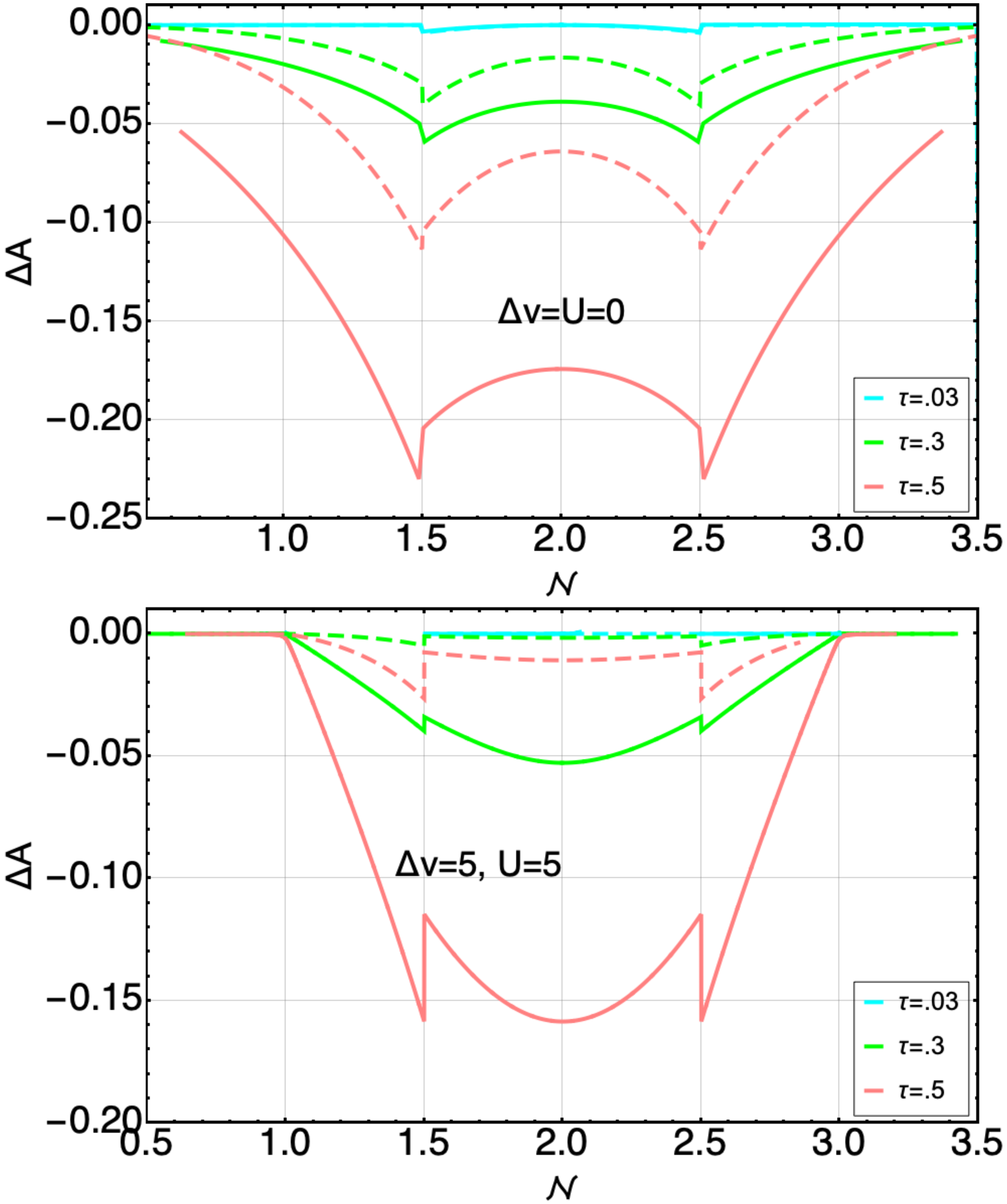

Figure 5.7: Comparing the absolute errors in the energy, ΔA. Solid lines are eq. 5.9 and dashed lines are eq. 5.11 plugged into eq. 5.1.

Chapter 6

Construction of an exact temperature dependent exchange correlation functional on a model system

This chapter is the most resent progress in an effort to understand the fundamentals of finite temperature DFT. Here we solve the full Fock space of the two site Hubbard model, for all particle numbers. This project is not currently finished, but will be submitted for publication soon.

As stated in chapter 4, current warm dense matter simulations use ground state(zero temperature) exchange correlation functionals for a variety of reasons, one of which is the fact that currently no good temperature dependent approximations exist. Hence, here we try to build an exact temperature dependent functional for the Hubbard model, that will hopefully bring some insight to the field of finite temperature DFT.

6.1 Extracting all energy components

Starting with the most simple case in the Hubbard model, that is the tight binding case, at $U = 0$ it is possible to write down the partition function to extract all energy components such that,

$$Z_{gc} = \prod_{\epsilon_\pm} \Big(1 + \exp\left((\mu - \epsilon_\pm)/\tau\right)\Big). \tag{6.1}$$

Here $\epsilon_\pm = \pm\sqrt{(t)^2 + \Delta v^2}/2$ and correspond to the energies for a single particle. Using the traditional derivatives found in statistical mechanics for the grand canonical ensemble it is possible to get

$$\begin{aligned} &\Omega = -\tau \log Z, \quad S = -\frac{\partial \Omega}{\partial \tau}\Big|_{\mu} \\ &\mathcal{N} = -\frac{\partial \Omega}{\partial \mu}\Big|_{\tau}, \quad A = \Omega + \mu N. \end{aligned} \tag{6.2}$$

Here $\Omega, S, \mathcal{N}$ and A correspond to the grand potential, entropy, average particle number, and free energy, respectively. Using the simple definition of the tight binding partition function it is possible to make literally hundreds of figures for all energy components (See Appendix), as function of both the chemical potential, μ and the average particle number $\mathcal{N}$. Below two sets of figures demonstrate that this seemingly simple model can provide information that has never been seen in this manner within the realm of finite temperature DFT.

Fig. 6.1 shows the most fundamental statistical mechanical quantities in the simplest possible case, the symmetric, tight-binding dimer, that is at $U = \Delta v = 0$. We plot the grand potential, the entropy, the free energy, chemical potential, and internal energy. The solid blue lines show their values at (almost) zero temperature, i.e., totally dominated by the ground state, and the other lines show what happens as the temperature is raised. The lowest panel shows the internal energy (just the energy at zero temperature), illustrating the straight-line behavior first deduced by PPLB, and the derivative discontinuity at $\mathcal{N} = 2$. At any finite temperature, this discontinuity is rounded (see red line), but becomes sharper as the temperature decreases.

We next consider the entropy, which has no direct analog in ground-state DFT. Nonetheless, it remains finite as the temperature vanishes, except at the end-points and the symmetry-point, $\mathcal{N} = 2$. As the temperature increases, the sharp dip near $\mathcal{N} = 2$ disappears. The middle panel shows the Helmholtz free energy, $A = E - \tau S$. Now, even the small increase in temperature to 0.1 shows up as significant rounding of the curve near $\mathcal{N} = 2$, and a decrease in free energy away from there, entirely due to entropic effects. The next panel shows the chemical potential, which is the derivative of the free energy with respect to the particle number, at each temperature. The coldest curve clearly shows the well-known step at $\mathcal{N} = 2$, where the ground-state orbital becomes doubly occupied. Again, significant rounding occurs even at temperatures of 0.1 (green curve), where one can see that the finite temperature curve passes through the center of the step. Lastly, we show the grand potential, which is not simply symmetric or antisymmetric, but includes also a linear term in $\mathcal{N}$.

Fig. 6.2 repeats the curves of Fig 6.1, but with the interaction turned on $U = 2$. The exact solutions (i.e., the interacting ones) are taken from the appendix of [147]. The dashed lines in the background are those of Fig. 6.1, for reference. The solid lines appear qualitatively similar to those of Fig. 6.1, but shifted due to the change in the energy eigenvalues, $\pm\epsilon$. In the statistical mechanics energetics we see the largest notable change. Now we see clear kinks in the energetics at integer particle numbers caused by the derivative discontinuity. There is also slight variation in the magnitude of these energy components. In the traditional DFT energies, we also see the derivative discontinuities appear, but they are more subtle, than in the previous figure.

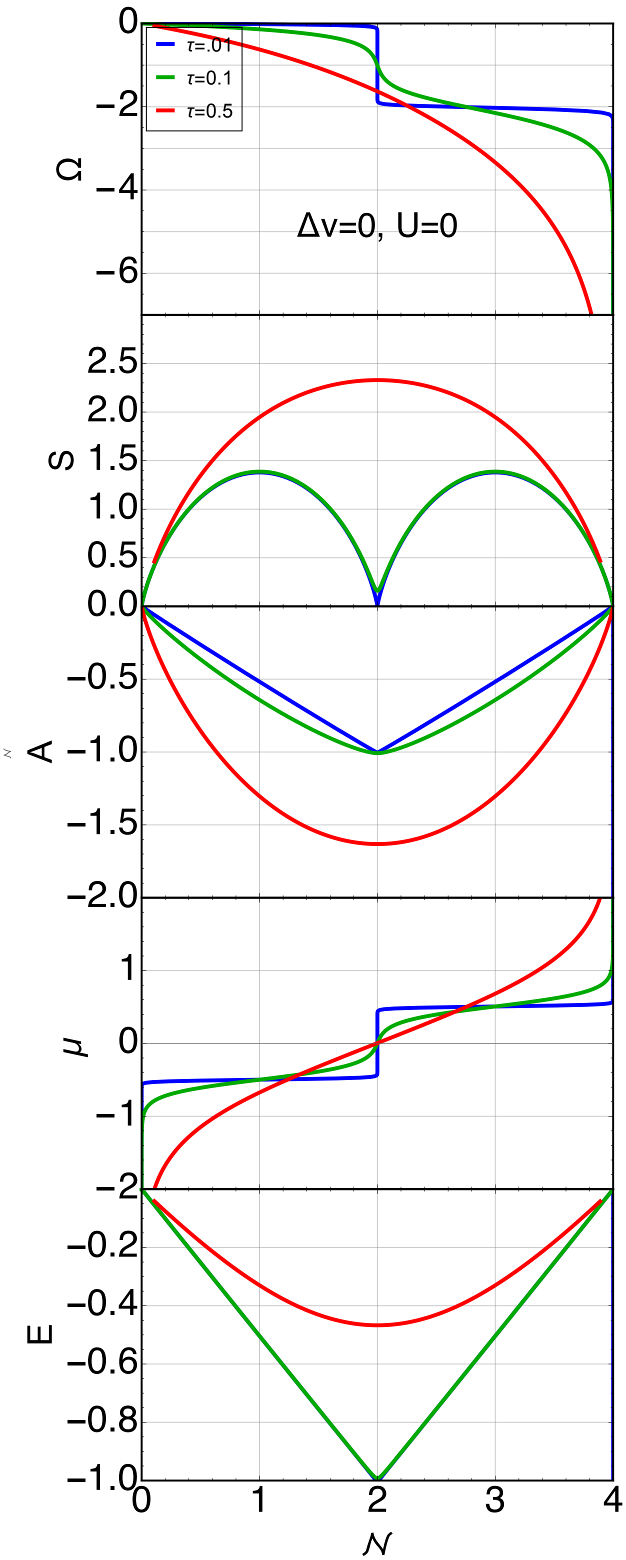

Figure 6.1: All statistical mechanics energy components for the temperature dependent dimer, grand potential (Ω), entropy (S), free energy (A), chemical potential (μ), and internal energy ($E = A + \tau S$) at the symmetric point ($\Delta v = 0$), with zero repulsion, $U = 0$, and increasing temperature, τ.

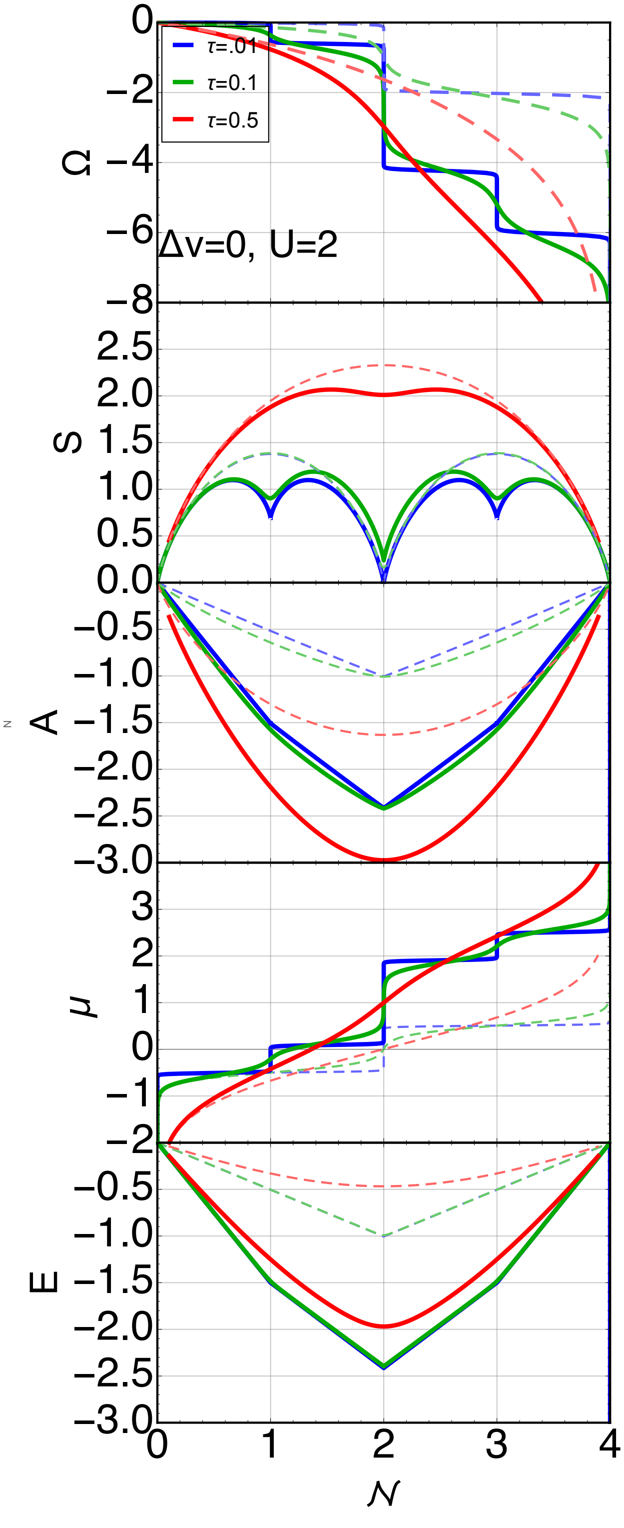

Figure 6.2: All statistical mechanics energy components for the temperature dependent dimer, grand potential (Ω), entropy (S), free energy (A), chemical potential (μ), and internal energy ($E = A + \tau S$) at slight asymmetry ($\Delta v = 0$), with the interaction turned on to $U = 2$, and increasing temperature, τ.

The next step towards constructing an exact temperature dependent functional would be to extract all temperature dependent KS components. All relevant KS were extracted numerically using a simple bisection algorithm . These figures can be seen below.

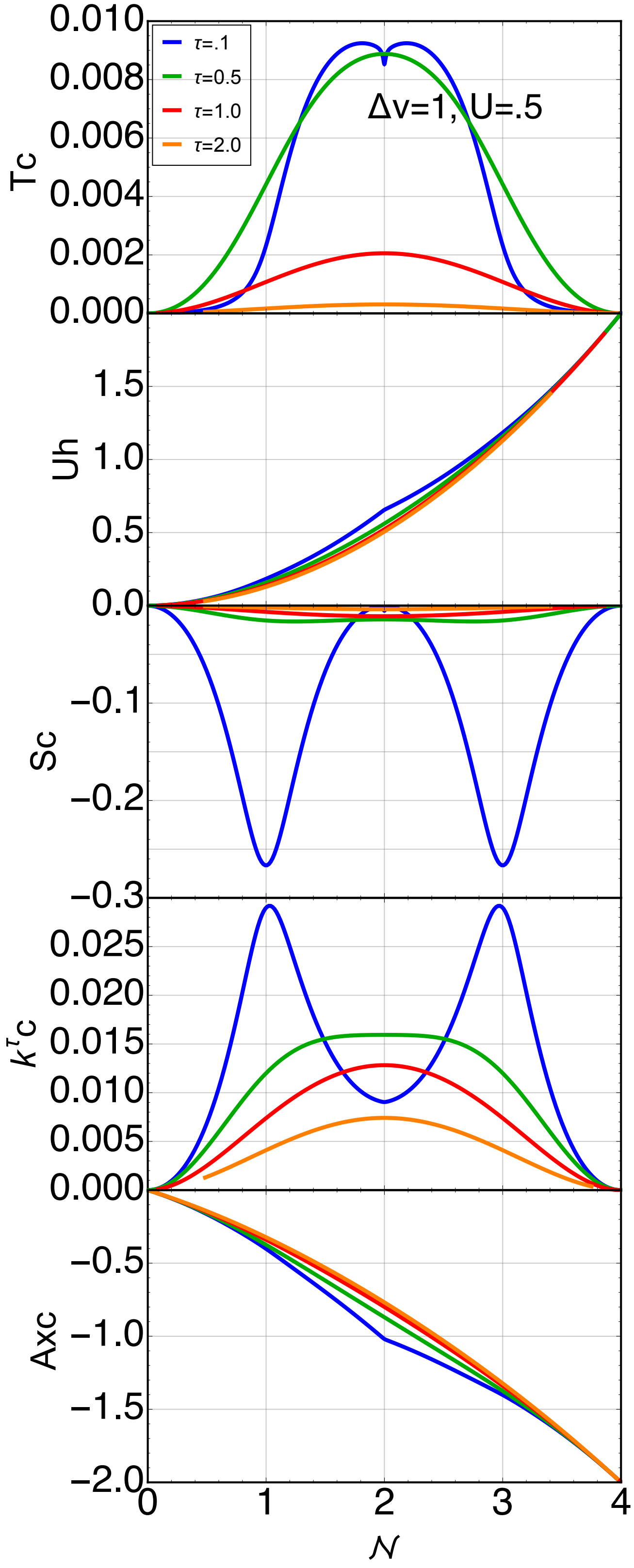

Figure 6.3: All KS energy components for the temperature dependent dimer, at slight asymmetry ($\Delta v = 1$), with weak interaction, $U = .5$, and increasing values of temperature, τ.

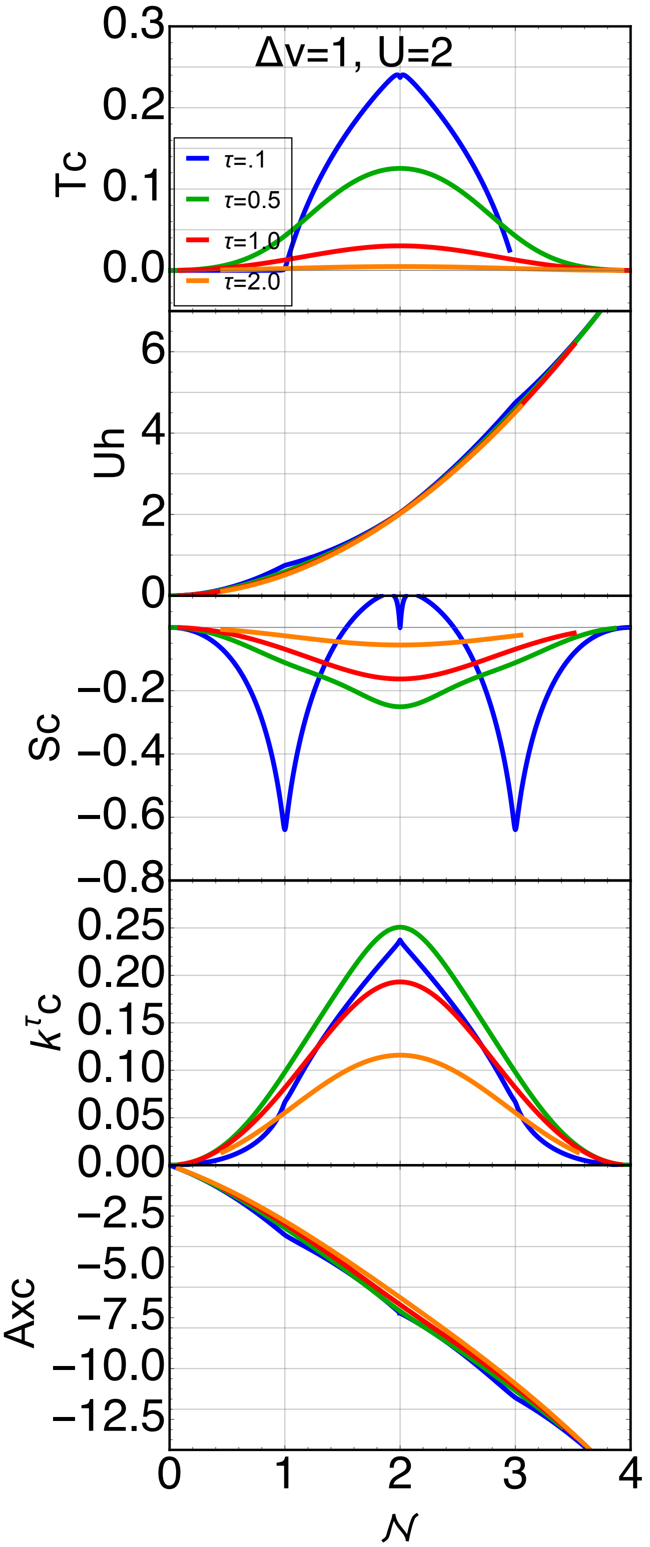

Figure 6.4: All KS energy components for the temperature dependent dimer, at slight asymmetry ($\Delta v = 1$), with repulsion set to U=2, and increasing values temperature, τ.

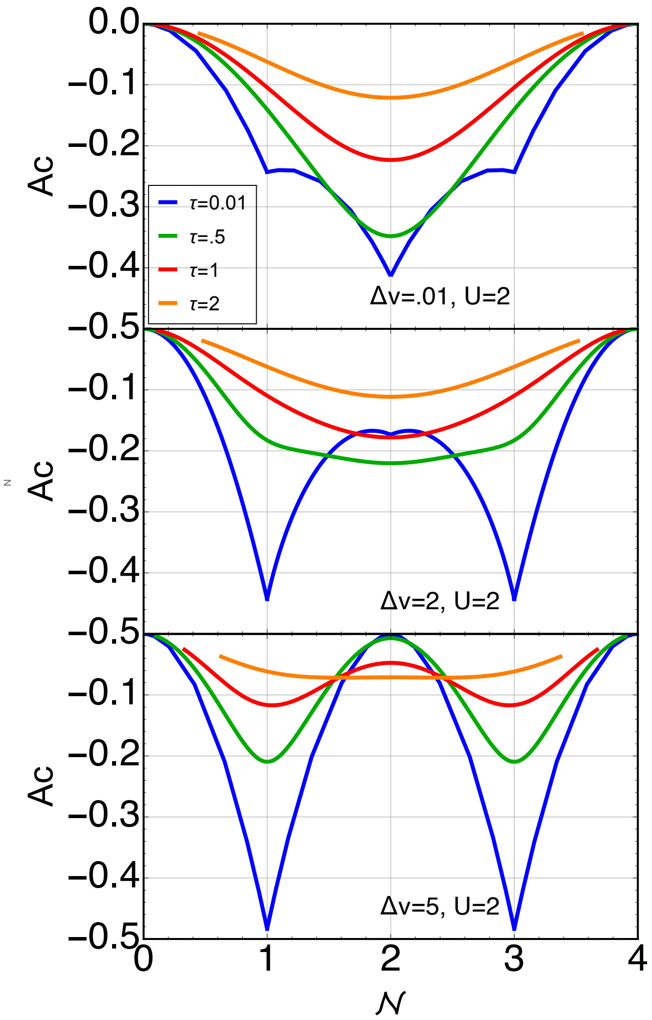

Figure 6.5: Various plots of A_C, plotted for all particle numbers.

Using the finite temperature KS components it is possible to extract the temperature dependent free energy, A^τ_C which cannot simply be extracted for many other systems.

6.2 Conclusions and future work

As stated earlier, real warm dense matter simulations usually use ground state approximations such that

$$A^{\tau}_{XC}[n] = E_{XC}[n] + \Delta A^{\tau}_{XC}, \tag{6.3}$$

where $E_{XC}[n]$ is the ground state functional that people typically approximate in the ground state case and $\Delta A^{\tau}_{XC}[n]$ is the difference in the exchange correlation energy and the ground state functional. In this project we aim to successfully build $A^{\tau}_{XC}[n]$ for the truncated Hubbard model. Since this can only be done in very few model systems exactly, we hope that extracting this information from this model will provide useful information in the future for building an $A^{\tau}_{XC}[n]$ for real systems.

6.3 Acknowledgments

F.S and K.B acknowledge support from the Department of Energy, Award No. DE-FG02-08ER46496.

Bibliography

[1] Basic research needs for high energy density laboratory physics. *The U.S. Department of Energy Office of Science and National Nuclear Security Administration*, 2009.

[2] M. M. Alam, S. Knecht, and E. Fromager. Ghost-interaction correction in ensemble density-functional theory for excited states with and without range separation. *Phys. Rev. A*, 94:012511, Jul 2016.

[3] F. Aryasetiawan and O. Gunnarsson. Exchange-correlation kernel in time-dependent density functional theory. *Phys. Rev. B*, 66:165119, Oct 2002.

[4] P. W. Ayers and W. Yang. Legendre-transform functionals for spin-density-functional theory. *The Journal of Chemical Physics*, 124(22):224108, 2006.

[5] A. D. Baczewski, L. Shulenburger, M. P. Desjarlais, S. B. Hansen, and R. J. Magyar. X-ray thomson scattering in warm dense matter without the chihara decomposition. *Phys. Rev. Lett.*, 116:115004, Mar 2016.

[6] B. Bennett, J. Johnson, G. Kerley, and G. Rood. Recent developments in the sesame equation-of-state library. Technical report, Los Alamos Scientific Lab., N. Mex.(USA), 1978.

[7] C. K. Birdsall and A. B. Langdon. *Plasma physics via computer simulation.* CRC Press, 2004.

[8] K. Burke. Perspective on density functional theory. *J. Chem. Phys.*, 136, 2012.

[9] K. Burke, J. C. Smith, P. E. Grabowski, and A. Pribram-Jones. Exact conditions on the temperature dependence of density functionals. *Phys. Rev. B*, 93:195132, May 2016.

[10] K. Burke, J. Werschnik, and E. K. U. Gross. Time-dependent density functional theory: Past, present, and future. *The Journal of Chemical Physics*, 123(6):062206, 2005.

[11] K. Burke, J. Werschnik, and E. K. U. Gross. Time-dependent density functional theory: Past, present, and future. *The Journal of Chemical Physics*, 123(6):062206, 2005.

[12] K. Capelle and V. L. C. Jr. Density functionals and model hamiltonians: Pillars of many-particle physics. *Physics Reports*, 528:91–159, 2013.

[13] R. Car and M. Parrinello. Unified approach for molecular dynamics and density-functional theory. *Phys. Rev. Lett.*, 55(22):2471–2474, Nov 1985.

[14] D. J. Carrascal, J. Ferrer, N. Maitra, and K. Burke. Linear response time-dependent density functional theory of the hubbard dimer. *Accepted arXiv:1802.09988*, 2018.

[15] D. J. Carrascal, J. Ferrer, J. C. Smith, and K. Burke. The hubbard dimer: a density functional case study of a many-body problem. *Journal of Physics: Condensed Matter*, 27(39):393001, 2015.

[16] M. E. Casida. Time-dependent density functional response theory of molecular systems: theory, computational methods, and functionals. In J. M. Seminario, editor, *Recent developments and applications in density functional theory.* Elsevier, Amsterdam, 1996.

[17] M. E. Casida and M. Huix-Rotllant. *Many-Body Perturbation Theory (MBPT) and Time-Dependent Density-Functional Theory (TD-DFT): MBPT Insights About What Is Missing In, and Corrections To, the TD-DFT Adiabatic Approximation*, pages 1–60. Springer International Publishing, Cham, 2016.

[18] R. J. Cave, F. Zhang, N. T. Maitra, and K. Burke. A dressed TDDFT treatment of the $2^1\mathrm{A}_g$ states of butadiene and hexatriene. *Chemical Physics Letters*, 389(1-3):39 – 42, 2004.

[19] D. Ceperley, M. Kalos, and K. Binder. *Monte Carlo methods in statistical physics.* Springer, Berlin, 1979.

[20] D. M. Ceperley and B. J. Alder. Ground state of the electron gas by a stochastic method. *Phys. Rev. Lett.*, 45:566–569, Aug 1980.

[21] D. Clery. Forbidden planets. *Science*, 353(6298):438–441, 2016.

[22] L. A. Curtiss, K. Raghavachari, P. C. Redfern, and J. A. Pople. Assessment of gaussian-2 and density functional theories for the computation of enthalpies of formation. *The Journal of Chemical Physics*, 106(3), 1997.

[23] W. T. D. Frydel and K. Burke. Adiabatic connection from accurate wavefunction calculations. *J. Chem. Phys.*, 112:5292, 2000.

[24] P. Davis, T. Döppner, J. Rygg, C. Fortmann, L. Divol, A. Pak, L. Fletcher, A. Becker, B. Holst, P. Sperling, et al. X-ray scattering measurements of dissociation-induced metallization of dynamically compressed deuterium. *Nature communications*, 7, 2016.

[25] M. P. Desjarlais. Density-functional calculations of the liquid deuterium hugoniot, reshock, and reverberation timing. *Phys. Rev. B*, 68:064204, Aug 2003.

[26] K. Deur, L. Mazouin, and E. Fromager. Exact ensemble density functional theory for excited states in a model system: Investigating the weight dependence of the correlation energy. *Phys. Rev. B*, 95:035120, Jan 2017.

[27] K. Deur, L. Mazouin, B. Senjean, and E. Fromager. Exploring weight-dependent density-functional approximations for ensembles in the hubbard dimer. *Arxiv:1803.00291*, May 2018.

[28] T. Dornheim, S. Groth, T. Sjostrom, F. D. Malone, W. M. C. Foulkes, and M. Bonitz. *Ab Initio* quantum monte carlo simulation of the warm dense electron gas in the thermodynamic limit. *Phys. Rev. Lett.*, 117:156403, Oct 2016.

[29] R. M. Dreizler and E. K. Gross. *Density Functional Theory:An Approach to the Quantum Many-Body Problem*, volume 1. 1984.

[30] A. Dreuw, J. L. Weisman, and M. Head-Gordon. Long-range charge-transfer excited states in time-dependent density functional theory require non-local exchange. *The J. of Chem. Phys.*, 119(6), 2003.

[31] K. P. Driver and B. Militzer. All-electron path integral monte carlo simulations of warm dense matter: Application to water and carbon plasmas. *Phys. Rev. Lett.*, 108:115502, Mar 2012.

[32] J. W. Dufty and S. Trickey. Finite temperature scaling in density functional theory. *Molecular Physics*, 114(7-8):988–996, 2016.

[33] J. W. Dufty and S. B. Trickey. Scaling, bounds, and inequalities for the noninteracting density functionals at finite temperature. *Phys. Rev. B*, 84:125118, Sep 2011.

[34] L. O. E.K.U. Gross and W. Kohn. Rayleigh-Ritz variational principle for ensembles of fractionally occupied states. *Phys. Rev. A*, 37:2805, 1988.

[35] M. Ernzerhof and G. E. Scuseria. Assessment of the Perdew–Burke–Ernzerhof exchange-correlation functional. *J. Chem. Phys*, 110:5029, 1999.

[36] H. Eshuis, J. Bates, and F. Furche. Electron correlation methods based on the random phase approximation. *Theoretical Chemistry Accounts*, 131(1):1–18, 2012.

[37] H. Eshuis, J. Yarkony, and F. Furche. Fast computation of molecular random phase approximation correlation energies using resolution of the identity and imaginary frequency integration. *The Journal of Chemical Physics*, 132(23):234114, 2010.

[38] V. S. Filinov, M. Bonitz, W. Ebeling, and V. E. Fortov. Thermodynamics of hot dense h-plasmas: path integral monte carlo simulations and analytical approximations. *Plasma Physics and Controlled Fusion*, 43(6):743, 2001.

[39] C. Filippi, C. J. Umrigar, and X. Gonze. Excitation energies from density functional perturbation theory. *The Journal of Chemical Physics*, 107(23):9994–10002, 1997.

[40] C. Filippi, C. J. Umrigar, and M. Taut. Comparison of exact and approximate density functionals for an exactly soluble model. *The Journal of Chemical Physics*, 100(2):1290–1296, 1994.

[41] O. Franck and E. Fromager. Generalised adiabatic connection in ensemble density-functional theory for excited states: example of the h2 molecule. *Molecular Physics*, 112(12):1684–1701, 2014.

[42] F. Furche. Molecular tests of the random phase approximation to the exchange-correlation energy functional. *Phys. Rev. B*, 64:195120, 2001.

[43] F. Furche. Developing the random phase approximation into a practical post-Kohn–Sham correlation model. *The Journal of Chemical Physics*, 129(11), 2008.

[44] F. Furche. Correlation energy in dft: Adiabatic connection random phase approximation. *Annual Review of Physical Chemistry*, 68(1), 2016.

[45] D. Gericke, M. Schlanges, and W. Kraeft. Stopping power of a quantum plasma . t-matrix approximation and dynamical screening. *Physics Letters A*, 222(4):241 – 245, 1996.

[46] X. Gonze and M. Scheffler. Exchange and correlation kernels at the resonance frequency: Implications for excitation energies in density-functional theory. *Phys. Rev. Lett.*, 82(22):4416–4419, May 1999.

[47] A. Görling and M. Levy. Hardness of molecules and the band gap of solids within the kohn-sham formalism: A perturbation-scaling approach. *Phys. Rev. A.*, 52:4493, 1995.

[48] T. Gould, L. Kronik, and S. Pittalis. Charge transfer excitations from exact and approximate ensemble kohn-sham theory. *The Journal of Chemical Physics*, 148(17):174101, 2018.

[49] T. Gould and S. Pittalis. Hartree and exchange in ensemble density functional theory: Avoiding the nonuniqueness disaster. *Phys. Rev. Lett.*, 119:243001, Dec 2017.

[50] F. Graziani, M. P. Desjarlais, R. Redmer, and S. B. Trickey, editors. *Frontiers and Challenges in Warm Dense Matter*, volume 96 of *Lecture Notes in Computational Science and Engineering*. Springer International Publishing, 2014.

[51] M. Greiner, P. Carrier, and A. Görling. Extension of exact-exchange density functional theory of solids to finite temperatures. *Phys. Rev. B*, 81(15):155119, Apr 2010.

[52] E. Gross and W. Kohn. Local density-functional theory of frequency-dependent linear response. *Phys. Rev. Lett.*, 55:2850, 1985.

[53] E. K. U. Gross, L. N. Oliveira, and W. Kohn. Density-functional theory for ensembles of fractionally occupied states. i. basic formalism. *Phys. Rev. A*, 37:2809–2820, Apr 1988.

[54] E. K. U. Gross, M. Petersilka, and T. Grabo. Conventional quantum chemical correlation energy versus density-functional correlation energy. *Chemical Applications of Density-Functional Theory*, 629:42–53, 1996.

[55] O. Gunnarsson and B. Lundqvist. Exchange and correlation in atoms, molecules, and solids by the spin-density-functional formalism. *Phys. Rev. B*, 13:4274, 1976.

[56] V. S. H. *Can. J. Phys.*, 58:1200, 1980.

[57] M. J. P. Hodgson, E. Kraisler, A. Schild, and E. K. U. Gross. How interatomic steps in the exact kohn–sham potential relate to derivative discontinuities of the energy. *The Journal of Physical Chemistry Letters*, 8(24):5974–5980, 2017. PMID: 29179553.

[58] D. Hofmann and S. Kümmel. Integer particle preference during charge transfer in kohn-sham theory. *Phys. Rev. B: Condens. Matter Mater. Phys.*, 86:201109, 2012.

[59] P. Hohenberg and W. Kohn. Inhomogeneous electron gas. *Phys. Rev.*, 136:B864–B871, Nov 1964.

[60] P. Hohenberg and W. Kohn. Thermal properties for the inhomogeneous electron gas. *Phys. Rev.*, 137, 1965.

[61] B. Holst, R. Redmer, and M. P. Desjarlais. Thermophysical properties of warm dense hydrogen using quantum molecular dynamics simulations. *Phys. Rev. B*, 77:184201, May 2008.

[62] S. X. Hu, L. A. Collins, T. R. Boehly, J. D. Kress, V. N. Goncharov, and S. Skupsky. First-principles thermal conductivity of warm-dense deuterium plasmas for inertial confinement fusion applications. *Phys. Rev. E*, 89:043105, Apr 2014.

[63] C.-J. Huang and C. J. Umrigar. Local correlation energies of two-electron atoms and model systems. *Phys. Rev. A*, 56:290–296, Jul 1997.

[64] J. Hubbard. Electron correlations in narrow energy bands. 276(1365):238–257, 1963.

[65] M. Huix-Rotllant, A. Ipatov, A. Rubio, and M. E. Casida. Assessment of dressed time-dependent density-functional theory for the low-lying valence states of 28 organic chromophores. *Chemical Physics*, 391(1):120 – 129, 2011. Open problems and new solutions in time dependent density functional theory.

[66] S. Ichimaru. *Rev. Mod. Phys.*, 54:1017, 1982.

[67] S. Ichimaru. *Statistical Plasma Physics.* Frontiers in Physics. Westview, Boulder, CO, 2004.

[68] S. Jiang, A. E. Lazicki, S. B. Hansen, P. A. Sterne, P. Grabowski, R. Shepherd, H. A. Scott, R. F. Smith, J. H. Eggert, and Y. Ping. Measurements of pressure-induced $k\beta$ line shifts in ramp compressed cobalt up to 8 mbar. *Phys. Rev. E*, 101:023204, Feb 2020.

[69] L. M. K. Deur and E. Fromager. Exact ensemble density functional theory for excited states in a model system: investigating the weight dependence of the correlation energy. *(Submitted)*, 2016.

[70] L. Kadanoff, G. Baym, and D. Pines. *Quantum Statistical Mechanics*. Advanced Books Classics Series. Addison-Wesley, 1994.

[71] V. V. Karasiev, T. Sjostrom, J. Dufty, and S. B. Trickey. Accurate homogeneous electron gas exchange-correlation free energy for local spin-density calculations. *Phys. Rev. Lett.*, 112:076403, Feb 2014.

[72] S.-H. Ke, H. U. Baranger, and W. Yang. Role of the exchange-correlation potential in ab initio electron transport calculations. *J. Chem. Phys.*, 126:201102, 2007.

[73] A. Kietzmann, R. Redmer, M. P. Desjarlais, and T. R. Mattsson. Complex behavior of fluid lithium under extreme conditions. *Phys. Rev. Lett.*, 101:070401, Aug 2008.

[74] M. D. Knudson and M. P. Desjarlais. Shock compression of quartz to 1.6 TPa: Redefining a pressure standard. *Phys. Rev. Lett.*, 103:225501, Nov 2009.

[75] M. D. Knudson, M. P. Desjarlais, A. Becker, R. W. Lemke, K. R. Cochrane, M. E. Savage, D. E. Bliss, T. R. Mattsson, and R. Redmer. Direct observation of an abrupt insulator-to-metal transition in dense liquid deuterium. *Science*, 348(6242):1455–1460, 2015.

[76] M. D. Knudson, M. P. Desjarlais, and D. H. Dolan. Shock-wave exploration of the high-pressure phases of carbon. *Science*, 322(5909):1822–1825, 2008.

[77] M. D. Knudson, M. P. Desjarlais, and A. Pribram-Jones. Adiabatic release measurements in aluminum between 400 and 1200 gpa: Characterization of aluminum as a shock standard in the multimegabar regime. *Phys. Rev. B*, 91:224105, Jun 2015.

[78] M. D. Knudson, D. L. Hanson, J. E. Bailey, C. A. Hall, J. R. Asay, and W. W. Anderson. Equation of state measurements in liquid deuterium to 70 gpa. *Phys. Rev. Lett.*, 87:225501, Nov 2001.

[79] M. Koentopp, K. Burke, and F. Evers. Zero-bias molecular electronics: Exchange-correlation corrections to landauer's formula. *Phys. Rev. B: Condens. Matter Mater. Phys.*, 73:121403, 2006.

[80] M. Koentopp, C. Chang, K. Burke, and R. Car. Density functional calculations of nanoscale conductance. *Journal of Physics: Condensed Matter*, 20(8):083203, 2008.

[81] W. Kohn and L. J. Sham. Self-consistent equations including exchange and correlation effects. *Phys. Rev.*, 140:A1133–A1138, Nov 1965.

[82] D. Kraus, A. Ravasio, M. Gauthier, D. Gericke, J. Vorberger, S. Frydrych, J. Helfrich, L. Fletcher, G. Schaumann, B. Nagler, et al. Nanosecond formation of diamond and lonsdaleite by shock compression of graphite. *Nature communications*, 7, 2016.

[83] G. Kresse and J. Furthmüller. Efficient iterative schemes for ab initio total-energy calculations using a plane-wave basis set. *Phys. Rev. B*, 54(16):11169–11186, Oct 1996.

[84] S. Kurth and J. P. Perdew. Role of the exchange-correlation energy: Nature's glue. *International Journal of Quantum Chemistry*, 77(5):814–818, 2000.

[85] K. R. L.A. Curtiss, P.C. Redfern and J. Pople. Assessment of gaussian-2 and density functional theories for the computation of ionization potentials and electron affinities. *J. Chem. Phys.*, 109:42, 1998.

[86] N. Lang and W. Kohn. *Phys. Rev. B*, 7:3541, 1973.

[87] D. Langreth and J. Perdew. The exchange-correlation energy of a metallic surface. *Solid State Commun.*, 17:1425, 1975.

[88] Y. T. Lee and R. More. An electron conductivity model for dense plasmas. *Physics of Fluids (1958-1988)*, 27(5):1273–1286, 1984.

[89] T. J. Lenosky, S. R. Bickham, J. D. Kress, and L. A. Collins. Density-functional calculation of the hugoniot of shocked liquid deuterium. *Phys. Rev. B*, 61:1–4, Jan 2000.

[90] B. G. Levine, C. Ko, J. Quenneville, and T. J. MartÍnez. Conical intersections and double excitations in time-dependent density functional theory. *Molecular Physics*, 104(5-7):1039–1051, 2006.

[91] M. Levy and J. Perdew. Hellmann-Feynman, virial, and scaling requisites for the exact universal density functionals. shape of the correlation potential and diamagnetic susceptibility for atoms. *Phys. Rev. A*, 32:2010, 1985.

[92] E. H. Lieb. Thomas-fermi and related theories of atoms and molecules. *Rev. Mod. Phys.*, 53:603–641, Oct 1981.

[93] E. H. Lieb and S. Oxford. Improved lower bound on the indirect coulomb energy. *International Journal of Quantum Chemistry*, 19(3):427–439, 1981.

[94] N. Lima, M. Silva, L. Oliveira, and K. Capelle. Density functionals not based on the electron gas: local-density approximation for a luttinger liquid. *Physical review letters*, 90(14):146402, 2003.

[95] W. Lorenzen, B. Holst, and R. Redmer. Demixing of hydrogen and helium at megabar pressures. *Phys. Rev. Lett.*, 102:115701, Mar 2009.

[96] N. T. Maitra. Undoing static correlation: long-range charge transfer in time-dependent density-functional theory. *J. Chem. Phys.*, 122:234104, 2005.

[97] N. T. Maitra. Perspective: Fundamental aspects of time-dependent density functional theory. *The Journal of Chemical Physics*, 144(22), 2016.

[98] N. T. Maitra, F. Zhang, R. J. Cave, and K. Burke. Double excitations within time-dependent density functional theory linear response. *The Journal of Chemical Physics*, 120(13):5932–5937, 2004.

[99] M. A. Marques, M. J. Oliveira, and T. Burnus. Libxc: A library of exchange and correlation functionals for density functional theory. *Computer Physics Communications*, 183(10):2272 – 2281, 2012.

[100] M. A. L. Marques, N. T. Maitra, F. M. S. Nogueira, E. K. U. Gross, and A. Rubio, editors. *Fundamentals of Time-Dependent Density Functional Theory*. Number 837 in Lecture Notes in Physics. Springer, Heidelberg, 2012.

[101] T. R. Mattsson and M. P. Desjarlais. Phase diagram and electrical conductivity of high energy-density water from density functional theory. *Phys. Rev. Lett.*, 97:017801, Jul 2006.

[102] J. M. McMahon, M. A. Morales, C. Pierleoni, and D. M. Ceperley. The properties of hydrogen and helium under extreme conditions. *Rev. Mod. Phys.*, 84:1607–1653, Nov 2012.

[103] Y. Miguel, T. Guillot, and L. Fayon. Jupiter internal structure: the effect of different equations of state. *arXiv preprint arXiv:1609.05460*, 2016.

[104] B. Militzer. Path integral monte carlo and density functional molecular dynamics simulations of hot, dense helium. *Phys. Rev. B*, 79:155105, Apr 2009.

[105] B. Militzer and D. M. Ceperley. Path integral monte carlo calculation of the deuterium hugoniot. *Phys. Rev. Lett.*, 85:1890–1893, Aug 2000.

[106] P. G. P. N. I. Gidopoulos and E. K. U. Gross. Spurious interactions, and their correction, in the ensemble-kohn-sham scheme for excited states. *Phys. Rev. Lett.*, 88:033003, 2002.

[107] Á. Nagy. Coordinate scaling and adiabatic connection formula for ensembles of fractionally occupied excited states. *International Journal of Quantum Chemistry*, 56(4):225–228, 1995.

[108] Á. Nagy. Excited states in density functional theory. *International Journal of Quantum Chemistry*, 70(4-5):681–691, 1998.

[109] N. Nettelmann, B. Holst, A. Kietzmann, M. French, R. Redmer, and D. Blaschke. Ab initio equation of state data for hydrogen, helium, and water and the internal structure of jupiter. *The Astrophysical Journal*, 683(2):1217–1228, aug 2008.

[110] J. F. Nossa, M. F. Islam, C. M. Canali, and M. R. Pederson. Electric control of a Fe4 single-molecule magnet in a single-electron transistor. *Phys. Rev. B: Condens. Matter Mater. Phys.*, 88:224423, 2013.

[111] J. R. O. *Rev. Mod. Phys.*, 61:689, 1989.

[112] U. D. of Energy. Basic research needs for high energy density laboratory physics: Report of the workshop on high energy density laboratory physics research needs. Technical report, Office of Science and National Nuclear Security Administration, 2009.

[113] L. N. Oliveira, E. K. U. Gross, and W. Kohn. Density-functional theory for ensembles of fractionally occupied states. ii. application to the he atom. *Phys. Rev. A*, 37:2821–2833, Apr 1988.

[114] P. J. P. What do the kohn sham orbitals really mean? *Density Functional Methods in Physics*, 28:497, 1985.

[115] J. Paier, R. Hirschl, M. Marsman, and G. Kresse. The perdew–burke–ernzerhof exchange-correlation functional applied to the g2-1 test set using a plane-wave basis set. *The Journal of chemical physics*, 122(23):234102, 2005.

[116] R. G. Parr and W. Yang. Density functional approach to the frontier-electron theory of chemical reactivity. *Journal of the American Chemical Society*, 106(14):4049–4050, 1984.

[117] J. Perdew. Density functional theory and the band gap problem. *Int. J. Quantum Chem. S*, 19:497, 1986.

[118] J. Perdew and Y. Wang. Accurate and simple analytic representation of the electron-gas correlation energy. *Phys. Rev. B*, 45:13244–13249, Jun 1992.

[119] J. P. Perdew, K. Burke, and M. Ernzerhof. Generalized gradient approximation made simple. *Phys. Rev. Lett.*, 77:3865–3868, Oct 1996.

[120] J. P. Perdew, J. A. Chevary, S. H. Vosko, K. A. Jackson, M. R. Pederson, D. J. Singh, and C. Fiolhais. Atoms, molecules, solids, and surfaces: Applications of the generalized gradient approximation for exchange and correlation. *Phys. Rev. B*, 46:6671–6687, Sep 1992.

[121] J. P. Perdew, M. Ernzerhof, and K. Burke. Rationale for mixing exact exchange with density functional approximations. *The Journal of Chemical Physics*, 105(22):9982–9985, 1996.

[122] J. P. Perdew, R. G. Parr, M. Levy, and J. L. Balduz. Density-functional theory for fractional particle number: Derivative discontinuities of the energy. *Phys. Rev. Lett.*, 49:1691–1694, Dec 1982.

[123] J. P. Perdew, A. Ruzsinszky, L. A. Constantin, J. Sun, and G. I. Csonka. Some fundamental issues in ground-state density functional theory: A guide for the perplexed. *Journal Of Chemical Theory and Computation*, 5(4):902–908, Apr 2009.

[124] J. P. Perdew and J. Smith. Can desorption be described by the local density formalism? *Surf. Sci.*, 141:L295, 1984.

[125] S. Pittalis, C. R. Proetto, A. Floris, A. Sanna, C. Bersier, K. Burke, and E. K. U. Gross. Exact conditions in finite-temperature density-functional theory. *Phys. Rev. Lett.*, 107:163001, Oct 2011.

[126] A. Pribram-Jones and K. Burke. Connection formulas for thermal density functional theory. *Phys. Rev. B*, 93:205140, May 2016.

[127] A. Pribram-Jones, P. E. Grabowski, and K. Burke. Thermal density functional theory: Time-dependent linear response and approximate functionals from the fluctuation-dissipation theorem. *Phys. Rev. Lett.*, 116:233001, Jun 2016.

[128] A. Pribram-Jones, S. Pittalis, E. Gross, and K. Burke. Thermal density functional theory in context. In F. Graziani, M. P. Desjarlais, R. Redmer, and S. B. Trickey, editors, *Frontiers and Challenges in Warm Dense Matter*, volume 96 of *Lecture Notes in Computational Science and Engineering*, pages 25–60. Springer International Publishing, 2014.

[129] A. Pribram-Jones, Z.-H. Yang, J. R. Trail, K. Burke, R. J. Needs, and C. A. Ullrich. Excitations and benchmark ensemble density functional theory for two electrons. *J. Chem. Phys.*, 140:18A541, 2014.

[130] S. Y. Quek, L. Venkataraman, H. J. Choi, S. G. Louie, M. S. Hybertsen, and J. B. Neaton. Aminegold linked single-molecule circuits: experiment and theory. *Nano Letters*, 7(11):3477–3482, 2007. PMID: 17900162.

[131] V. Rizzi, T. N. Todorov, J. J. Kohanoff, and A. A. Correa. Electron-phonon thermalization in a scalable method for real-time quantum dynamics. *Phys. Rev. B*, 93:024306, Jan 2016.

[132] S. Root, R. J. Magyar, J. H. Carpenter, D. L. Hanson, and T. R. Mattsson. Shock compression of a fifth period element: Liquid xenon to 840 GPa. *Phys. Rev. Lett.*, 105(8):085501, Aug 2010.

[133] S. Root, R. J. Magyar, J. H. Carpenter, D. L. Hanson, and T. R. Mattsson. Shock compression of a fifth period element: Liquid xenon to 840 gpa. *Phys. Rev. Lett.*, 105:085501, Aug 2010.

[134] S. Root, L. Shulenburger, R. W. Lemke, D. H. Dolan, T. R. Mattsson, and M. P. Desjarlais. Shock response and phase transitions of mgo at planetary impact conditions. *Phys. Rev. Lett.*, 115:198501, Nov 2015.

[135] E. Runge and E. K. U. Gross. Density-functional theory for time-dependent systems. *Phys. Rev. Lett.*, 52(12):997, Mar 1984.

[136] J. P. S. Kurth and P. Blaha. Molecular and solid-state tests of density functional approximations: Lsd, gga's, and meta-gga's. *Int. J. Quantum Chem.*, 75:889, 1999.

[137] F. Sagredo and K. Burke. Accurate double excitations from ensemble density functional calculations. *The Journal of Chemical Physics*, 149(13):134103, 2018.

[138] L. Schimka, J. Harl, A. Stroppa, A. Grüneis, M. Marsman, F. Mittendorfer, and G. Kresse. Accurate surface and adsorption energies from many-body perturbation theory. *Nature Materials*, 9(9):741–744, 2010.

[139] P. R. T. Schipper, O. V. Gritsenko, and E. J. Baerends. Kohn-sham potentials corresponding to slater and gaussian basis set densities. *Theoretical Chemistry Accounts: Theory, Computation, and Modeling (Theoretica Chimica Acta)*, 98:16–24, 1997. 10.1007/s002140050273.

[140] T. Schoof, M. Bonitz, A. Filinov, D. Hochstuhl, and J. Dufty. Configuration path integral monte carlo. *Contributions to Plasma Physics*, 51(8):687–697, 2011.

[141] T. Schoof, S. Groth, J. Vorberger, and M. Bonitz. *Ab Initio* thermodynamic results for the degenerate electron gas at finite temperature. *Phys. Rev. Lett.*, 115:130402, Sep 2015.

[142] N. Schuch and F. Verstraete. Computational complexity of interacting electrons and fundamental limitations of density functional theory. *Nat. Phys.*, 5:732–735, 2009.

[143] F. Schwabl. *Statistical Mechanicss.* Springer-Verlag, 2002.

[144] B. Senjean and E. Fromager. Unified formulation of fundamental and optical gap problems in density-functional theory for ensembles. *Arxiv:1805.08715*, May 2018.

[145] B. Senjean, E. D. H. rd, M. M. Alam, S. Knecht, and E. Fromager. Combining linear interpolation with extrapolation methods in range-separated ensemble density functional theory. *Molecular Physics*, 114(7-8):968–981, 2016.

[146] T. Sjostrom and J. Dufty. Uniform electron gas at finite temperatures. *Phys. Rev. B*, 88:115123, Sep 2013.

[147] J. C. Smith, A. Pribram-Jones, and K. Burke. Exact thermal density functional theory for a model system: Correlation components and accuracy of the zero-temperature exchange-correlation approximation. *Phys. Rev. B*, 93:245131, Jun 2016.

[148] J. C. Smith, F. Sagredo, and K. Burke. Warming up density functional theory. *Frontiers of Quantum Chemistry*, pages 249–271, 2018.

[149] R. F. Smith, J. H. Eggert, R. Jeanloz, T. S. Duffy, D. G. Braun, J. R. Patterson, R. E. Rudd, J. Biener, A. E. Lazicki, A. V. Hamza, J. Wang, T. Braun, L. X. Benedict, P. M. Celliers, and G. W. Collins. Ramp compression of diamond to five terapascals. *Nature*, 511(7509):330–3, Jul 2014.

[150] P. Sperling, E. J. Gamboa, H. J. Lee, H. K. Chung, E. Galtier, Y. Omarbakiyeva, H. Reinholz, G. Röpke, U. Zastrau, J. Hastings, L. B. Fletcher, and S. H. Glenzer. Free-electron x-ray laser measurements of collisional-damped plasmons in isochorically heated warm dense matter. *Phys. Rev. Lett.*, 115:115001, Sep 2015.

[151] G. Stefanucci and R. Van Leeuwen. *Nonequilibrium Many-Body Theory of Quantum Systems: A Modern Introduction.* Cambridge University Press, 2013.

[152] J. C. Stewart and J. Pyatt, Kedar D. Lowering of Ionization Potentials in Plasmas. *Astrophysical Journal*, 144:1203, June 1966.

[153] N. Q. Su, C. Li, and W. Yang. Describing strong correlation with fractional-spin correction in density functional theory. *Proceedings of the National Academy of Sciences*, 115(39):9678–9683, 2018.

[154] J. Sun, A. Ruzsinszky, and J. P. Perdew. Strongly constrained and appropriately normed semilocal density functional. *Phys. Rev. Lett.*, 115:036402, Jul 2015.

[155] F. Tasnádi and Á. Nagy. Ghost- and self-interaction-free ensemble calculations with local exchange-correlation potential for atoms. *Journal of Physics B: Atomic, Molecular and Optical Physics*, 36(20):4073, 2003.

[156] A. Theophilou. The energy density functional formalism for excited states. *J. Phys. C*, 12:5419, 1979.

[157] A. Tkatchenko and M. Scheffler. Accurate Molecular Van Der Waals Interactions from Ground-State Electron Density and Free-Atom reference data. *Phys. Rev. Lett.*, 102:073005, Feb 2009.

[158] C. Toher, A. Filippetti, S. Sanvito, and K. Burke. Self-interaction errors in density-functional calculations of electronic transport. *Phys. Rev. Lett.*, 95:146402, 2005.

[159] D. J. Tozer. Relationship between long-range charge-transfer excitation energy error and integer discontinuity in kohn-sham theory. *J. Chem. Phys.*, 119:12697, 2003.

[160] S. Tretiak and V. Chernyak. Resonant nonlinear polarizabilities in the time-dependent density functional theory. *The Journal of Chemical Physics*, 119(17):8809–8823, 2003.

[161] C. A. Ullrich. *Time-Dependent Density-Functional Theory*. Oxford University Press, Oxford, 2012.

[162] C. A. Ullrich. Density-functional theory for systems with noncollinear spin: orbital-dependent exchange-correlation functionals and their application to the hubbard dimer. *Arxiv:1805.06417*, May 2018.

[163] C. J. Umrigar and X. Gonze. Accurate exchange-correlation potentials and total-energy components for the helium isoelectronic series. *Phys. Rev. A*, 50(5):3827–3837, Nov 1994.

[164] C. J. Umrigar and M. Nightingale. *Quantum Monte Carlo Methods in Physics and Chemistry*, volume 525. Springer, 1999.

[165] M. van Faassen, P. L. de Boeij, R. van Leeuwen, J. A. Berger, and J. G. Snijders. Ultranonlocality in time-dependent current-density-functional theory: Application to conjugated polymers. *Phys. Rev. Lett.*, 88:186401, Apr 2002.

[166] U. von Barth and L. Hedin. A local exchange-correlation potential for the spin polarized case. *Journal of Physics C: Solid State Physics*, 5(13):1629, 1972.

[167] L. O. Wagner, E. M. Stoudenmire, K. Burke, and S. R. White. Guaranteed convergence of the kohn-sham equations. *Phys. Rev. Lett.*, 111:093003, Aug 2013.

[168] Y. Wang and J. P. Perdew. *Phys. Rev. B*, 43:8911, 1991.

[169] S. R. White. Density matrix formulation for quantum renormalization groups. *Phys. Rev. Lett.*, 69(19):2863–2866, Nov 1992.

[170] B. Wilson, V. Sonnad, P. Sterne, and W. Isaacs. Purgatorio—a new implementation of the inferno algorithm. *Journal of Quantitative Spectroscopy and Radiative Transfer*, 99(1):658–679, 2006.

[171] H. F. Wilson and B. Militzer. Rocky core solubility in jupiter and giant exoplanets. *Phys. Rev. Lett.*, 108:111101, Mar 2012.

[172] H. F. Wilson, M. L. Wong, and B. Militzer. Superionic to superionic phase change in water: Consequences for the interiors of uranus and neptune. *Phys. Rev. Lett.*, 110:151102, Apr 2013.

[173] Z.-h. Yang, A. Pribram-Jones, K. Burke, and C. A. Ullrich. Direct extraction of excitation energies from ensemble density-functional theory. *Phys. Rev. Lett.*, 119:033003, Jul 2017.

[174] Z.-h. Yang, J. R. Trail, A. Pribram-Jones, K. Burke, R. J. Needs, and C. A. Ullrich. Exact and approximate Kohn-Sham potentials in ensemble density-functional theory. *Phys. Rev. A*, 90:042501, Oct 2014.

[175] F. Zhang and K. Burke. Adiabatic connection for near degenerate excited states. *Phys. Rev. A*, 69(5):052510, May 2004.

[176] P. Ziesche, S. Kurth, and J. P. Perdew. Density functionals from LDA to GGA. *Computational Materials Science*, 11(2):122 – 127, 1998.

Appendix A

Too many finite temperature figures

Using this simple model system, a substantial amount of information can be extracted. Some of those figures are shown below, and have never been made. They provide substantial insight to how specific energy components behave depending on the on $\Delta v, U$ and τ. Here all figures of N are really figures of $\mathcal{N}$, and $x = \Delta v$.

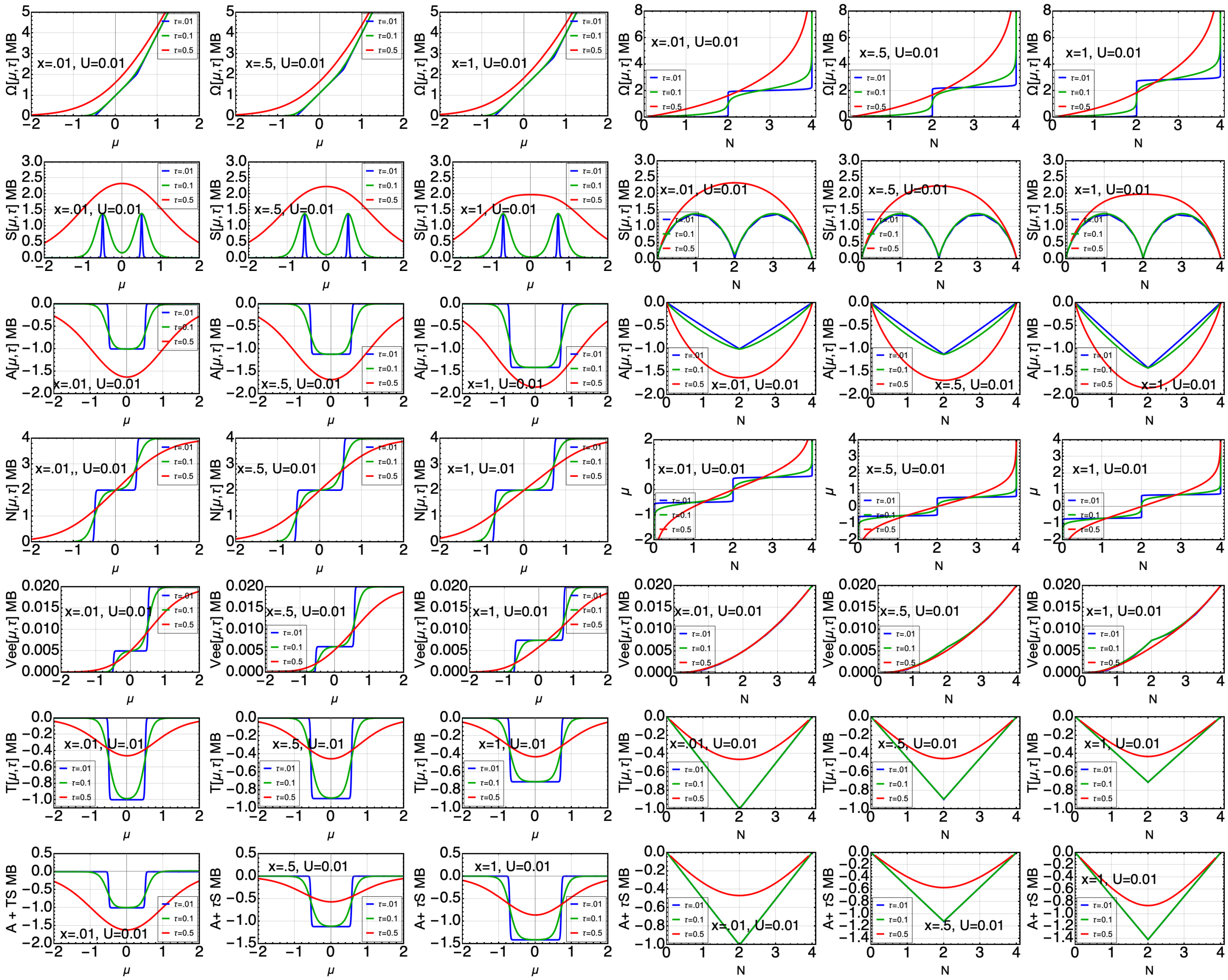

Figure A.1: Many body figures for $\Omega, S, A, N, T, Vee, A + \tau S$ for $U = 0$.

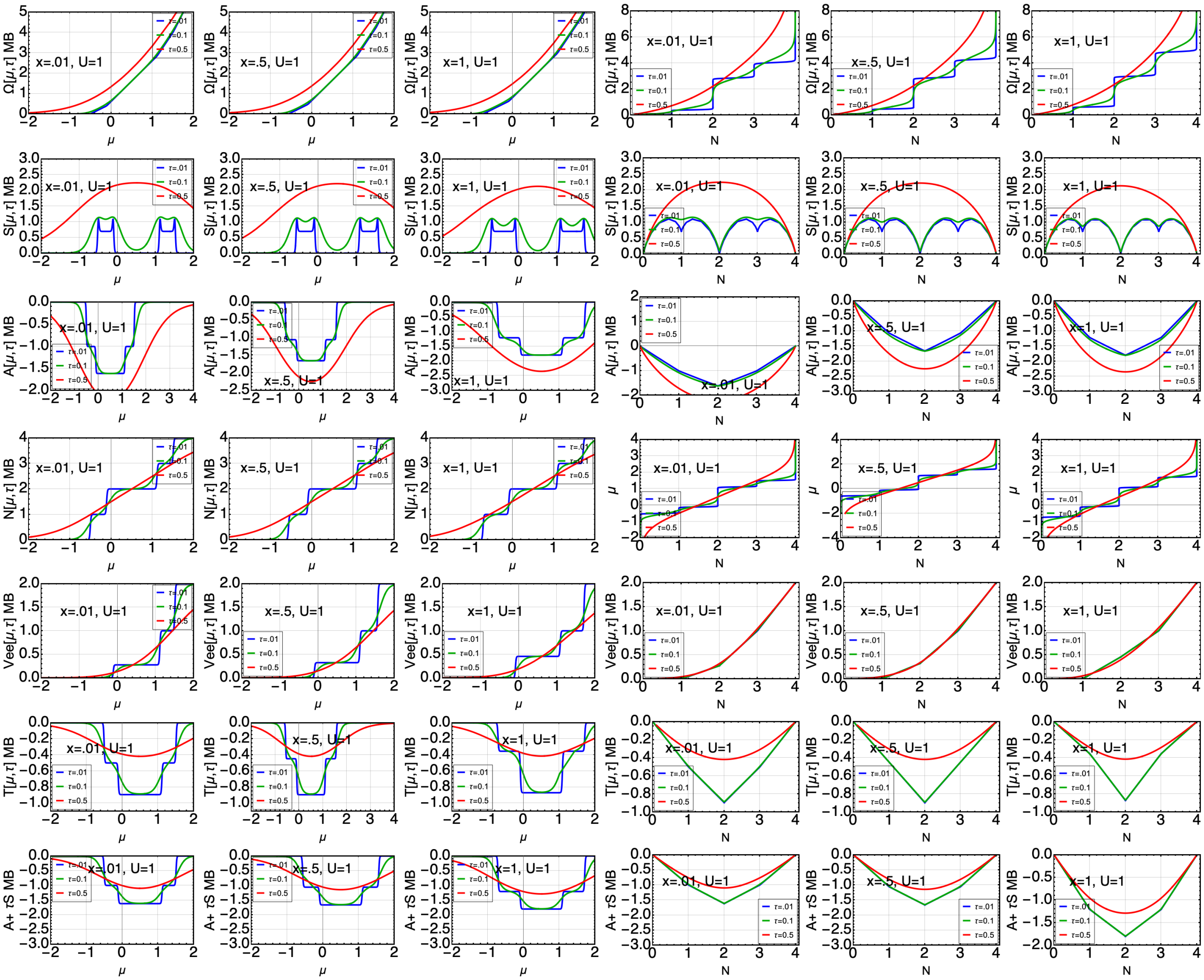

Figure A.2: Many body figures for $\Omega, S, A, N, T, Vee, A + \tau S$ for $U = 1$.

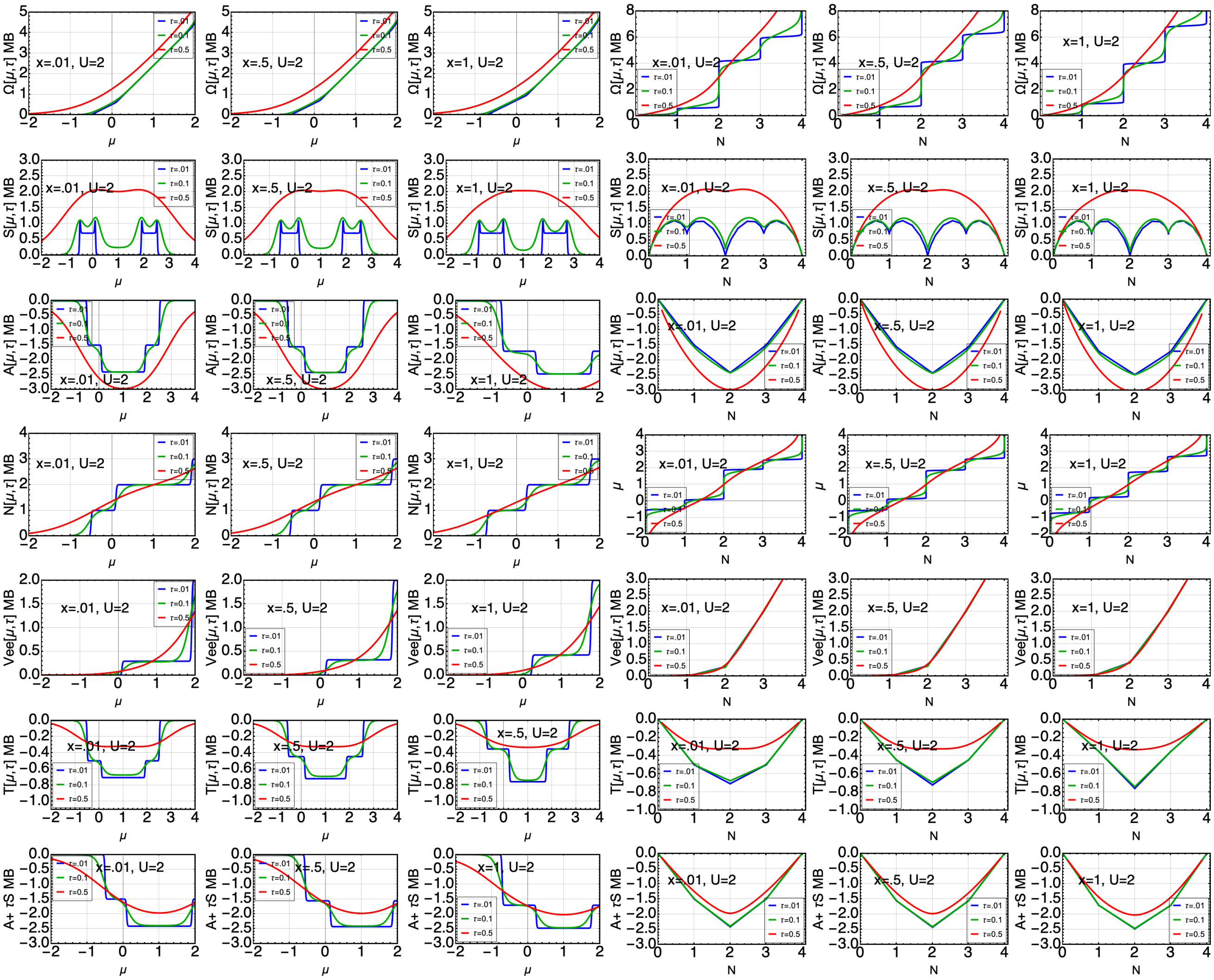

Figure A.3: Many body figures for $\Omega, S, A, N, T, Vee, A + \tau S$ for $U = 2$.